

1-2017

TARGETING APOPTOTIC PATHWAYS TO OVERCOME DRUG RESISTANCE IN ACUTE MYELOID LEUKEMIA

Rongqing Pan

Follow this and additional works at: https://digitalcommons.library.tmc.edu/utgsbs_dissertations

 Part of the [Biology Commons](#), [Cancer Biology Commons](#), and the [Medicine and Health Sciences Commons](#)

Recommended Citation

Pan, Rongqing, "TARGETING APOPTOTIC PATHWAYS TO OVERCOME DRUG RESISTANCE IN ACUTE MYELOID LEUKEMIA" (2017). *The University of Texas MD Anderson Cancer Center UTHealth Graduate School of Biomedical Sciences Dissertations and Theses (Open Access)*. 728.
https://digitalcommons.library.tmc.edu/utgsbs_dissertations/728

This Dissertation (PhD) is brought to you for free and open access by the The University of Texas MD Anderson Cancer Center UTHealth Graduate School of Biomedical Sciences at DigitalCommons@TMC. It has been accepted for inclusion in The University of Texas MD Anderson Cancer Center UTHealth Graduate School of Biomedical Sciences Dissertations and Theses (Open Access) by an authorized administrator of DigitalCommons@TMC. For more information, please contact digitalcommons@library.tmc.edu.

**TARGETING APOPTOTIC PATHWAYS TO OVERCOME DRUG RESISTANCE IN
ACUTE MYELOID LEUKEMIA**

by

Rongqing Pan, M.S.

APPROVED:

Michael Andreeff, M.D., Ph.D.
Advisory Professor

Pierre McCrea, Ph.D.

Marina Konopleva, Ph.D.

Sean Post, Ph.D.

Peng Huang, Ph.D.

APPROVED:

Dean, The University of Texas
Graduate School of Biomedical Sciences at Houston

**TARGETING APOPTOTIC PATHWAYS TO OVERCOME DRUG RESISTANCE IN ACUTE
MYELOID LEUKEMIA**

A

DISSERTATION

Presented to the Faculty of

**The University of Texas
Health Science Center at Houston**

And

**The University of Texas
MD Anderson Cancer Center**

Graduate School of Biomedical Sciences

in Partial Fulfillment
of the Requirements
for the Degree of

DOCTOR OF PHILOSOPHY

by

Rongqing Pan, M.S.

Houston, Texas
January 2017

Copyright © 2017 Rongqing Pan

All rights reserved

Dedication

I dedicate this dissertation to

my parents who taught me to be

passionate, hard-working and patient.

Thank you both for your love and support.

Acknowledgement

This dissertation could not have been accomplished without the help, guidance, and advice of many people.

I would like to express my sincere appreciation to my mentor, **Dr. Michael Andreeff** for his support and guidance on the course to pursue my Ph.D. degree. Dr. Andreeff gave me the freedom to think independently, the support to learn from trial and error, and the guidance to keep me on the right track.

I would also like to thank all members of my supervisory committee, **Drs. Marina Konopleva, Peng Huang, Pierre McCrea, Sean Post, Hui-Kuan Lin, David McConkey, and Elsa Flores**, for their helpful guidance and thoughtful perspectives in the committee meetings. I am especially grateful to Dr. Konopleva, who has been like a second mentor to me.

I would like to take this opportunity to thank all current and past members of the **Andreeff Lab** and the **Konopleva Lab**. Thanks to Vivian Ruvolo, Teresa McQueen, Peter Ruvolo, Ye Chen, Hong Mu, Numsen Hail, Twee Tsao, Christopher Benton, Lokesh Battula, Jared Burks, Lina Han, Bing Carter, Weiguo Zhang, Kensuke Kojima, Wendy Schober, Po Yee Mak, Sujana Piya, Rodrigo Jamaco, Zhihong Zeng, Sesha Duvvuri, Almed Al Rawi, Qi Zhang, Karine Harutyunyan and all others for their willingness to share their knowledge and expertise. In addition, I would like to thank all of our collaborators, Drs. Anthony Letai, Leah Hogdal, Joel Leverson, Gwen Nichols, John Reed, Maurizio Pellecchia, Markus Muschen and others for their contributions.

Finally, I would like to express my gratitude to my parents for their unconditional love and support and for teaching me the value of kindness, perseverance, and hard work.

Abstract

TARGETING APOPTOTIC PATHWAYS TO OVERCOME DRUG RESISTANCE IN ACUTE MYELOID LEUKEMIA

Rongqing Pan, M.S.

Supervisory Professor: Michael Andreeff, M.D., Ph.D.

Evasion of apoptosis is integral to tumorigenesis and drug resistance. BCL-2 and p53 proteins represent two focal nodes in convergent apoptosis signaling. Upregulation of anti-apoptotic BCL-2 family members and inactivation of p53 functions are two canonical approaches exploited by cancer cells to escape apoptosis. In the current study, we find that BCL-2 protein is highly expressed in acute myeloid leukemia (AML) cells. BCL-2-specific inhibitor ABT-199 potently induces mitochondrial apoptosis in AML cells and effectively kills AML stem/progenitor cells. Our biomarker studies demonstrate that both BH3 profiling and the expression profiling of BCL-2 proteins may serve as predictive biomarkers for the efficacy of ABT-199. Despite the initial success, we find that MCL-1 protein renders cancer cells resistant to ABT-199. Next we investigated whether p53 activation could overcome MCL-1-mediated resistance to BCL-2 inhibitor ABT-199. We demonstrate that p53 activation by MDM2 inhibitor RG7388 effectively overcomes the acquired or inherent resistance to ABT-199 both *in vitro* and *in vivo*. Mechanistic studies indicate that ABT-199 induces stabilizing phosphorylation of MCL-1. Surprisingly, p53 activation mediates the conversion from stabilized MCL-1 to destabilized MCL-1. Further mechanistic studies demonstrate that p53 activation inhibits N-Ras/Raf/MEK/ERK signaling and releases GSK3 activity to

modulate MCL-1 phosphorylation and promote Mcl-1 degradation. Additionally, p53 activation also induces pro-apoptotic proteins such as PUMA and BAX to counteract MCL-1, thus overcoming Mcl-1 mediated resistance at multiple levels. During the course of this study, we find that AML cells resistant to BCL-2 inhibition may also be resistant to p53 activation. We demonstrate that p53-induced p21^{Cip1} protein confer tumor resistance by promoting reversible G1 arrest. Importantly, BCL-2 inhibition switches the outcomes of p53 activation from pro-survival G1 arrest to apoptosis, thus overcoming AML resistance to p53 activation. The combination of BCL-2 inhibition and p53 induction markedly prolongs survival in three resistant mouse models of AML. These results collectively indicate that p53 activation and BCL-2 inhibition reciprocally overcome apoptosis resistance to either strategy alone. Our study provides novel mechanistic insights into the mechanisms of apoptosis resistance and forms the concept for an international phase II trial in AML.

Table of Contents

Copyright.....	iii
Dedication	iv
Acknowledgement	v
Abstract	vi
Table of Contents.....	viii
List of Figures	xii
List of Tables.....	xiv
Chapter 1 Introduction	1
1.1 Overview.....	2
1.2 Apoptosis Pathways	4
1.3 The BCL-2 Protein Family	5
1.4 BH3 Mimetics as Cancer Therapeutics.....	6
1.5 MCL-1 as a Cancer Therapeutic Target	7
1.6 p53 Protein in Cancer	8
1.7 Acute Myeloid Leukemia and Therapies.....	10
Chapter 2 Selective BCL-2 Inhibition by ABT-199 Causes On-Target Cell Death That Can Be Predicted by BH3 Profiling.....	12
2.1 Chapter Introduction	14
2.2 Materials and Methods	16
2.2.1 Cell lines.....	16
2.2.2 Measurement of Apoptosis, Live Cell Number and IC ₅₀ Values	16

2.2.3 Quantitative Western Blot.....	17
2.2.4 <i>MCL1</i> Knockdown by Lentiviral shRNA.....	18
2.2.5 BH3 Profiling of Cell Lines.....	18
2.2.6 Isolation and Treatment of Primary AML Cells	19
2.2.7 Apoptosis of AML Stem/Progenitor Cells.....	19
2.2.8 <i>In vivo</i> Study of ABT-199 Efficacy in AML Mouse Models.....	20
2.2.9 Immunohistochemical Analysis	21
2.2.10 Microarray-Based Gene Expression Profiling in AML.....	21
2.2.11 iBH3 of Primary AML Patient Cells	22
2.2.12 Statistical Analysis.....	23
2.3 Results.....	23
2.3.1 BCL-2 inhibitor ABT-199 Kills AML Cell Lines Potently and Quickly	23
2.3.2 ABT-199 Sensitivity Correlates with BCL-2 Protein Levels.....	25
2.3.3 ABT-199 Operates Selectively on BCL-2 Dependent Mitochondria	27
2.3.4 ABT-199 Efficiently Kills Primary AML Myeloblasts.....	29
2.3.5 ABT-199 Induces Apoptosis in AML Stem/Progenitor Cells (LSPCs).....	33
2.3.6 BH3 Profiling Predicts AML Myeloblast Killing by ABT-199.....	35
2.3.7 BH3 Profiling Predicts Response to ABT-199 in AML Xenograft Models ...	37
Chapter 3 p53 Activation and BCL-2 Inhibition Reciprocally Overcome Apoptosis	
Resistance to Either Strategy Alone: The Novel Mechanisms and Superior	
Antileukemic Efficacy	40
3.1 Chapter Introduction	41
3.2 Materials and Methods	42
3.2.1 Cell Lines and Tissue Culture.....	42

3.2.2 Generation of AML Cells with Acquired Resistance to ABT	43
3.2.3 Concurrent Apoptosis and Cell Cycle Analysis.....	43
3.2.4 Immunoblotting and Antibodies	44
3.2.5 Stable Overexpression of MCL-1	45
3.2.6 Isolation and Treatment of Primary AML Cells	45
3.2.7 Animal Studies	46
3.2.8 Gene Knockdown by shRNA	47
3.2.9 Immunohistochemical (IHC) Analysis	48
3.2.10 Measurement of Apoptosis, Live Cell Number and IC ₅₀ Values	48
3.2.11 Statistical Analysis.....	48
3.3 Results.....	48
3.3.1 RG Activates p53 and Induces Apoptosis in a p53-Dependent Manner	48
3.3.2 p53 Activation Overcomes Acquired Resistance to BCL-2 Inhibition	52
3.3.3 p53 Activation Abrogates Inherent Resistance to BCL-2 Inhibition	56
3.3.4 p53 Activation Induces Pro-Apoptotic Proteins and Reverses ABT–Induced Upregulation of MCL-1	59
3.3.5 p53 Activation Inhibits pERK and Activates GSK3 to Modulate MCL-1 Phosphorylation.....	60
3.3.6 p53 Downregulates N-Ras and Downstream MAPK Signaling and Releases GSK3 Activity	64
3.3.7 BCL-2 Inhibition Reciprocally Overcomes Resistance to p53 Activation by Switching Cellular Response from Pro-Survival G1 Arrest to Apoptosis	65
3.3.8 p53 Activation and BCL-2 Inhibition Reciprocally Overcome Resistance of Primary AML Cells.....	69

Chapter 4 Discussion and Future Directions	72
4.1 Discussion	73
4.2 Future Directions and Unanswered Questions	79
4.2.1 To Systematically Study Mechanisms of Resistance to BCL-2 inhibitor ABT-199	79
4.2.2 To Study Mechanisms of Acquired Resistance to the Combination of BCL-2 Inhibition and p53 Activation	81
4.2.3 To Illustrate the Underlying Mechanism by Which p53 Negatively Regulates Ras	82
4.2.4 To Study the Mechanism by Which ABT-199 Elevates MCL-1 Expression	83
4.2.5 To Test the BCL-2 Inhibition/p53 Activation Strategy in immunocompetent Mice or in immunodeficient Mice with Humanized Immune System	84
4.2.6 To Study the Efficacy of Concurrent BCL-2 Inhibition and p53 Activation in killing Leukemia Stem Cells (LSCs)	85
Bibliography	87
Vita	105

List of Figures

Figure 2.1 Selective inhibition of BCL-2 by ABT-199 kills AML cell lines quickly and effectively.....	24
Figure 2.2 Sensitivity to ABT-199 positively correlates with endogenous BCL-2 protein level and negatively correlates with BCL-XL protein level in AML cell lines.....	26
Figure 2.3 ABT-199 functions selectively on BCL-2 dependent mitochondria in AML cell lines.	28
Figure 2.4 ABT-199 efficiently kills primary AML myeloblasts as a single agent.....	31
Figure 2.5 Clinical characteristics of AML patients do not correlate with ABT-199 sensitivity.	34
Figure 2.6 BH3 profiling predicts AML myeloblast killing by ABT-199.....	36
Figure 2.7 BH3 profiling predicts AML progression in a primary AML xenograft model	38
Figure 3.1 MDM2 inhibitor RG activates p53 and induces apoptosis in a p53-dependent manner.....	50
Figure S3.1 related to Figure 3.1.	51
Figure 3.2 Sensitive AML cell lines acquire resistance to BCL-2 inhibitor ABT; p53 activator RG overcomes the acquired resistance <i>in vitro</i> and <i>in vivo</i>	54
Figure S3.2 related to Figure 3.2. MCL-1 overexpression confers resistance to BCL-2 inhibitor ABT, which can be abrogated by p53 activator RG.....	55
Figure 3.3 p53 activation by RG abrogates inherent resistance to ABT.....	57
Figure S3.3 related to Figure 3.3. MCL-1 inhibition overcomes inherent ABT resistance in OCI-AML3 cells.	58
Figure 3.4 p53 negatively regulates N-Ras and downstream MAPK/GSK3 signaling to modulate MCL-1 phosphorylation and degradation.	62

Figure S3.4 related to Figure 3.4.	63
Figure 3.5 BCL-2 inhibition reciprocally overcomes resistance to p53 activation via shifting cellular response from G1 arrest to apoptosis.	67
Figure S3.5 related to Figure 3.5.	68
Figure 3.6 BCL-2 inhibition and p53 activation reciprocally overcome drug resistance of AML primary samples <i>in vitro</i> and in a PDX mouse model of resistance.	70
Figure 4.1 Low doses of ABT-RG combination synergizes with idarubicin, cytarabine and sorafinib.	77

List of Tables

Table 2.1 Clinical characteristics of AML patients.....	30
---	----

Chapter 1 Introduction

1.1 Overview

Drug resistance is always a potential concern with targeted therapeutics. Most targeted compounds focus on upstream nodes of cancer signaling pathways. Although the initial response might be promising, acquired resistance is often inevitable due to various compensatory mechanisms mediated by complex cancer signaling networks¹⁻³. For most cancer treatments, including chemotherapy, radiotherapy, and targeted therapies, induction of apoptosis represents the principal mechanism by which malignant cells are eliminated⁴⁻⁶. Therefore, targeting the downstream apoptosis machinery appears to be a promising strategy since it directly elicits cell death and possibly minimizes the development of drug resistance. p53 and BCL-2 family proteins are central regulators of the apoptosis machinery. Upregulation of anti-apoptotic BCL-2 family proteins and inactivation of p53 are two canonical approaches exploited by cancer cells to escape apoptosis^{5,7-9}. This thesis is composed of two interrelated projects to target the mitochondrial apoptosis pathway, by inhibiting BCL-2 and activating p53, to induce apoptotic cell death and to overcome drug resistance of AML cells.

In the first project (Chapter 2), we found that BCL-2 protein, a key regulator of the mitochondrial apoptosis pathway, is highly expressed in AML. The advent of ABT-199, a selective and potent BCL-2 inhibitor, allows us to study whether BCL-2 inhibition could effectively induce mitochondrial apoptosis *in vitro* and in pre-clinical mouse models. In Chapter 2, we tested the hypothesis that AML cells dependent on BCL-2 for survival would be sensitive to BCL-2 inhibitor ABT-199 and the cellular response to ABT-199 could be predicted by BH3 profiling. We studied the efficacy and mechanism

of action of ABT-199 in cell lines, patient samples, and mouse models. We also evaluated the expression profiling of BCL-2 proteins and BH3 profiling as predictive biomarkers for cellular response to BCL-2 inhibitor ABT-199. This study has been translated into a Phase II clinical trial to treat AML patients.

Both the results of the first project as well as the results of the clinical trial indicate that BCL-2 inhibition by ABT-199 is an effective treatment for AML in preclinical and clinical settings^{10,11}. However, we found that expression of another anti-apoptotic protein MCL-1 renders AML cells resistant to ABT-199. In the second project (Chapter 3), we investigated whether p53 activation could overcome MCL-1 mediated resistance to BCL-2 inhibition and elucidated the detailed mechanisms through which p53 negatively modulated the expression of MCL-1. During the course of this study, we found that AML p53 wild type cell lines such as OCI-AML3 could also be resistant to p53 activation. We studied the roles of p21 in mediating apoptosis resistance to p53 activation and tested the hypothesis that BCL-2 inhibition could overcome resistance to p53 activation by shifting cell response from cell cycle arrest to apoptosis. The mechanistic and efficacy studies were conducted with three types of drug-resistant models of AML. Either BCL-2 inhibition or p53 activation alone had limited efficacy in these three resistant models. However, the combination of the two strategies achieved remarkable efficacy and markedly prolonged mouse survival. We illustrated, both mechanistically and therapeutically, BCL-2 inhibition and p53 activation can reciprocally overcome apoptosis resistance to either strategy alone. Our results provide important mechanistic insights as well as critical preclinical evidence proposing the use of p53-reactivating compounds in combination with BCL-2 inhibitors in leukemia patients, and

warrant an international phase II trial to assess the clinical benefit of our proposed combination therapy.

1.2 Apoptosis Pathways

Apoptosis is a form of highly regulated and programmed cell death that occurs in multicellular organisms. Apoptosis is evolutionarily conserved from nematodes to humans and plays essential roles in diverse biological progresses including embryo development, tissue homeostasis, aging, and immunity^{9,12}. Excessive apoptosis can cause a number of diseases such as neurodegenerative diseases and ischaemic heart failure, while inadequate apoptosis leads to diseases associated with excessive accumulation of cells, such as cancer, autoimmune disease, and chronic inflammation^{9,13,14}.

Two canonical pathways regulate apoptosis in mammalian cells, namely the mitochondrial (or intrinsic) pathway and the death receptor-mediated (or extrinsic) pathway^{13,15}. Mitochondrial apoptosis pathway is tightly regulated by BCL-2 family proteins. Diverse cytotoxic stimuli such as DNA damage, oncogenic stress, and developmental cues can shift the balance of BCL-2 family anti-apoptotic and pro-apoptotic proteins towards the initiation of mitochondrial apoptosis^{9,16}. The subsequent activation of pro-apoptotic Bax and Bak proteins leads to the release of cytochrome c and other intermembrane space proteins from the mitochondria. Released cytochrome c next binds cytosolic Apaf-1 protein to form apoptosome, which in turn cleaves and activates pro-caspase-9. Activated caspase-9 (one initiator caspase) next cleaves and activates effector caspases such as caspase-3, -6 and -7 to execute apoptotic cell death^{12,13}.

The death receptor-mediated pathway involves binding of extracellular ligands of TNF family (such as Trail, FasL and TNF α) to transmembrane death receptors (DR4/5, Fas and TNFR1, respectively), leading to activation of caspase-8^{13,14}. Active caspase-8, similar as caspase-9, cleaves and activates effector caspases-3 and -7 to induce extrinsic apoptosis. In addition, caspase-8 also mediates the proteolysis of BID and the truncated form of BID (tBID) can potentially promote the mitochondrial apoptosis pathway to amplify the apoptotic response^{9,13}. Numerous studies have shown that evasion of apoptosis is a hallmark of cancer. Dysregulated apoptotic machinery, especially the abnormal mitochondrial pathway, is widely associated with tumor initiation, progression and therapeutic resistance^{5,9,17,18}. For this reason, targeting apoptotic pathway might be a promising direction for the development of novel cancer therapies.

1.3 The BCL-2 Protein Family

The BCL-2 family includes at least 16 members of interacting proteins, which together form a rheostat to regulate mitochondrial outer membrane permeabilization (MOMP) and regulate mitochondrial apoptosis pathway^{5,9,17}. BCL-2 family protein can be classified into three functionally different groups. The first group comprises of anti-apoptotic proteins including BCL-2, MCL-1, BCL-XL, BFL-1/A1, and BCL-W, all of which share four BCL-2 homology domains (i.e., BH1, BH2, BH3, and BH4 domains). These anti-apoptotic proteins can bind and sequester the other two groups of pro-apoptotic proteins to prevent apoptosis from happening^{14,17,18}. The second group consists of three proteins, Bax, Bak, and Bok, all of which are multi-domain pro-apoptotic proteins sharing BH1, BH2 and BH3 domains. When activated, Bax, Bak, and Bok adopt a pro-death conformation and oligomerize to form channels in the

mitochondrial outer membranes. As a result, cytochrome c, as well as other intermembrane space proteins such as Omi and Diablo, will be released from mitochondria to initiate mitochondrial apoptosis^{12,19}.

Members of the third group are BH3-only pro-apoptotic proteins including Puma, Bim, Bid, Bad, Noxa, Hrk, Bmf, and Bik. BH3-only proteins, as the name implies, share only one BCL-2 homology domain BH3. All members in this group are able to bind and counteract at least one anti-apoptotic protein. For example, Hrk binds BCL-XL; Noxa binds MCL-1 and BFL-1; Bad or Bmf binds BCL-2, BCL-W and BCL-XL; whereas Puma, Bid, and Bim bind all five anti-apoptotic BCL-2 proteins^{14,17}. The BH3-only proteins can be further divided into two subsets: sensitizers (i.e., Bad, Noxa, Hrk, Bmf, and Bik) and activators (i.e., Bim, Bid, and Puma)²⁰⁻²². In addition to inhibiting anti-apoptotic members, BH3-only activator proteins also directly interact with and activate Bax and Bak to promote their conformational changes and oligomerization to form channels across mitochondrial outer membrane^{23,24}. BH3-only sensitizers cannot activate Bax and Bak but instead bind and sequester anti-apoptotic proteins to prevent them from interacting with Bax, Bak and BH3-only activators. The dynamic interaction of the three groups of BCL-2 proteins determines the survival or death of cells under various physiological or pathological stimuli.

1.4 BH3 Mimetics as Cancer Therapeutics

Over the past three decades, research on BCL-2 family proteins and mitochondrial apoptosis has led to the development of small molecules mimicking the BH3 domains of BH3-only proteins. This type of compounds, termed as BH3 mimetics, can dock into the binding grooves of BCL-2 anti-apoptotic proteins, replace and release the sequestered pro-apoptotic proteins to directly induce mitochondrial apoptosis of cancer

cells^{4,5}. ABT-737²⁵ and its orally-bioavailable counterpart ABT-263/navitoclax²⁶ represent a breakthrough in the development of BH3 mimetics⁹. ABT-737 and ABT-263 have submicromolar affinities for BCL-2, BCL-XL and BCL-W. Although both of the two BH3 mimetics have shown promising efficacy from bench to bedside studies, on-target thrombocytopenia caused by BCL-XL inhibition limits the usage and efficacy of ABT-263 in the clinical settings⁵. Recently, Souers, *et al.* reported the re-engineering of ABT-263 to generate ABT-199 (venetoclax), a first-in-class BCL-2 specific inhibitor²⁷. ABT-199 has significantly enhanced avidity and specificity for BCL-2 protein compared to its predecessors ABT-737 and ABT-263²⁷. ABT-199 has shown potent efficacy against several cancers, earned several Breakthrough Therapy Designations, and was recently approved by US FDA for the treatment of chronic lymphocytic leukemia with chromosomal 17q deletion. Nevertheless, ABT-199, as well as its predecessors ABT-737 and ABT-263, binds poorly to MCL-1. Thus, tumor cells expressing high levels of MCL-1 are usually very resistant to these agents^{11,28-31}. Overexpression of the anti-apoptotic BCL-2 proteins, especially MCL-1 and BCL-2, has been widely implicated in resistance to conventional chemotherapy and novel targeted therapeutics. Therefore, development of selective and potent BH3 mimetics to inhibit these antiapoptotic proteins has become a pressing pharmacologic need for treatment of refractory malignancies.

1.5 MCL-1 as a Cancer Therapeutic Target

MCL-1 amplification and aberrant overexpression have been shown to be one of the most common genetic aberrations in hematological malignancies and in solid tumors, including leukemia, lymphoma, multiple myeloma, melanoma, lung, colorectal, breast, pancreatic, prostate as well as ovarian and cervical cancers^{4,9,32}. In particular, it

has been shown that MCL-1 is essential for the survival of AML cells^{28,33}. Gores, *et al.* reported that MCL-1 ablation resulted in almost complete loss of viable AML cells in MCL-1 knockout mouse models²⁸. Furthermore, elevated MCL-1 expression confers cancer cell resistance to aforementioned BCL-2 inhibitors and a number of widely used anticancer chemotherapeutics^{4,9}. These facts, collectively, established MCL-1 as one key target for antitumor therapies.

The advent of BCL-2 inhibitors such as ABT-737 and ABT-199 has had a profound impact in the field of targeting mitochondrial apoptotic pathways^{4,5}. ABT-199 is currently intensively investigated as monotherapy or in combination with other therapies in various cancers. Nevertheless, the development of MCL-1 inhibitors progressed more slowly and lagged behind, perhaps because MCL-1 binding groove is more rigid than BCL-2 groove³⁴. As mentioned above, the emerging roles of MCL-1 in tumorigenesis, tumor progression, and therapeutic resistance make it an important cancer target. Tremendous efforts have been made towards the development of MCL-1 specific inhibitors. However, the reported MCL-1 inhibitors, small molecules or stabled peptides, are still at an early stage and only have moderate affinity for MCL-1³³. Therefore, highly potent MCL-1-selective BH3 mimetics have been eagerly awaited, as both tool compounds and therapeutic agents.

1.6 p53 Protein in Cancer

p53, arguably the most important tumor suppressor gene, was identified by Lionel Crawford, David Lane, Arnold Levine, and Lloyd Old nearly four decades ago. p53 protein senses DNA damage and other stresses (e.g., oncogene activation, hypoxia, and nutrient deprivation) and triggers diverse biological responses such as apoptosis, cell cycle arrest, and senescence^{35,36}. The best-characterized function of p53 is as a

transcription factor to induce or repress the expression of many genes and microRNAs. p53 expression can be regulated at transcriptional, translational and post-translational modification (PTM) levels^{25,26}. Among them, the regulation of p53 protein stability by MDM2 is a critical mechanism through which p53 activity is dynamically modulated. MDM2, an E3 ubiquitin ligase of p53, not only targets p53 for degradation through the ubiquitin-proteasome pathway, but also directly inhibits the transcriptional functions of p53 by binding to its transcriptional activation domain^{35,37,38}. Notably, p53 also transcriptionally induces MDM2 mRNA expression, thus creating a negative feedback loop to control p53 activity^{39,40}.

p53 mutations have long been implicated in carcinogenesis and therapeutic resistance. In genetic mouse models, p53 deletion leads to the spontaneous development of tumors, establishing the role of p53 as a tumor suppressor gene. p53 is also the most frequently mutated gene in human solid tumors, with about half of all solid tumors carrying p53 mutations^{8,41,42}. Interestingly, p53 mutation is rare in the majority of hematological malignancies such as AML, MDS, MM, CLL, CML, and ALL^{43,44}. However, wild type p53 functions can be suppressed by MDM2, which is frequently overproduced through gene amplification or overexpression in tumors with wild-type p53. We have reported that MDM2 is highly expressed in most primary AML samples, and its overexpression is strongly associated with poor prognosis^{45,46}.

A number of strategies have been devised to reactive p53 functions, e.g., using small molecules to disrupt p53-MDM2 interaction, p53 gene therapies, and designing drugs to restore the wild type functions of mutant p53^{8,42}. The development of Nutlins, a set of small molecule inhibitors of p53-MDM2 interaction, represents a breakthrough in this field^{8,47}. To date, a number of pharmaceutical companies have developed their own

MDM2 small molecule inhibitors and are evaluating these compounds in pre-clinical studies and in early phase clinical trials. The recently developed RG7388 (abbreviated here as RG) is a second-generation MDM2 inhibitor with greater potency, selectivity, and bioavailability compared to its predecessors nutlins⁴⁸. RG will be used in Chapter 3 to mediated non-genotoxic activation of p53. We first demonstrated that RG could robustly activate p53 and that RG-induced apoptosis was highly dependent on p53, indicating that RG can serve as an ideal compound to study p53 activation. Since p53 is also a critical regulator of mitochondrial apoptosis, next we studied whether p53 activation by RG could abrogate MCL-1 mediated resistance to BCL-2 inhibitor ABT-199 in several resistance models of AML.

1.7 Acute Myeloid Leukemia and Therapies

Acute myeloid leukemia (AML) is a hematopoietic malignancy characterized by the rapid accumulation of abnormally differentiated, non-functional myeloid cells^{49,50}. The current 5-yr survival rate is 26% for AML patients and this disease accounts for over 10,000 deaths per year in US^{51,52}. Acute promyelocytic leukemia (APL) is the M3 subtype of AML and represents 10-12% of all AML cases. Nowadays, APL can be effectively treated with all-trans retinoic acid (ATRA) and arsenic trioxide (ATO)⁵³. The long-term cure of APL patients with ATRA and ATO therapy represents the only therapeutic breakthrough over the past two decades for AML treatment.

Except for APL, current AML treatment relies largely on induction chemotherapy and bone marrow/stem cell transplantation. Induction therapy with cytarabine and an anthracycline compound remains a standard of care in AML⁵¹. However, most AMLs develop chemoresistance during the course of treatment and AML patients tend to relapse after initial response^{54,55}. The fact that only 10-20% of AML patients are cured

by chemotherapy highlights the urgent need for novel treatment options. Although bone marrow transplantation is potentially curative, only 25% of AML patients are eligible for this therapy and only half of transplanted patients can survive long-term⁵¹. The 5-year survival rate has only marginally increased over the past few decades and 70% of AML patients still die from this hematological malignancy^{51,52,56}. Consequently, there is a substantial unmet need for new AML therapeutic regimens.

Chapter 2 Selective BCL-2 Inhibition by ABT-199 Causes On-Target Cell Death That Can Be Predicted by BH3 Profiling

Copyright disclosure:

This chapter is largely based upon (Pan, R., Hogdal, L. J., Benito, J. M., Bucci, D., Han, L., Borthakur, G., Cortes, J., DeAngelo, D. J., Debose, L., Mu, H., Dohner, H., Gaidzik, V. I., Galinsky, I., Golfman, L. S., Haferlach, T., Harutyunyan, K. G., Hu, J., Levenson, J. D., Marcucci, G., Muschen, M., Newman, R., Park, E., Ruvolo, P. P., Ruvolo, V., Ryan, J., Schindela, S., Zweidler-McKay, P., Stone, R. M., Kantarjian, H., Andreeff, M., Konopleva, M. & Letai, A. G. Selective BCL-2 inhibition by ABT-199 causes on-target cell death in acute myeloid leukemia. *Cancer discovery* 4, 362-375, doi:10.1158/2159-8290.CD-13-0609 (2014)), and re-printed with permission from the journal.

Attributions:

Chapter 2 was the result of a productive collaboration between myself and Leal Hogdal in Dr. Anthony Letai's lab at Dana-Farber Cancer Institute, Harvard Medical School. The data was collected and compiled by myself with the exception of Figures 2.3, 2.4B-C, 2.5, and 2.6C.

Permissions from Cancer Discovery (one AACR Journal)

Rac, Karola

Today at 1:28 PM

RK

To: Pan, Rongqing

RE: Request for permission to reproduce 1st-authored paper as part of doctoral dissertation



Hello,

Authors of articles published in AACR journals are permitted to use their article or parts of their article in the following ways without requesting permission from the AACR. All such uses must include appropriate attribution to the original AACR publication. Authors may do the following as applicable:

1. Reproduce parts of their article, including figures and tables, in books, reviews, or subsequent research articles they write;
2. Use parts of their article in presentations, including figures downloaded into PowerPoint, which can be done directly from the journal's website;
3. Post the accepted version of their article (after revisions resulting from peer review, but before editing and formatting) on their institutional website, if this is required by their institution. The version on the institutional repository must contain a link to the final, published version of the article on the AACR journal website. The posted version may be released publicly (made open to anyone) 12 months after its publication in the journal;
4. Submit a copy of the article to a doctoral candidate's university in support of a doctoral thesis or dissertation.

Kind regards,
Karola

AACR JOURNALS - MUST HAVE CONTENT | ANYTIME, ANYWHERE

Karola Rac

ASSISTANT DIRECTOR, INSTITUTIONAL SALES AND OUTREACH
Publishing Division



American Association for Cancer Research
615 Chestnut Street, 17th Floor | Philadelphia, PA 19106-4404
215-446-7231 Direct | 267-765-1006 Fax
karola.rac@aacr.org | www.AACR.org



2.1 Chapter Introduction

Acute myeloid leukemia is a hematopoietic neoplasia characterized by the rapid, clonal growth of the myeloid lineage of blood cells. The disease affects approximately 14,000 adults in the United States each year and unfortunately, despite recent advances in the treatment of AML, 10,400 people die from their disease⁵⁷. Most AML patients become resistant to chemotherapy at some point in their course and succumb to their disease. Therefore, it is necessary to prevent chemo-resistance or enhance chemo-sensitivity in a selective fashion to lead to a higher cure rate and a lower toxic burden.

A novel strategy to treat cancer cells is to directly stimulate the mitochondrial apoptotic pathway in them. ABT-263 (navitoclax), which functions as a small molecule mimetic of the BH3 domain of the BH3-only sensitizer protein BAD, efficiently binds to BCL-2, BCL-XL and BCL-W, releasing bound pro-apoptotic proteins and causing MOMP in BCL-2 dependent cancer cells²⁶. In early clinical trials, navitoclax showed potency in the treatment of chronic lymphocytic leukemia (CLL) and small-cell lung cancer^{30,58}. However, treatment with navitoclax causes on-target, dose-limiting thrombocytopenia because platelets are dependent on BCL-XL for their survival⁵⁹. The dose-dependent thrombocytopenia limited navitoclax's use in many malignancies, particularly leukemias where patients often present with pre-existing thrombocytopenia. This prompted the development of ABT-199, a modified BH3-mimetic derivative of ABT-263 which maintains specificity for BCL-2, but lacks affinity for BCL-XL²⁷. The remodeled drug has shown cancer killing efficacy in CLL *in vivo*, myc-driven

lymphomas in mice and estrogen receptor-positive breast cancer while sparing platelets^{27,60,61}.

AML bulk and stem cells might be dependent on BCL-2 for survival and BCL-2 inhibition by ABT-737 causes cell death in AML cells²⁹. Importantly, BCL-2 inhibition relatively spares normal hematopoietic stem cells^{62,63}. Thus, the first goal of the present study is to evaluate the anti-cancer effects of ABT-199 on AML and compare its efficacy with ABT-737/ABT-263, drugs that have both shown activity in the *ex vivo* treatment of AML cell lines and AML primary patient samples and in human clinical trials²⁹. The second goal is to determine if BH3-profiling can be used as a tool to predict cellular response to ABT-199 treatment.

BH3-profiling is a method to determine the mitochondrial priming level of a cell by exposing cellular mitochondria with standardized amounts of peptides derived from the BH3 domains of BH3-only proteins and determining the rate of MOMP, as measured by either cytochrome c release or depolarization across the inner mitochondrial membrane⁶⁴. Previously, we have shown that the priming status of the cell is predictive of the cell's chemo-responsiveness in that the more primed the cell is, the more sensitive the cell is to various chemotherapeutics^{62,65}. Furthermore, BH3-profiling can also identify anti-apoptotic addictions^{62,65,66}. For instance, the BAD BH3-only peptide binds with high affinity with BCL-2, BCL-XL and BCL-W, while the HRK BH3 peptide binds with high affinity only to BCL-XL. Thus, MOMP following BAD peptide incubation suggests an anti-apoptotic dependency on BCL-2, BCL-XL or BCL-W, while MOMP following HRK peptide incubation indicated dependency on BCL-XL. Using this tool, we can identify AML cells which depend on BCL-2 for survival and that are more likely to die following

BCL-2 inhibition. Thus, we hypothesize that cells that are addicted to BCL-2 for survival will be sensitive to ABT-199 and that we can predict this response by BH3 profiling.

2.2 Materials and Methods

2.2.1 Cell lines

The AML cell lines were purchased from the American Type Culture Collection (Manassas, VA) or Deutsche Sammlung von Mikroorganismen und Zellkulturen (Braunschweig, Germany) or were kindly provided by Dr. James Griffin (Dana-Farber Cancer Institute, Boston, MA). HL-60 cell lines with stable overexpression of BCL-2 or BCL-XL, and the control cell line with empty vector, were kindly provided by Dr. Kapil N. Bhalla (The Methodist Hospital Research Institute, Houston, TX). AML cell lines were cultured in RPMI 1640 medium supplemented with 10% or 20% fetal bovine serum, 10mM L-glutamine, 100 U/ml penicillin and 10 mg/ml streptomycin. Cells were kept at 37°C in a humidified atmosphere of 5% CO₂.

2.2.2 Measurement of Apoptosis, Live Cell Number and IC₅₀ Values

Exponentially growing cells were treated with different compounds or dimethyl sulfoxide (DMSO) as indicated in each figure and figure legend. DMSO served as drug vehicle and its final concentration was less than 0.1%. After treatment, cells were collected, stained with Annexin V (AnnV) and propidium iodide (PI; Sigma-Aldrich, St Louis, MO, USA), and analyzed by flow cytometry. Briefly, cells were washed twice by centrifugation (1000g, 5 min) with 2 mL AnnV binding buffer (ABB; 10mM HEPES, 140mM NaCl, and 5mM CaCl₂ at pH 7.4). After washing, cells were resuspended in 0.1 mL ABB containing fluorochrome-conjugated AnnV and incubated in darkness at room temperature for 15 min. The cells were washed again with 2 mL ABB and then

resuspended in 0.3 mL ABB. PI was added at a final concentration of 1 µg/mL before analysis by a Gallios flow cytometer (Beckman Coulter, Indianapolis, IN, USA). To determine absolute cell number, CountBright Absolute Counting Beads (Life Technologies, Carlsbad, CA, USA) were also added. Data were analyzed by Kaluza software version 1.3 (Beckman Coulter). Calcosyn 2.0 software (Biosoft, Great Shelford, UK) was used to calculate IC₅₀ values and combination index, based on the absolute number of live cells (*i.e.*, AnnV/PI⁺). AnnV-FITC and AnnV-APC were purchased, respectively, from Roche Applied Sciences (Indianapolis, IN, USA) and BD Biosciences (San Jose, CA, USA).

2.2.3 Quantitative Western Blot

Cells were subjected to lysis at a density of 1 x 10⁶/50 µL in protein lysis buffer (0.25 M Tris-HCl, 2% sodium dodecylsulfate, 4% β-mercaptoethanol, 10% glycerol, 0.02% bromophenol blue) supplemented with 1x protease/phosphatase inhibitor cocktail (#5872, Cell Signaling Technology, Beverly, MA, USA). Cell lysates were then loaded onto polyacrylamide gels with sodium dodecyl sulfate (Bio-Rad, Hercules, CA, USA). After electrophoresis, proteins were transferred to polyvinylidene difluoride membranes. The transblotted membranes were blocked for 1 h and then probed with appropriate primary antibodies (dilution as recommended by manufacturers) overnight at 4°C. Next, the membranes were washed three times for a total of 30 min and then incubated with secondary antibodies in darkness at room temperature for 1 h. After another three washes, Odyssey infrared imaging system and companion software (LI-COR Biosciences, Lincoln, NE, USA) were used to scan immunoblot membranes and to quantify band intensity according to the manufacturer's manual. The ratio of band intensity of BCL-2 proteins relative to that of loading control was normalized to the ratio

in untreated OCI-AML3 cells. Antibodies used for quantitative Western blot were: BCL-2 (#M0887, Dako, Carpinteria, CA), BCL-XL (# 2764, Cell Signaling Technology, Danvers, MA), MCL-1 (#559027, BD Biosciences, San Diego, CA), α -Tubulin and β -Actin (loading controls, #T6199 and #A5441, Sigma-Aldrich, St. Louis, MO).

2.2.4 MCL1 Knockdown by Lentiviral shRNA

MCL1 was knocked down by lentiviral transduction using a MCL1-specific shRNA transfer vector targeting residues 2421-2440 on RefSeq NM_021960.4. Lentivirus was prepared by co-transfection of HEK293T cells (ATCC) with an equal molar mix of transfer vector and packaging plasmid (psPAX2 and pMD2.G, Addgene, Cambridge, MA) using JetPrime transfection reagent as directed by the manufacturer (Polyplus, Illkirch, France). Fresh lentiviral supernatants were passed through 0.45 μ m surfactant-free cellulose acetate membranes; polybrene was added to 8 μ g/mL, and the virus stock was used at once to spinoculate OCI-AML3 cells as described before⁶⁷. Infected cells were selected with 0.5 μ g/mL puromycin. In parallel, control cells were transduced using lentivirus delivering a hairpin targeting GFP in pLKO.1 (Addgene). Knockdown was verified by Western blot analysis.

2.2.5 BH3 Profiling of Cell Lines

AML cell lines were seeded at a density of 4×10^5 cells/mL in 10% FBS RPMI media supplemented with 10 mM L-glutamine, 100 U/ml penicillin and 10 mg/ml streptomycin 24 h before BH3 profiling. Two million cells of each cell line were pelleted at 400 xg for 5 minutes at RT and resuspended in 2 mL DTEB (135 mM Trehalose, 10 mM HEPES-KOH, 0.1% w/v BSA, 20 μ M EDTA, 20 μ M EGTA, 50 mM KCl, 5 mM succinate, final pH 7.4). Cell lines were profiled by using the plate-based JC-1 BH3 profiling assay previously described⁶². Cells were permeabilized with digitonin, exposed

to BH3 peptides, and mitochondrial transmembrane potential loss was monitored using the ratiometric dye JC-1.

2.2.6 Isolation and Treatment of Primary AML Cells

Primary AML cells were obtained by informed consent from the Dana-Farber Cancer Institute, Leukemia Group, the Pasquarello Tissue Bank at the Dana-Farber Cancer Institute, the University of Texas MD Anderson Cancer Center, Leukemia Tissue Bank Shared Resource from the Ohio State University Comprehensive Cancer Center and the Germany-Austrian Study Group according to protocols approved by the Institute's Institutional Review Board. Samples were Ficoll purified, used immediately or viably frozen in 90% FBS/10% DMSO. Fresh (Figures 2.4A, 2.4D and 2.4E) or thawed (Figure 2.4B) mononuclear cells were resuspended in culture medium. Cells were treated with ABT-199, ABT-263 or ABT-737 for appropriate time. Cells were then washed with PBS and resuspended in Annexin binding buffer. Cell viability was assessed by FACS analysis following concurrent Annexin V and PI (or 7-AAD) staining.

2.2.7 Apoptosis of AML Stem/Progenitor Cells

AML mononuclear cells were isolated by Ficoll density centrifugation and cultured with 100 nM ABT-199 or ABT-737 as described above. After 24 h, AML cells were washed twice in Annexin binding buffer (ABB) and resuspended in 100 μ L ABB containing 1:100 dilution of Annexin-V-APC (#550475), 1:50 dilution of CD45-APC-Cy7 (#557833), CD34-FITC (#555821), CD38-PE-Cy7 (#335790) and CD123-PerCP-Cy5.5 (#58714) (all from BD Biosciences) for 20 minutes at room temperature in dark. Following staining, cells were washed with ABB and resuspended in 95 μ L ABB containing 5 μ L DAPI. Cells were analyzed by Gallios Flow Cytometer (Beckman Coulter). Results were expressed as percentage of specific apoptosis calculated by the

formula: $100 \times (\% \text{ apoptosis of treated cells} - \% \text{ apoptosis of control cells}) / (100 - \% \text{ apoptosis of control cells})$.

2.2.8 *In vivo* Study of ABT-199 Efficacy in AML Mouse Models

All animal studies were conducted in accordance with the guidelines approved by the Institutional Animal Care and Use Committees at the University of Texas MD Anderson Cancer Center. Twenty female NOD SCID gamma (NSG) mice (6-week-old, Jackson Laboratory, Bar Harbor, MA) were intravenously injected with luciferase-labeled MOLM-13 cells (0.7×10^6 cells/100 μ L) and randomly divided into two groups. Four days post injection, the mice were treated with vehicle or ABT-199 (100 mg/kg body weight) daily by oral gavage for 2 weeks. For oral dosing, ABT-199 (10 mg/mL) was formulated in 60% phosal 50 propylene glycol, 30% polyethyleneglycol-400, and 10% ethanol. Bioluminescence imaging (BLI) was used to monitor tumor burden on different time points. Briefly, mice were anaesthetized and injected intraperitoneally with firefly luciferase substrate D-luciferin and then imaged noninvasively using IVIS-200 *in vivo* imaging system (PerkinElmer, Waltham, MA). Three mice from each group were sacrificed by CO₂ asphyxiation after 15 d. Bone marrow, spleen, and liver were collected for H&E and immunohistochemical staining. The remaining seven mice in each group were followed for survival.

For primary AML derived xenograft models, NSG mice were sub-lethally irradiated (250 cGy) the day prior to intravenous injection of 10^5 PDX21 patient-derived AML cells. Three weeks following injection and after confirmation of AML engraftment, the mice were randomly divided into two groups and treated with 100 mg/kg ABT-199 or vehicle via gavage daily for 2 weeks. All mice were then sacrificed and femur bone

marrows were analyzed for leukemia burden by CD45 flow cytometry (using anti-human CD45-PE antibody #555483, BD Biosciences, San Jose, CA).

2.2.9 Immunohistochemical Analysis

Immunohistochemistry was performed as described previously⁶⁸. Briefly, the tissue was formalin-fixed, paraffin-embedded, sectioned into 5 µm thickness and mounted onto microscope slides. Tissue sections were then deparaffinized and rehydrated using xylene and ethanol in decreasing concentration. Samples were stained with hematoxylin and eosin (H&E) for histopathological evaluation. For immunohistochemical staining, the tissue sections were incubated with primary antibody against human CD45 (#555480, BD Biosciences, San Jose, CA), followed by sequential incubation with biotinylated secondary antibody, peroxidase labeled streptavidin and 3,3' diaminobenzidine tetrahydrochloride/H₂O₂ (Dako), which resulted in a brown precipitate at the antigen site. Images were taken using an optical microscope under the same magnification.

2.2.10 Microarray-Based Gene Expression Profiling in AML

The expression of BCL-2 family genes was determined using oligonucleotide microarrays (HG-U133 Plus 2.0, Affymetrix) in 288 AML samples comprising all cytogenetic groups, and in 103 normal samples (healthy BM and non-leukemia conditions) as described in Haferlach et al.⁶⁹ All samples in this study were obtained from untreated patients at the time of diagnosis. Cells used for microarray analysis were collected from the purified fraction of mononuclear cells after Ficoll density centrifugation. The study design adhered to the tenets of the Declaration of Helsinki and was approved by the ethics committees of the participating institutions before its initiation. The analysis is conducted at logarithm-2 transformed gene expression

intensities. Correlation analysis based on Pearson correlation coefficient and Spearman's rank correlation coefficient was performed to identify probe sets that have consistent expression pattern corresponding to a common gene. Two-sample t-test was performed for each two-group comparison, and the *P* value threshold of 0.005 was used to moderately control for multiple testing.

2.2.11 iBH3 of Primary AML Patient Cells

Thawed cells were washed 1x with PBS and stained with 1:100 Invitrogen Live/Dead– near IR stain (#10119, Life Technologies, Grand Island, NY) in FACS Buffer (2% FBS PBS, 1:100) for 20 min on ice, washed with FACS buffer and subsequently stained with CD45-V450 (#642275; BD Biosciences; San Jose, CA) 1:100 FACS buffer on ice for 20 min. Cells were pelleted at 400 x g for 5 min at RT and resuspended in DTEB. 100 µL of cells in DTEB was added to each tube containing twice the final concentration of each peptide treatment in 100 µL of DTEB with 0.002% w/v digitonin. Mitochondria in the permeabilized cells were exposed to peptides for 60 minutes at RT before the addition of 200 µL 4% v/v formaldehyde at RT for 15 minutes, quenched with 50 µL of 100 mM Tris/2.5 M glycine pH 8.2 for 5 minutes at RT, and pelleted at 1500 x g for 5 minutes at RT. Cells were stained with anti-cytochrome c-Alexa488 (#560263, BD Bioscience) 1:100 in 0.1% Saponin/1%BSA/PBS overnight at 4°C and diluted 1:5 in PBS an hour before FACS on a LSR Fortessa flow cytometer (BD Bioscience) to quantify cytochrome c loss calculated from the median fluorescence intensity (MFI) as

$$\% \text{ cyto c loss} = 100 \times (1 - \frac{[MFI_{\text{sample}} - MFI_{\text{isotype}}]}{[MFI_{\text{DMSO}} - MFI_{\text{isotype}}]})$$

AML blasts were identified by low-mid CD45/low SSC-A.

2.2.12 Statistical Analysis

Statistical analyses were performed using GraphPad Prism software v6.0 (GraphPad, La Jolla, CA). Unless otherwise indicated, the results are expressed as the mean \pm standard error of the mean (SEM) from at least three independent experiments. Differences with P values ≤ 0.05 were considered statistically significant.

2.3 Results

2.3.1 BCL-2 inhibitor ABT-199 Kills AML Cell Lines Potently and Quickly

As an initial test of the potential utility of ABT-199 in AML, we exposed AML cell lines to increasing concentrations of ABT-199 for 48 h and then determined the IC₅₀ values. Comparisons were made with ABT-737. As shown in Figure 2.1A, the IC₅₀ of ABT-199 ranged from <10 nM to >1000 nM, and sensitivity to ABT-737 roughly tracked sensitivity to ABT-199. Prior experience with CLL, a disease for which excellent clinical activity of ABT-199 has been observed, has revealed that CLL cells are killed in an on-target fashion, and that the killing was evident within 4 h⁷⁰. Therefore, we tested whether ABT-199 could rapidly induce apoptosis in a sensitive AML cell line MOLM-13. In Figure 1B and 1C, it can be seen that cell growth is inhibited and cell apoptosis is observed within just a few hours of exposure to ABT-199.

To demonstrate that the efficacy seen was consistent with tolerable *in vivo* delivery of ABT-199, we tested the effect of ABT-199 on an aggressive mouse xenograft model of MOLM-13. NOD SCID gamma (NSG) mice were injected with luciferase-labeled MOLM-13 cells and monitored by bioluminescence imaging (BLI) for tumor development. After confirmation of AML engraftment in the bone marrow (Figure 2.1D, day 4), the mice were treated with ABT-199 (100 mg/kg) by daily oral gavage for 2

Figure 2.1

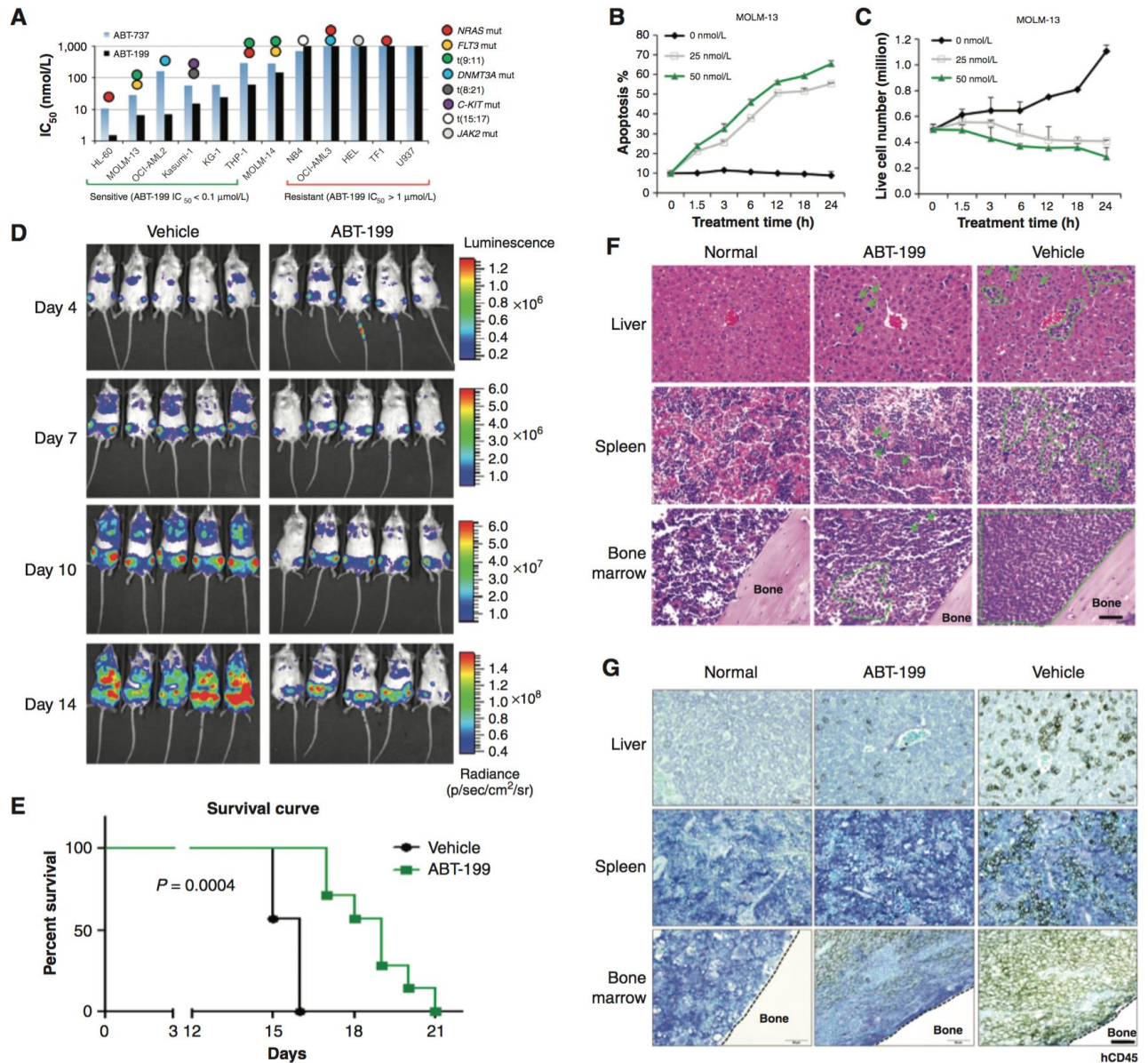


Figure 2.1 Selective inhibition of BCL-2 by ABT-199 kills AML cell lines quickly and effectively.

(A) AML cell lines were treated with ABT-199 or ABT-737 for 48 h. CalcuSyn software was used to calculate the IC_{50} values based on the number of viable cells (i.e., Annexin V/PI). (B) MOLM-13 AML cells were treated with indicated concentrations of ABT-199. Apoptosis induction was determined by Annexin V/PI flow cytometry. (C) Viable (i.e., Annexin V/PI-) cell counts were quantified by FACS analysis using CountBright counting beads. (D) Serial bioluminescence images of mice bearing MOLM-13 tumors treated with the vehicle or ABT-199 (treatment started on day 4). (E) Kaplan-Meier survival curves for mice treated as described in E ($n = 7$ per arm). (F) H&E staining of histological sections of liver, spleen, and bone marrow 15 d post leukemia cell injection. Age- and sex-matched mice without tumor were used as controls. Representative MOLM-13 cells are indicated by arrows. Representative engraftment areas are circled in green. (G). Immunohistochemical staining of histological sections of liver, spleen, and bone marrow with human CD45 antibody 15 d post leukemia cell injection. Scale bar equals 50 μm .

weeks. Serial BLI images showed that ABT-199 treatment markedly inhibited leukemia progression, which translated into prolonged overall survival when compared to vehicle-treated mice ($P = 0.0004$, Figure 2.1E). ABT-199 treated mice also carried significantly lower leukemia burden in bone marrow, spleen and liver as indicated by hematoxylin and eosin staining (H&E, Figure 2.1F) and immunohistochemical analysis of human CD45 (Figure 2.1G).

2.3.2 ABT-199 Sensitivity Correlates with BCL-2 Protein Levels

Next we tested whether there were correlations between BCL-2 protein expression levels and cell line sensitivity to ABT-199, which supported an on-target action of killing via competition for the BH3 binding site of BCL-2. Relative levels of several BCL-2 family proteins were measured by Western blot and densitometry (Figure 2.2A). Spearman analysis was performed to evaluate the correlation between IC₅₀ values and protein expression. Levels of BCL-2 correlated with sensitivity to ABT-199, while levels of BCL-XL inversely correlated with ABT-199 sensitivity (Figure 2.2B). Levels of MCL-1 demonstrated a trend to anti-correlation with sensitivity to ABT-199, but the trend was not statistically significant (Figure 2.2B). These observations supported the on-target effects of ABT-199.

The OCI-AML3 cell line was relatively resistant to ABT-199 and ABT-737 (Figure 2.1A). A quantitative immunoblot showed that OCI-AML3 cells had high expression of BCL-2 and MCL-1 and relatively low level of BCL-XL (Figure 2.2A). If ABT-199 is a BH3 mimetic specific for BCL-2, then MCL-1 knockdown should significantly sensitize OCI-AML3 cells to this compound. To test this, MCL-1 protein level was reduced by 85% in OCI-AML3 cells by lentiviral transduction using a previously validated *MCL1*-specific shRNA (Figure 2.2C). Indeed, MCL-1 knockdown greatly increased sensitivity

Figure 2.2

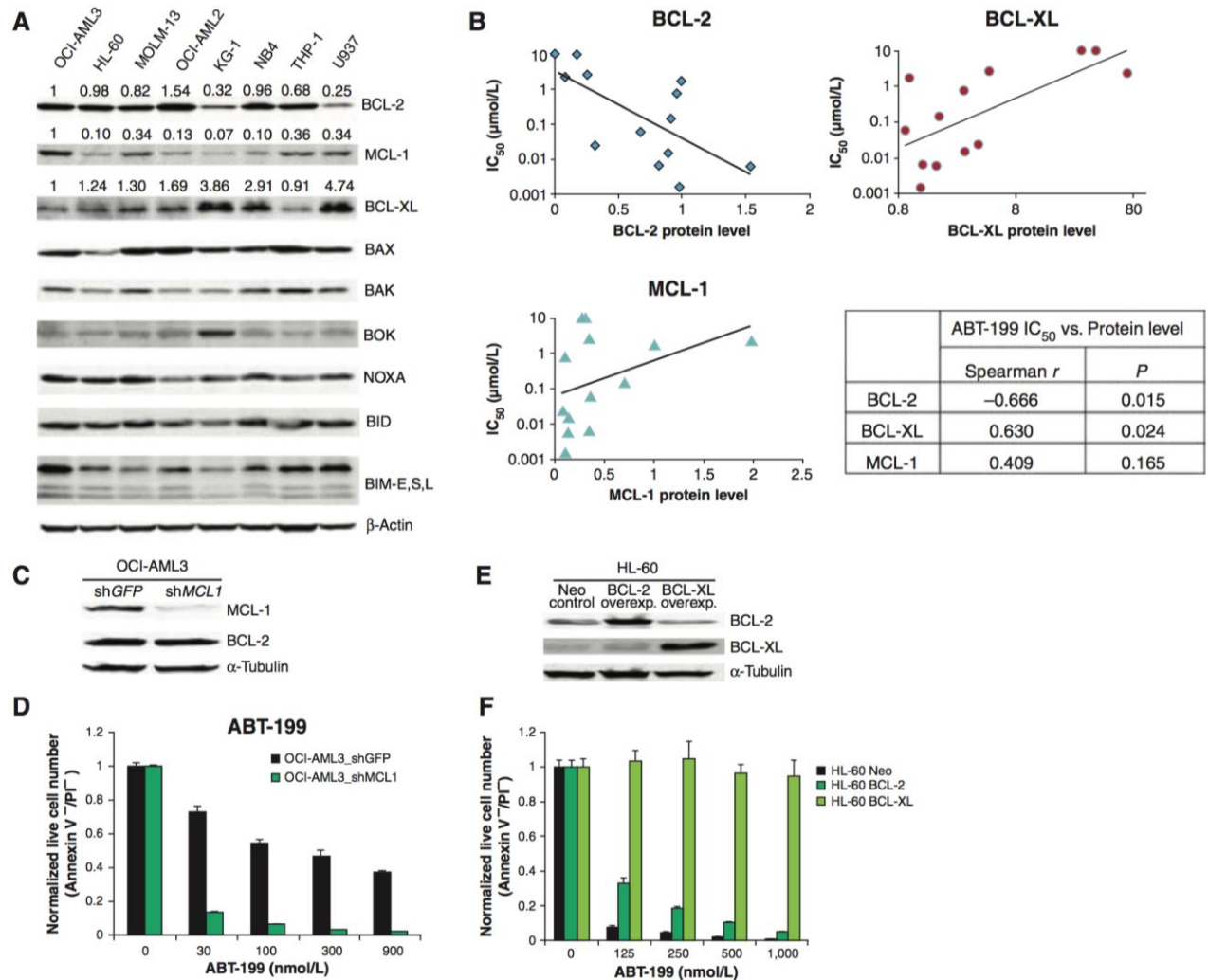


Figure 2.2 Sensitivity to ABT-199 positively correlates with endogenous BCL-2 protein level and negatively correlates with BCL-XL protein level in AML cell lines.

(A) Western blot analysis of BCL-2 family proteins in untreated AML cells. The band intensity was quantified using Odyssey v2.0 software, and displayed numerically as a ratio of the band intensity detected in the OCI-AML3 cells. (B) Significant correlations were observed between ABT-199 IC₅₀ values and BCL-2/BCL-XL protein levels. The non-parametric one-tailed Spearman test was used to determine the correlation coefficient. The p values provided are nominal p values not corrected for multiple comparisons. (C) MCL-1 knockdown by 85% was achieved by lentiviral shRNA. (D) MCL-1 knockdown significantly sensitized OCI-AML3 cells to ABT-199. (E) Western blot analysis showing HL-60 AML cells transfected to stably overexpress BCL-XL or BCL-2. (F) Overexpression of BCL-XL or BCL-2 in HL-60 cells confers complete resistance to ABT-199-induced apoptosis.

to ABT-199 (Figure 2.2D). HL-60 cells with high levels of BCL-2 protein and relatively low BCL-XL and MCL-1 expression are very sensitive to ABT-199 (Figure 2.1A). BCL-XL overexpression conferred strong resistance to ABT-199 in HL-60 cells, while BCL-2 overexpression made HL-60 cells moderately resistant to ABT-199 (Figures 2.2E-F). All these results are consistent with a killing mechanism operating via selective targeting of BCL-2 in AML cells.

2.3.3 ABT-199 Operates Selectively on BCL-2 Dependent Mitochondria

If ABT-199 is killing cancer cells via displacement of pro-apoptotic proteins from BCL-2, it should be operating on mitochondria. As one would expect if this were the case, we observed a correlation between direct mitochondrial toxicity and cellular toxicity for ABT-199 and ABT-737 in the 12 cell lines studied in Figure 2.1A (Figures 2.3A-B). We also tested whether detection of BCL-2 dependence using mitochondrial exposure to the BAD BH3 peptide correlated with cellular sensitivity to these agents. We found that while there was a good correlation between mitochondrial sensitivity to the BAD peptide and drug sensitivity for the most sensitive cell lines, there was a group of relatively drug-resistant cell lines that still demonstrated mitochondrial sensitivity to the BAD BH3 peptide (Figures 2.3C-D). A clue to the reason for this was revealed by the tendency of these cell lines to have mitochondria that were also quite sensitive to the HRK peptide, an indicator of BCL-XL dependence. To ensure that we were studying BCL-2 dependence specifically, especially in these less drug-sensitive cells, we made a correction, by subtracting the HRK signal from the BAD signal. In Figures 2.3E-F, we used this modified metric to observe a good correlation between mitochondrial BCL-2 dependence and cellular sensitivity.

Figure 2.3

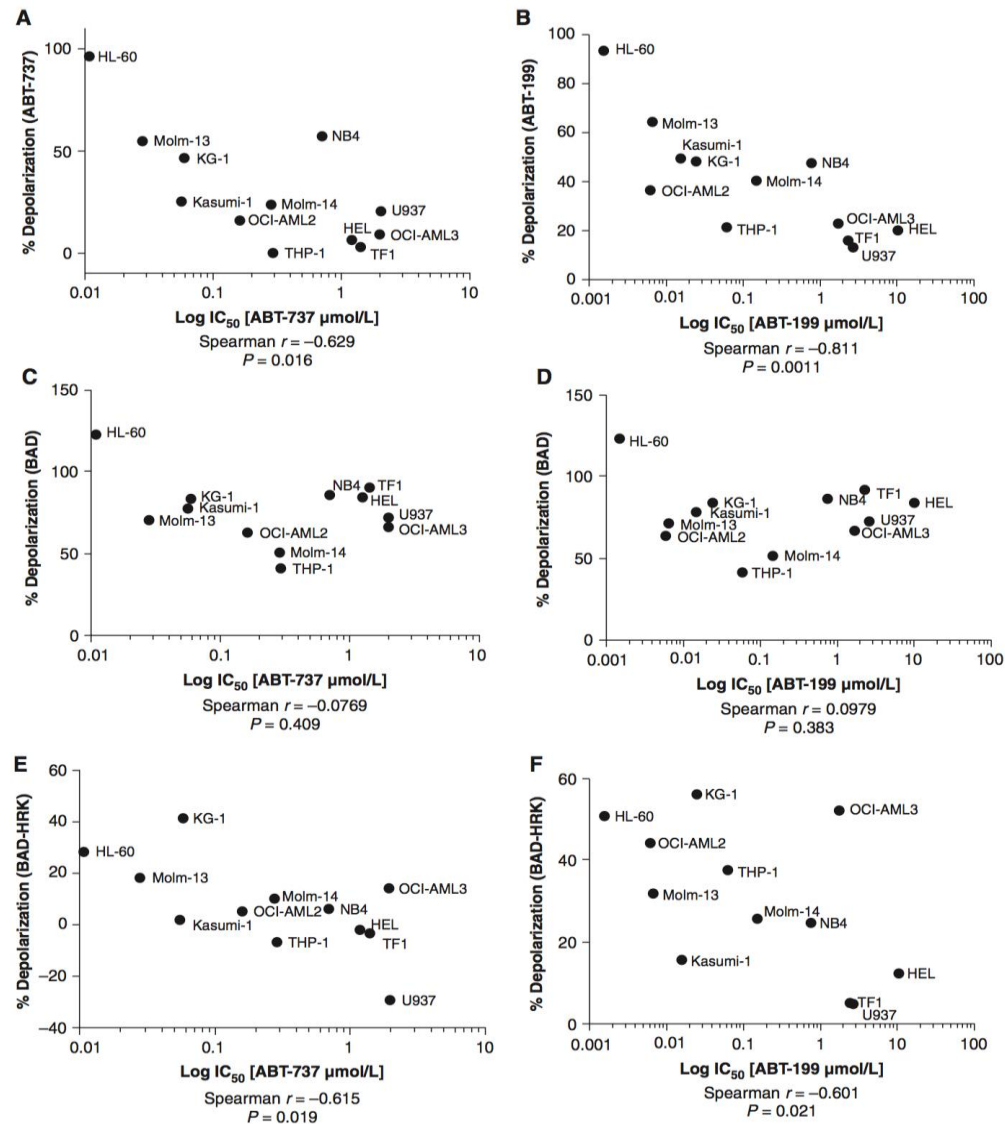


Figure 2.3 ABT-199 functions selectively on BCL-2 dependent mitochondria in AML cell lines.

(A) The IC₅₀ values of AML cell lines treated with ABT-737 from Figure 2.1A were correlated with the mitochondrial response of ABT-737 (1 μ M). Mitochondrial response was measured by JC1 based BH3 profiling. (B) IC₅₀ values of cell lines treated with ABT-199 from Figure 2.1A were correlated with the mitochondrial response of mitochondrial ABT-199 (0.1 μ M) (C). IC₅₀ values of AML cells treated with ABT-737 were correlated with the response to the BAD BH3 (80 μ M). The mitochondrial responses to the BAD BH3 peptide were measured by JC1 based BH3 profiling. (D). IC₅₀ values of AML cell treated with ABT-199 from Figure 2.1A were correlated with the mitochondrial response of the BAD BH3 (80 μ M) peptide. (E). IC₅₀ values of AML cells treated with ABT-737 were correlated with the response to the BAD BH3 (80 μ M) – HRK BH3 (80 μ M). The mitochondrial responses to the BAD and HRK BH3 peptides were measured by JC1 based BH3 profiling. (F). IC₅₀ values of AML cells treated with ABT-199 from Figure 2.1A were correlated with the mitochondrial response of the BAD BH3 (80 μ M) – HRK BH3 (80 μ M) peptide. Statistical correlation was performed using a one-tailed Spearman r using GraphPad Prism 6.

2.3.4 ABT-199 Efficiently Kills Primary AML Myeloblasts

We observed ABT-199 selectively kills BCL-2 dependent cell lines. Therefore, we next wanted to test the sensitivity of primary patient AML samples to ABT-199. Clinical and genetic data for both sets of AML samples is available in Table 2.1. AML myeloblasts from patient bone marrow or peripheral blood were exposed to ABT-199 for 48 h in minimum essential medium alpha supplemented with cytokines. It is notable that the primary cells were quite sensitive, with median IC₅₀ values less than 10 nM (Figure 2.4A). Note that this is significantly lower than the IC₅₀ observed in the AML cell lines (Figure 2.1A). Note also that this is comparable to the sensitivity observed for *ex vivo* exposure of CLL cells, a disease in which ABT-199 has shown clinical activity in most patients treated.

Because prolonged *ex vivo* culture by itself can promote sensitivity to apoptosis of AML myeloblasts, we wanted to test whether we would see sensitivity at shorter time points as well. Therefore, we tested sensitivity of AML myeloblasts to ABT-199 at 8 h (Figure 2.4B). Again, AML myeloblasts proved to be sensitive to ABT-199 with a median IC₅₀ of 20 nm. Indeed, when we reduced exposure times further, to 2 hours, we could still see induction of apoptosis by ABT-199 in AML myeloblasts (Figure 2.4C). Similarly rapid induction of cell death has been observed for the clinically sensitive CLL, consistent with a direct action of ABT-199 on AML myeloblast mitochondria, promoting apoptosis in the absence of a requirement for additional cell signaling extrinsic to the mitochondria.

Table 2.1 Clinical characteristics of AML patients

UPIN	DX	Source	Blast (%)	Status	Cyto-genetics	Molecular Mutations					ABT-199 IC50 (nM)	ABT-737 IC50 (nM)	ABT-263 IC50 (nM)
						NPM1	FLT3	NRAS	JAK	Others			
3841772	AML	PB	57	Relapsed Refractory, post-2 SCT	Complex	-	-	-	-	-	356.2	63.3	-
4031144	AML	PB	98	Primary Refractory	-3, +8	-	-	+(G12D)	-	-	0.8	2.5	-
3891338	AML	PB	71	Primary Refractory	inv(3)	-	-	+(G13R)	-	-	0.6	1.2	-
4081468	AML	PB	86	Pre-treatment	Complex incl -5, -7	U	-	U	U	U	7.5	9.2	-
4081654	AML	BM	69	Relapsed Refractory	del(3q)	+	-	-	-	K-RAS, GATA2, RUNX1	0.5	1.8	-
		PB	99							1.9	7.4	-	
4030094	AML	PB	98	Primary Refractory	t(9;11) and other	-	-	-	-	CEBPA	84.8	179.3	-
2422940	AML	BM	80	Refractory	inv(3)	-	-	-	-	-	0.6	1.7	-
4031936	AML	PB	99	Relapsed Refractory	inv(3)	-	+	-	-	IDH1	0.5	3.1	-
3913992	AML	PB	82	Primary Refractory	-	-	-	-	-	-	6530.3	238.5	-
3831282	AML	PB	78	Primary Refractory	-	-	-	-	-	-	0.9	3.5	-
3788196	AML	PB	85	Primary Refractory	-	-	-	-	-	-	1.1	4.2	-
3873322	AML	PB	98	Primary Refractory Post-SCT	-	-	+	-	-	-	1.2	2.1	-
3686032	AML	PB	52	New AML from CMML	-	-	-	+	-	-	1.6	4.6	-
3846024	AML	BM	99	Relapsed Refractory	-	-	-	-	-	-	0.9	5.8	-
4015568	AML	PB	87	New therapy-related AML	t(9;11)	-	-	+	-	-	1.4	14.8	-
3866160	AML	BM	77	Relapsed post-SCT	Diploid	+	-	-	-	DNMT3	1209.5	308.4	-
3798414	AML	PB	99	AML from MDS, refractory	del(12p)	-	-	+	-	-	1.7	3.4	-
3871344	AML	PB	69	Refractory AMML	Diploid	-	-	-	-	-	0.6	2.4	-
3898404	AML	PB	55	AML from MDS	del(5q), -7	-	-	+	-	-	4.3	16.2	-
3899418	AML	PB	81	Relapsed	Diploid	+	-	-	-	DNMT3	2.7	6	-
3899936	AML	PB	74	AML from MDS	N/A	-	-	-	-	-	> 5000	> 5000	-
3821772	AML	PB	93	Refractory, Relapsed post-SCT	Complex	-	-	-	-	CEBPA	3.9	21.8	-
5	AML	PB	5	Relapsed	trisomy 11	-	-	U	U	-	9.3	-	5.4
9	AML	PB	10	Relapsed AML from MDS	normal	-	+	U	U	-	21.2	-	4.1
10	AML	BM	83	Pre-treatment	normal	+	+	U	U	-	43.5	-	4.2
13	AML	BM	46	Relapsed Refractory	normal	+	+	U	U	-	20.7	-	28.1
15	AML	BM	16	AML from MDS	trisomy 8	-	-	U	U	-	139.3	-	347.5
16	AML	PB	35	relapsed AML	normal	+	+	U	U	-	19.9	-	5
19	AML	PB	75	Relapsed Refractory	Monosomy 7	U	-	U	U	-	88.7	-	11.7
30	AML	BM	35	Pre-treatment	MLL gene rearrangement	-	-	U	U	-	219.3	-	148.6
31	AML	BM	80	Pre-treatment	Complex	-	-	U	U	-	0.6	-	0.7
33	AML	BM	63	Pre-treatment	normal	+	-	U	U	-	52.1	-	212.3
34	AML	BM	80	Pre-treatment	normal	+	+	U	U	-	9.4	-	8.5
35	AML	PB	48	Relapsed, Refractory	normal	+	-	U	U	-	0.4	-	0.4
1002	AML	BM	51	Pre-treatment	t(16;16)	U	U	U	U	-	13	-	20.8
1003	AML	BM	44	Pre-treatment	normal	-	-	U	U	-	2.3	-	2.7
1005	AML	BM	69	Pre-treatment	inversion 16	-	+	U	U	-	1.3	-	2.8
1001	AML	BM	88	Pre-treatment	normal	U	+	U	U	-	168.3	-	11.1
1004	AML	BM	78	Pre-treatment	46,XX,inv(16)(p13q22)[20]	U	U	U	U	-	192.8	-	555.9
37	AML	BM	79	AML from MDS	normal	-	+	U	U	-	11.2	-	6.7
40	AML	BM	73	Relapsed Refractory	complex	-	-	U	U	-	0.6	-	2.5
41	AML	BM	13	Pre-treatment	complex	-	+	U	U	-	124.2	-	123.6
44	AML	BM	69	Pre-treatment	normal	+	-	U	U	-	1.4	-	3.3
1006	AML	BM	U	Pre-treatment	unknown	U	U	U	U	-	132.4	-	108.9
1009	AML	BM	96	Pre-treatment	unknown	+	-	U	U	-	75.7	-	31.8
1010	AML	BM	93	Pre-treatment	normal	-	-	U	U	-	8.3	-	2.2
1011	AML	BM	94	Pre-treatment	normal	-	+	U	U	-	28.1	-	2.3
1013	AML	BM	88	Pre-treatment	normal	U	+	U	U	-	2.3	-	3.1
1015	AML	BM	65	Pre-treatment	46,XY[20].nuc ish(PML,RARA)x2[100]	U	+	U	U	-	16.3	-	24
1017	AML	BM	61	Pre-treatment	inv(16)(p13q22)[20]	U	U	U	U	-	10.3	-	8.3
571	AML	BM	94	Pre-treatment	No info	U	U	U	U	-	43.8	-	9.3
958	AML	BM	95	Pre-treatment	No info	U	U	U	U	-	27.1	-	3
1044	AML	BM	93	Pre-treatment	No info	U	U	U	U	-	43.1	-	10.4
2924	AML	BM	91	Pre-treatment	No info	U	U	U	U	-	10.8	-	1.1
1012	AML	BM	53	Pre-treatment	normal	+	-	U	U	-	321.4	-	2009.1
1019	AML	BM	45	Pre-treatment	normal	-	-	U	U	-	9.1	-	6.6
1014	AML	BM	65	Pre-treatment	normal	+	+	U	U	-	95.3	-	28.6

Abbreviations: BM, bone marrow; PB, peripheral blood; “+”, Positive; “-”, None detected; U, unknown.

Figure 2.4

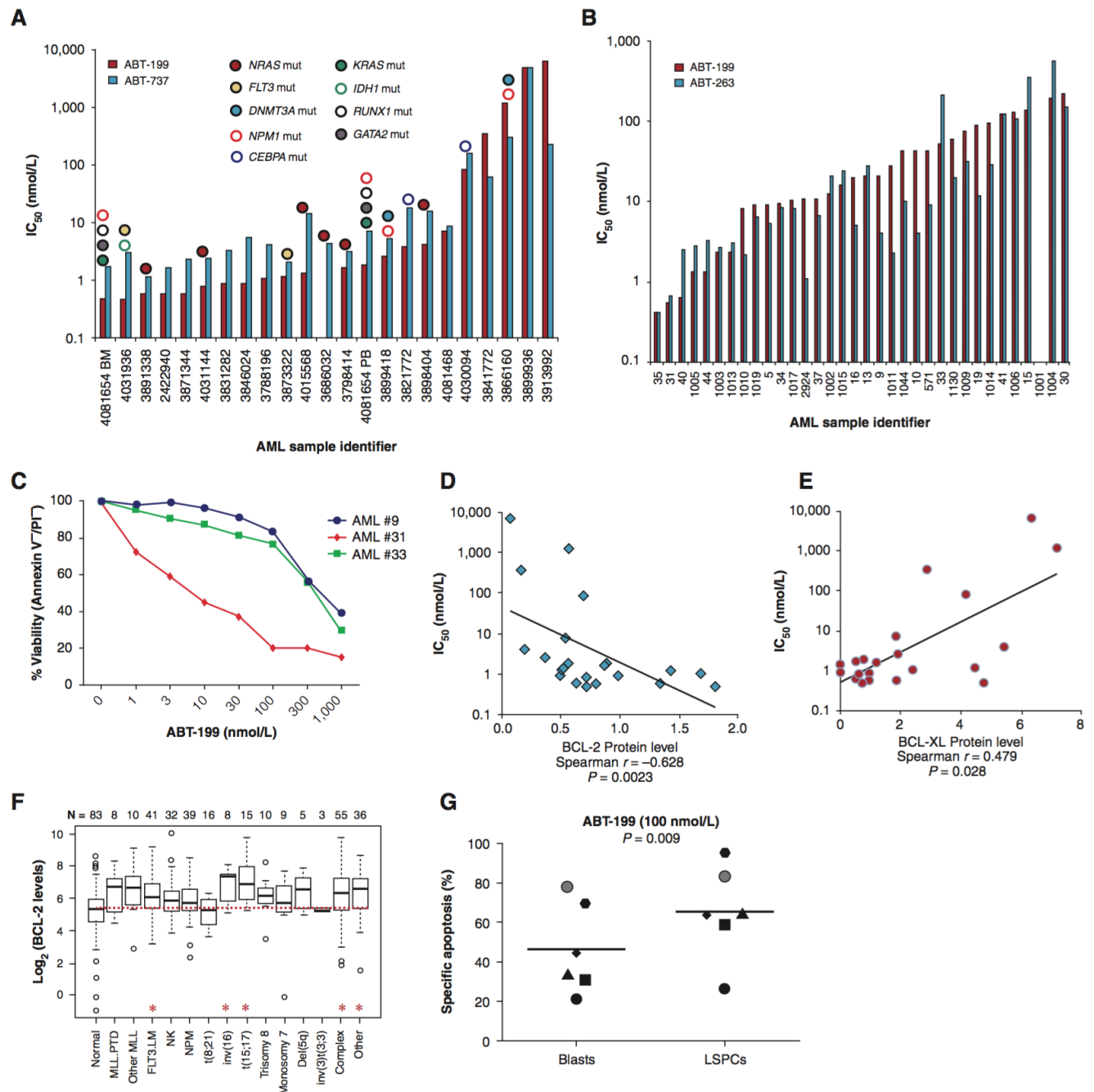


Figure 2.4 ABT-199 efficiently kills primary AML myeloblasts as a single agent.

(A) IC₅₀ determination for ABT-199 and ABT-737 treatment of primary AML samples. Fresh mononuclear cells from AML patients were isolated from bone marrow or peripheral blood and treated for 48 h. The IC₅₀ values were calculated based on viable (i.e., Annexin V/PI) cell numbers determined by FACS analysis. Samples with ABT-199 IC₅₀ < 0.1 μ M were defined as “sensitive”, while those with ABT-199 IC₅₀ > 1 μ M were defined as “resistant”. (B) Frozen primary AML myeloblasts were thawed treated with ABT-199 and ABT-263 for 8 h in the absence of fetal bovine serum. Viability was assessed by Annexin/PI- via FACS analysis and

Figure 2.4 Legend (continued)

IC50 values were calculated using GraphPad Prism software. **(C)** Thawed primary AML samples were treated for 2 h with 1-1000 nM of ABT-199 and viability was assessed by Annexin V-PI- by FACS analysis **(D)** Nonparametric Spearman correlation analysis shows a significant ($p = 0.017$) negative correlation between ABT-199 IC50 values and BCL-2 protein levels. **(E)** A non-significant ($p = 0.069$) positive correlation was observed between ABT-199 IC50 values and BCL-XL protein levels. **(F)** Boxplots represent the quartiles and range of log2 values of mRNA expression for BCL-2 genes in different subgroups of AML and normal bone marrows. The median is indicated by the black line in each box. Numbers on top indicate number of patients in each specified subgroup. Differences in gene expression with P values ≤ 0.005 were considered statistically significant, as denoted by *. **(G)** Patient AML samples treated with 100 nM ABT-199 for 24 hours were subjected to FACS analysis of specific apoptosis based on Annexin V staining in the bulk AML myeloblast and CD34+/CD38-/CD123+ LSC-containing population.

Upon testing of additional cryopreserved AML patient samples, including AML cells with diploid cytogenetics and mutations in *FLT3*, *NRAS*, and *NPM1* genes, 20 out of 25 (80%) were sensitive to ABT-199 (100 nM). However, samples from patients with complex cytogenetics and *JAK2* mutation ($n = 9$) were largely insensitive to ABT-199 (1 of the 9, or 11.1% response rate, $P = 0.0005$ by two-tailed Fisher exact test). Further we found no correlation between ABT-199 sensitivity and FAB classification or *NPM1* or *FLT3* mutational status. There was no difference in ABT-199 sensitivity between samples sensitive or resistant to conventional induction chemotherapy (Figure 2.5), consistent with prior findings with ABT-737⁶². We next tested whether sensitivity to ABT-199 correlated with protein expression for primary AML myeloblasts. As we found with AML cell lines, sensitivity to ABT-199 correlated directly with BCL-2 expression and inversely with BCL-XL expression as measured by quantitative Western blot (Figure 2.4D-E). AML myeloblasts also demonstrate higher BCL-2 mRNA expression than normal bone marrow samples (Figure 2.4F).

2.3.5 ABT-199 Induces Apoptosis in AML Stem/Progenitor Cells (LSPCs)

We next tested whether ABT-199 is capable of inducing cell death not only in AML blasts, but also in the phenotypically defined AML stem/progenitor cells characterized by $CD34^+CD38^-CD123^+$ immunophenotype⁷¹. Samples from six ABT-199-sensitive AML patients with high blast counts were incubated with ABT-199 for 24 h, and apoptosis induction was determined by Annexin V flow cytometry in electronically gated AML blasts ($CD45^{\text{dim}}SSC^{\text{low}}$) and AML stem/progenitor cells ($CD45^{\text{dim}}SSC^{\text{low}}CD34^+CD38^-CD123^+$). ABT-199 induced apoptotic cell death in both bulk AML blasts and AML stem/progenitor cells (Figure 2.4G). It appeared that AML

Figure 2.5

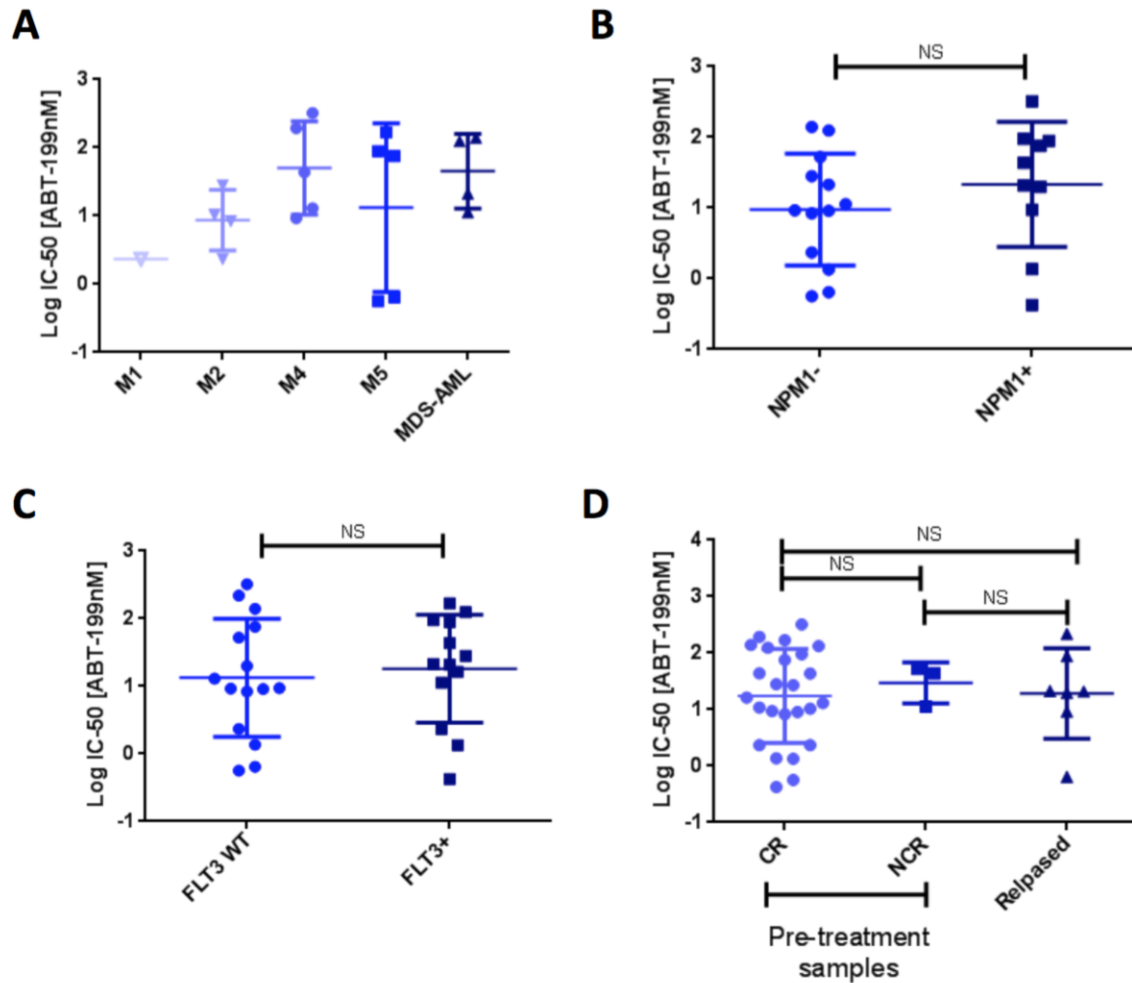


Figure 2.5 Clinical characteristics of AML patients do not correlate with ABT-199 sensitivity.

(A) Patients from Figure 4B were classified by their FAB status (French-American-British classification). There was no significant difference between the IC₅₀ values between various cohorts (note, M1 was not included in the analysis because there were not enough samples to perform the analysis). (B) Patient samples used in Figure 4B were stratified by their nucleophosmin 1 status (an *NPM1* mutation is a good prognostic factor). There was no difference in IC₅₀ values between patients who had an *NPM1* mutation and those who were WT. (C) Patient samples used in Figure 4B were stratified by their *FLT3* status (an *FLT3* mutation is a poor prognostic factor). There was no difference in IC₅₀ values between patients who had an *FLT3* mutation and those who were WT. (D) Patient samples used in Figure 4B were stratified into newly diagnosed patients who achieved a complete response (CR), newly diagnosed patients who did not achieve a CR and relapsed patients. There is no difference in ABT-199 IC₅₀ values between the three groups. A Mann-Whitney t test was used for these comparisons.

stem/progenitor cells are more sensitive to ABT-199 ($P = 0.009$), consistent with previous report that leukemia stem cells overexpress BCL-2 and are dependent on BCL-2 for energy homeostasis and survival⁷².

2.3.6 BH3 Profiling Predicts AML Myeloblast Killing by ABT-199

We next tested whether killing of primary AML myeloblasts by ABT-199 acted as a true BH3 mimetic in an on-target fashion on BCL-2 dependent mitochondria. If this were the case, we would expect that mitochondria sensitive to the BAD BH3 peptide should also be sensitive to the ABT-199. Indeed, we found an extremely tight correlation between mitochondrial sensitivity to BAD BH3 and ABT-199 across 30 independent patient samples (Figure 2.6A). No such correlation was observed for the comparison of the BCL-XL selective peptide HRK BH3 and the IC₅₀ of ABT-199, supporting BCL-2 selective action of ABT-199 (Figure 2.6B). We observed a weak anti-correlation between cellular sensitivity to ABT-199 and sensitivity to the MCL-1 selective peptide NOXA BH3 (Figure 2.6C). This suggests that there is a minor tendency for MCL-1 dependent mitochondria to be less sensitive to ABT-199.

In other diseases, BH3 profiling has proven a useful tool for predicting the cytotoxic effect of BH3 mimetic small molecules^{73,74}. Here we tested whether BH3 profiling using the BAD BH3 peptide predicted cytotoxicity from ABT-199, and found that the correlation was very good (Figure 2.6D). In addition, the mitochondrial effect of ABT-199 correlated well with the cytotoxic effect (Figure 2.6E), again supporting a direct mitochondrial effect of ABT-199, consistent with a mechanism of action of direct competition for the BH3 binding site of BCL-2 on mitochondria.

Figure 2.6

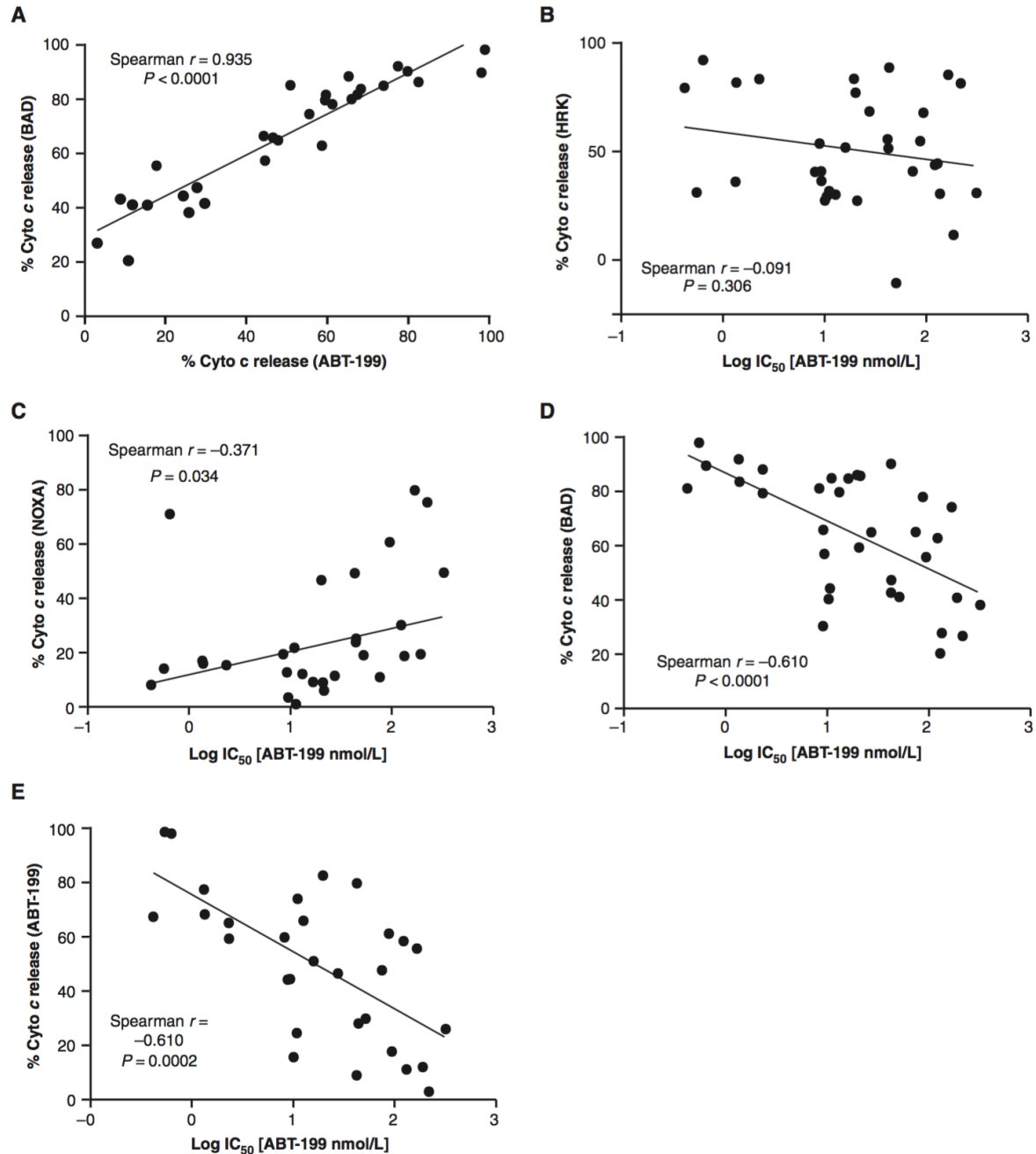


Figure 2.6 BH3 profiling predicts AML myeloblast killing by ABT-199

(A) Intracellular BH3 (iBH3) profiling was performed on thawed primary AML cells using the BAD BH3 (80 μ M) and ABT-199 (1 μ M). The mitochondrial sensitivity to BAD BH3 and ABT-199 were positively correlated. (B) There is no correlation between the IC_{50} of primary AML samples from Figure 2.4B with the BCL-XL specific BH3 peptide HRK (80 μ M). (C) The IC_{50} of primary AML samples from Figure 2.4B were correlated with the NOXA (80 μ M), a MCL-1 specific NOXA BH3 peptide. (D) The ABT-199 IC_{50} of primary AML samples from Figure 2.4B were correlated with the BAD BH3 peptide (80 μ M). (E) The ABT-199 IC_{50} from Figure 2.4B was correlated with the ABT-199 mitochondrial response (1 μ M). All correlations were tested using a one-tailed Spearman r correlation using GraphPad Prism software.

2.3.7 BH3 Profiling Predicts Response to ABT-199 in AML Xenograft Models

Tumor xenograft models established by inoculation of cancer cell lines into immunodeficient mice have been used widely for testing novel therapies. However, cultured tumor cells can undergo changes in their gene expression patterns after prolonged passage *in vitro*. Therefore, the preclinical results obtained from patient-tumor derived xenograft (PDX) models may offer superior modeling of the human disease, especially for testing target-oriented therapies. We have shown that ABT-199 was very effective in a murine AML cell line xenograft model (Figure 2.1E). As a more clinically relevant test of ABT-199's anti-leukemic efficacy *in vivo*, NSG mice were injected with primary AML cells from two different patients (R and S) and monitored for leukemia engraftment by measurements of human CD45⁺ cells in peripheral blood. After confirmation of AML engraftment, the mice were randomly divided into vehicle and treatment groups. Treated mice received ABT-199 for 2 weeks, after which all the mice were sacrificed, and bone marrows were examined for AML tumor burden by human CD45 flow cytometry. FACS analysis showed that ABT-199 treatment significantly reduced leukemia burden in murine bone marrows in mice injected with cells from patient S (mean, 70 ± 16% human CD45⁺ cells in bone marrow of control mice and 32.7 ± 12% in ABT-199 treated mice, $P = 0.0004$, Figure 2.7A). We did not observe a decrease in tumor burden in mice injected with cells from patient R (mean 70.3 ± 8.1% human CD45⁺ cells in bone marrow of control mice and 74.3 ± 6.4% in ABT-199 treated mice, $P = 0.1930$, Figure 2.7B).

Since we observed a difference in response in the xenograft model following ABT-199 treatment, we asked whether the response to ABT-199 could be predicted by BH3

Figure 2.7

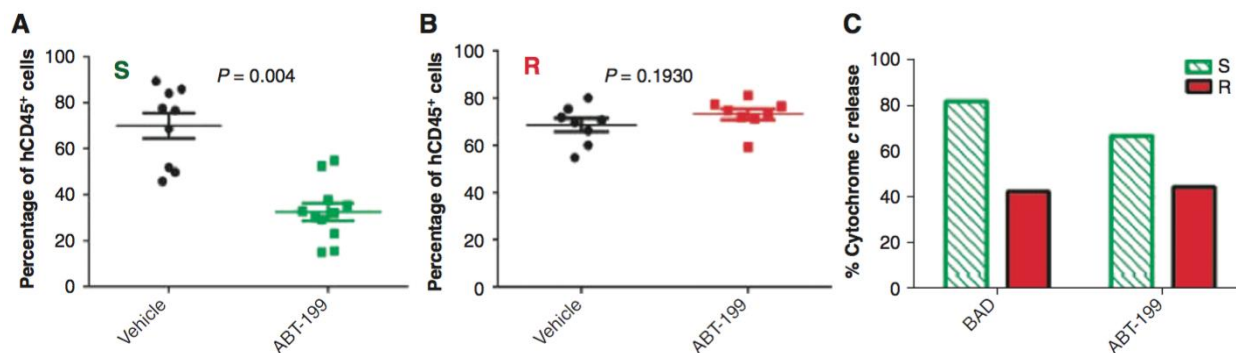


Figure 2.7 BH3 profiling predicts AML progression in a primary AML xenograft model

(A-B) NSG mice were injected with primary AML cells as described under Methods. Mice were treated with ABT-199 100 mg/kg oral daily dose starting 3 weeks after AML cell injection, for two weeks. The graph represents % of human CD45⁺ leukemic cells in the murine bone marrow in mice sacrificed upon completion of the therapy. A non-parametric, unpaired, two-tailed *t*-test was used to evaluate the significance of mean difference. (C) Intracellular BH3 profiling using the BAD BH3 (80 μ M) and ABT-199 (10 μ M) was performed on pre-treatment patient samples.

profiling. In a blinded fashion, pre-treatment AML myeloblasts from each model were subjected to BH3 profiling in which mitochondria were exposed to the BAD BH3 peptide as well as ABT-199 itself. We found that mitochondria from AML myeloblasts from patient S released more cytochrome c following incubation with the BAD peptide or ABT-199 compared to patient R (Figure 2.7C). These results provide evidence that ABT-199 kills AML myeloblasts by the expected mechanism of inhibition of mitochondrial BCL-2. Furthermore, these results suggest that BH3 profiling might predict the response of AML primary cells to ABT-199 *in vivo*.

**Chapter 3 p53 Activation and BCL-2 Inhibition Reciprocally
Overcome Apoptosis Resistance to Either Strategy Alone:
The Novel Mechanisms and Superior Antileukemic Efficacy**

3.1 Chapter Introduction

Evasion of apoptosis is integral to tumorigenesis and drug resistance^{7,17}. Upregulation of anti-apoptotic BCL-2 family members and inactivation of p53 functions are two canonical approaches exploited by cancer cells to escape apoptosis^{5,7,8,17}. Both approaches shift the balance of anti- and pro-apoptotic proteins toward survival and render cancer cells resistant to various therapies. Tremendous efforts to develop BCL-2 inhibitors culminated in ABT-199 (abbreviated here as ABT), a selective and potent BCL-2 inhibitor that showed promising efficacy in several cancers^{4,5,27}. The advent of ABT allows scientists to specifically study BCL-2 inhibition in cancers.

TP53, arguably the most important tumor suppressor gene, is mutated in ~50% of human solid tumors but rarely in hematological malignancies^{75,76}. However, wild-type p53 functions are frequently suppressed by MDM2, an E3 ubiquitin ligase that targets p53 for proteasomal degradation^{77,78}. Nutlins, the first-generation MDM2 inhibitors, represented a breakthrough in the development of p53-reactivating compounds⁴⁷. The recently developed RG7388 (RG) is a second-generation MDM2 inhibitor with greater potency, selectivity, and bioavailability compared to its predecessors Nutlin-3a and RG7112⁴⁸. In the current study, we first demonstrated that RG could robustly activate p53 and that RG-induced apoptosis was highly dependent on p53, indicating that RG can serve as an ideal compound to study p53 activation.

We have reported previously that targeting BCL-2 by ABT effectively induced apoptosis in AML cells. However expression of MCL-1, another critical anti-apoptotic protein, renders leukemia cells resistant to BCL-2 selective ABT or its predecessor ABT-737^{11,29,79}. In the current study, we initially hypothesized that p53 activation by RG could overcome resistance to BCL-2 inhibition by inducing pro-apoptotic proteins such

as Puma and Noxa to counteract MCL-1. To our surprise, p53 activation also negatively regulated N-Ras protein to downregulate the Ras/Raf/MEK/ERK pathway. This, in turn, activated GSK3 protein to promote MCL-1 phosphorylation and degradation, thus overcoming MCL-1-mediated resistance. Moreover, we found that leukemia cells that are resistant to BCL-2 inhibition can also be resistant to p53 activation. In fact, p53 activation induced high levels of p21^{WAF1/Cip1}, which then mediated reversible G1 arrest and protected cancer cells from apoptosis induction by p53. We developed a novel method to simultaneously analyze apoptosis and cell cycle distribution of viable cells and unambiguously illustrated that BCL-2 inhibition can switch the outcomes of p53 activation from pro-survival G1 arrest to apoptotic cell death, thus overcoming the apoptosis resistance to p53 activation. We demonstrated, both mechanistically and therapeutically, that BCL-2 inhibition and p53 activation could reciprocally overcome apoptosis resistance to either strategy alone *in vitro* and in three resistant mouse models of leukemia.

3.2 Materials and Methods

3.2.1 Cell Lines and Tissue Culture

Acute myeloid leukemia (AML) and other cell lines were purchased from the American Type Culture Collection (Manassas, VA, USA) or Deutsche Sammlung von Mikroorganismen und Zellkulturen (Braunschweig, Germany) and maintained according to the vendors' instructions. OCI-AML3, MOLM-13, MV-4-11, KG1, HL-60 and THP1 were validated by short tandem repeat DNA fingerprinting using the Amp-FISTR Identifier kit according to the manufacturer's instructions (Thermo Fisher Scientific, Waltham, MA). Cells were cultured at 37°C in a humidified atmosphere containing 5%

CO₂. Exponentially growing parental and generated cells were used for all *in vitro* and *in vivo* studies.

3.2.2 Generation of AML Cells with Acquired Resistance to ABT

Parental MOLM-13 and MV-4-11 cells were cultured in RPMI-1640 medium (10% fetal bovine serum [FBS]) supplemented with escalating doses of ABT (starting at IC₅₀ doses for each cell line). Every 2 days, the cells were pelleted by centrifugation (1000g, 5 min) and resuspended in fresh medium with ABT. Cell viability was monitored by Vi-CELL viability analyzer (Beckman Coulter). Once the viability reached $\geq 90\%$, the concentration of ABT was increased by one fold. The generated cells were at least 30 times more resistant than their parental cells (Figure 2.2A).

3.2.3 Concurrent Apoptosis and Cell Cycle Analysis

Exponentially growing cells were treated with vehicle, ABT, RG or ABT-RG combination for the indicated time. Then Edu (10 mM in phosphate-buffered saline solution [PBS]) was added to a final concentration of 10 μ M. After incubation under optimal growth conditions for 1 h, cells were washed with 3 mL ice-cold ABB buffer and pelleted by centrifugation at 4°C (1000g, 5 min). Supernatant was carefully removed by aspiration without disturbing the cell pellet. The cells were then placed on ice, mixed with 50 μ L ABB containing 5 μ L AnnV-Alexa488 (Life Technologies) and incubated in darkness for 15 min. After staining, cells were washed again with ice-cold ABB. The cells were fixed, permeabilized and then incubated with Click-iT Plus reaction cocktail (Life Technologies) according to the manufacturer's instructions. After the Click-iT reaction, cells were mixed well with 0.5 mL of FxCycle PI/RNase solution (Life Technologies) by gentle vortexing. Following 30 min of incubation in darkness at 37°C, CountBright™ Counting Beads were added and the samples were analyzed by flow

cytometry for apoptosis (AnnV⁺) and cell cycle distribution of AnnV⁻ live cells (Figure 2.5G for gating strategy).

3.2.4 Immunoblotting and Antibodies

Cells were subjected to lysis at a density of $1 \times 10^6/50 \mu\text{L}$ in protein lysis buffer (0.25 M Tris-HCl, 2% sodium dodecylsulfate, 4% β -mercaptoethanol, 10% glycerol, 0.02% bromophenol blue) supplemented with 1x protease/phosphatase inhibitor cocktail (#5872, Cell Signaling Technology, Beverly, MA, USA). Cell lysates were then loaded onto polyacrylamide gels with sodium dodecyl sulfate (Bio-Rad, Hercules, CA, USA). After electrophoresis, proteins were transferred to polyvinylidene difluoride membranes. The transblotted membranes were blocked for 1 h and then probed with appropriate primary antibodies (dilution as recommended by manufacturers) overnight at 4°C. Next, the membranes were washed three times for a total of 30 min and then incubated with secondary antibodies in darkness at room temperature for 1 h. After another three washes, Odyssey infrared imaging system and companion software (LI-COR Biosciences, Lincoln, NE, USA) were used to scan immunoblot membranes and to quantify band intensity according to the manufacturer's manual. The ratios of proteins of interest/loading control in treated samples were normalized to their counterparts in untreated cells. Antibodies for immunoblotting were purchased from the following sources: p53 (sc-126), MDM2 (sc-5304), BCL-2 (sc-7382), MCL-1 (sc-819), Puma (sc-28226), ERK (sc-1647), N-Ras (sc-31) and GSK3 (sc-7291) from Santa Cruz Biotechnology (Dallas, TX, USA); pERK (T202/Y204, 4370), pMEK (S217/S221, 9121), MEK (4694), AKT (2920), pAKT(S473, 9271), pGSK3 (S21/S9, 8566), PARP-1 (9542), Bim (2819), Bak (12105), caspase-3 (9664), caspase-9 (9508), pMCL-1 (T163, 14765), B-Raf (9433), pB-Raf (S445, 2696), JNK (9252) and pJNK (T183Y185, 9255) from Cell

Signaling Technology; Bax (B8554) and β -Actin (A2228) from Sigma-Aldrich; NOXA (ab13654) and pMCL-1 (T163S159, ab111574) from Abcam; p21 (OP64) from EMD Millipore (Darmstadt, Germany). IRDye 680 donkey anti-rabbit and IRDye 800 donkey anti-mouse secondary antibodies were purchased from Li-COR Biosciences.

3.2.5 Stable Overexpression of MCL-1

MCL-1 expression cassette was delivered into MV-4-11 and MOLM-13 cells by lentiviral transduction. Briefly, the open reading frame of human *MCL1* cDNA (IMAGE:3826638) was inserted between the NheI and BamHI sites of a commercially available lentiviral transfer vector pCDH-EF1-MCS-BGH-PGK-GFP-T2A-Puro (System Biosciences, Mountain View, CA, USA). After verification of the construction by Sanger sequencing, lentivirus was prepared and used to transfect AML cells as described above. In parallel, control cells were transduced with lentivirus delivering GFP coding sequence. Infected cells were selected with puromycin starting at 0.5 μ g/mL. Increased expression of MCL-1 was verified by immunoblot analysis.

3.2.6 Isolation and Treatment of Primary AML Cells

Primary samples from AML patients at The University of Texas MD Anderson Cancer Center were obtained with informed consent according to protocols approved by the Institutional Review Board. Mononuclear cells were isolated from peripheral blood or bone marrow samples by Ficoll density centrifugation. The primary cells were used immediately or resuspended in 90% FBS plus 10% DMSO and viably cryopreserved in liquid nitrogen for future use. The isolated cells were treated with different compounds or combinations in RPMI-1640 medium supplemented with 10% FBS (final concentration of DMSO vehicle < 0.1%). After 48 h, cell viability was determined by flow cytometry following concurrent AnnV and PI staining. Samples with

a spontaneous apoptosis rate > 30% were excluded from our analysis.

3.2.7 Animal Studies

All animal studies were performed in accordance with protocols approved by MD Anderson Cancer Center Institutional Animal Care and Use Committees. NOD SCID gamma (NSG) mice (6 wk old; Jackson Laboratory, Bar Harbor, ME, USA) were intravenously injected with AML cell lines or primary patient cells as indicated in schematic outlines for each mouse model (Figures 3.2D, 3.3G, and 3.6C). After confirmation of engraftment, the mice were randomly assigned to four groups (n = 10 per group) and treated with vehicle, ABT (100 mg/kg), RG (100 mg/kg) or the combination daily by oral gavage. ABT was prepared weekly in 10% ethanol, 30% polyethyleneglycol-400, and 60% phosal 50 propylene glycol (provided by AbbVie). RG was formulated daily in 4% DMA, 30% PEG400 and 66% Gelucire 44-14 (provided by Roche). Leukemic burden of luciferase-labeled OCI-AML3 or MOLM-13-R cells was monitored by bioluminescence imaging at multiple time points. Briefly, mice were anesthetized and injected intraperitoneally with firefly luciferase substrate D-luciferin (Gold Biotechnology, St. Louis, MO, USA) and then imaged by IVIS-200 *in vivo* imaging system (PerkinElmer, Waltham, MA, USA). After treatment for the indicated time, three mice were randomly selected from each group and euthanized by CO₂ asphyxiation. Left femur, spleen, and liver were harvested for IHC staining with human CD45 antibody. For the PDX mouse model of resistance, BM cells from the right femur were also collected and stained with human CD45-PE and murine CD45-APC antibodies (BD Biosciences) followed by flow cytometry analysis. The remaining seven mice in each group were monitored for survival.

3.2.8 Gene Knockdown by shRNA

p53, MCL-1 and p21 encoding genes (*TP53*, *MCL1*, and *CDKN1A*) were knocked down by lentivirus delivering well-validated shRNAs in pLKO.1 vector (Addgene, Cambridge, MA, USA). In parallel, control cells were transduced with lentivirus delivering a hairpin targeting GFP. Briefly, lentivirus was prepared by co-transfection of log-phase HEK293T cells with an equimolar mix of transfer vector psPAX2 and packaging plasmid pMD2.G (Addgene) using JetPrime transfection reagent according to the manufacturer's instructions (Polyplus, Illkirch, France). Lentiviral supernatants were harvested 48 h after transfection by centrifugation (800g, 10 min) at room temperature. The supernatant was then filtered through 0.45 μ M surfactant-free cellulose acetate membranes to remove lentivirus-producing cells. Polybrene (Chemicon, Temecula, CA, USA) was added to a final concentration of 8 μ g/mL, and the virus stock was used immediately to transfect AML cell lines. Exponentially growing cells were resuspended at a concentration of 0.5×10^6 cells per mL of virus stock, transferred to 12-well tissue plates, and centrifuged for 45 min (1300 g, 30°C). After adding one volume of fresh virus stock, the cells were centrifuged again and incubated in a tissue culture incubator (37°C, 5% CO₂) for 1 h. The cells were then washed twice with growth medium to remove the polybrene and returned to the tissue culture incubator. After two doubling times (42–44 h), infected cells were subjected to selection with 0.5 μ g/mL puromycin (Invitrogen, San Diego, CA, USA). Generated knockdown cells were assessed by immunoblot using MCL-1, p53 and p21 antibodies. Because of the low basal expression of p53 and p21 in OCI-AML3, MOLM-13 and MV-4-11 cells, the control and knockdown cells were treated with 1 μ M RG for 12 h prior to immunoblot analysis.

3.2.9 Immunohistochemical (IHC) Analysis

IHC analysis of human CD45 was performed as described in Methods section of Chapter 2. The monoclonal mouse anti-human CD45 antibody (M0701) was purchased from DAKO (Carpinteria, CA, USA). Images were acquired by an OLYMPUS BX43 microscope with DP72 digital color camera and companion software CellSens (Olympus, Upper Saucon Township, PA, USA).

3.2.10 Measurement of Apoptosis, Live Cell Number and IC₅₀ Values

As described in the Method section of Chapter 2.

3.2.11 Statistical Analysis

Statistical analyses were performed using Prism software v6.0 (GraphPad Software, La Jolla, CA, USA). The log-rank test was used to compare mouse survival curves. For *in vitro* studies, statistical significance was determined by the two-tailed unpaired Student's *t*-test. A *P* value < 0.05 was considered statistically significant. NS, not significant, **P* < 0.05, ***P* < 0.01, ****P* < 0.001, *****P* < 0.0001. Unless otherwise indicated, data represent the mean ± standard deviation from at least three independent experiments.

3.3 Results

3.3.1 RG Activates p53 and Induces Apoptosis in a p53-Dependent Manner

We first tested whether the MDM2 inhibitor RG depends on wild type p53 for its activity using Annexin V (AnnV) and propidium iodide (PI) co-staining followed by flow cytometry analysis (Figure 3.1A). In three p53 wild-type (p53^{wt}) AML cell lines (MV-4-11, OCI-AML3, and MOLM-13), RG induced a rapid accumulation of p53 as well as a time- and dose-dependent apoptosis induction and growth inhibition (Figures 3.1B-C,

S3.1A-B). In contrast, RG did not trigger apoptosis in p53^{null} HL-60 or p53^{mutant} KG1 and THP1 cells (Figure 3.1D). Furthermore, stable p53 knockdown substantially attenuated RG efficacy in three p53^{wt} cell lines (Figures 3.1E-F). These results demonstrate that RG can effectively activate p53 and induce apoptosis in a p53-dependent manner, indicating that RG can be used as a superior tool compound to study p53 activation.

MV-4-11 and MOLM-13 are sensitive to the BCL-2-specific inhibitor ABT (IC₅₀ values < 20 nM). Combining p53 activator RG with ABT at a 5:1 or 1:1 ratio augmented apoptosis and reduced live cell numbers to a significantly greater extent than either agent alone (Figures S3.1C-D). RG decreased ABT's IC₅₀ values from 11.6 to 2.2 nM for MV-4-11 and from 15.2 to 3.6 nM for MOLM-13. The combination index (CI) values also indicated a strong synergy between BCL-2 inhibitor ABT and p53 activator RG in ABT-sensitive cells (Figure S3.1E).

Figure 3.1

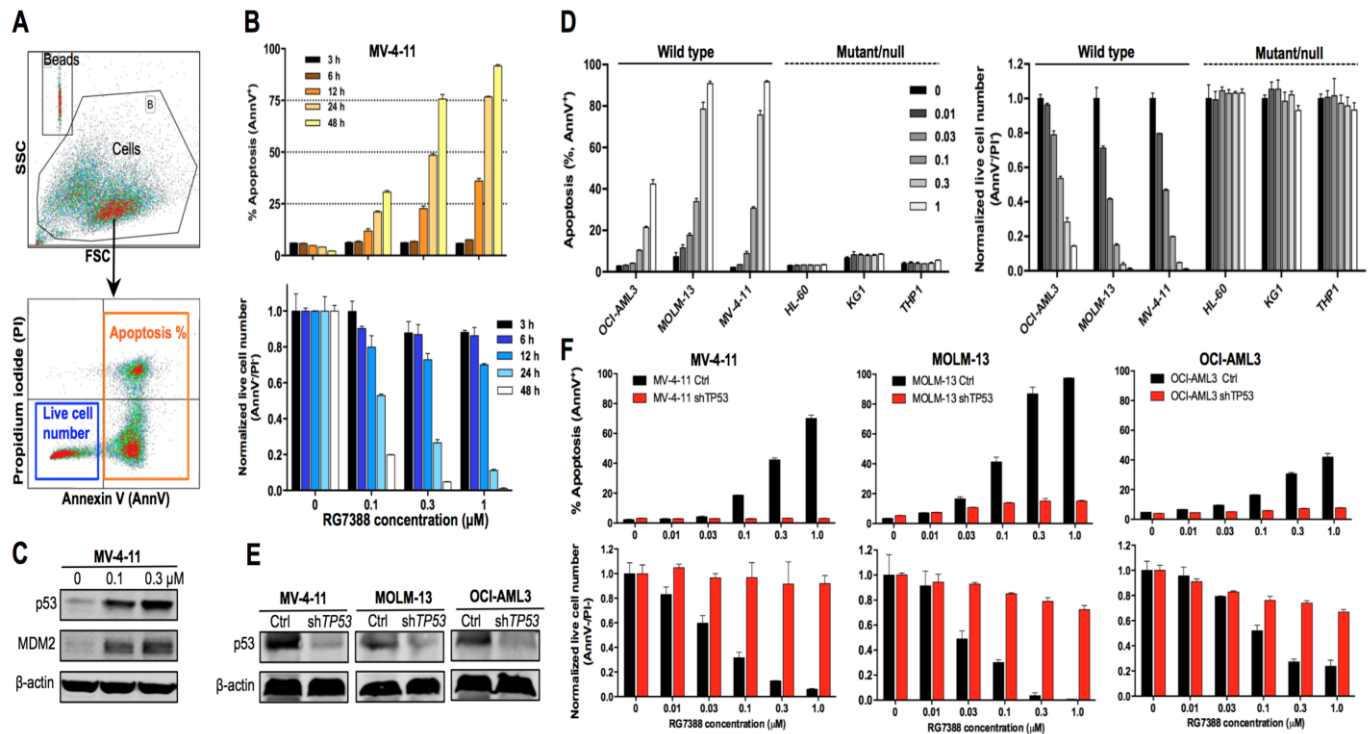


Figure 3.1 MDM2 inhibitor RG activates p53 and induces apoptosis in a p53-dependent manner.

(A) Flow cytometry plots showing gating strategy to determine apoptosis (AnnV⁺) and the numbers of live cells (AnnV⁻/PI⁻). (B) Time- and dose-dependent induction of apoptosis and reduction of live cell numbers by RG in MV-4-11 cells. (C) Immunoblot of MV-4-11 cells treated with RG for 8 h. β-actin served as loading control. (D) RG induced apoptosis and reduction of live cell numbers in p53^{wt} cells but not in p53^{null} HL-60 or p53^{mutant} KG1 and THP1 cells. (E) Immunoblot showing stable p53 knockdown by lentiviral shRNA in three AML cell lines (Because of low basal expression of p53, cells were treated with 1 μM RG for 12 h to increase p53 levels prior to immunoblot). (F) p53 knockdown reduced apoptosis induction and cell killing by RG.

AML cells were treated with indicated concentration of RG for 48 h (D, F). The cell numbers were enumerated by flow analysis using CountBright counting beads and normalized to untreated controls (B, D, F). All data in bar graphs represent the means of triplicate experiments. Error bars, mean ± SD.

Figure S3.1

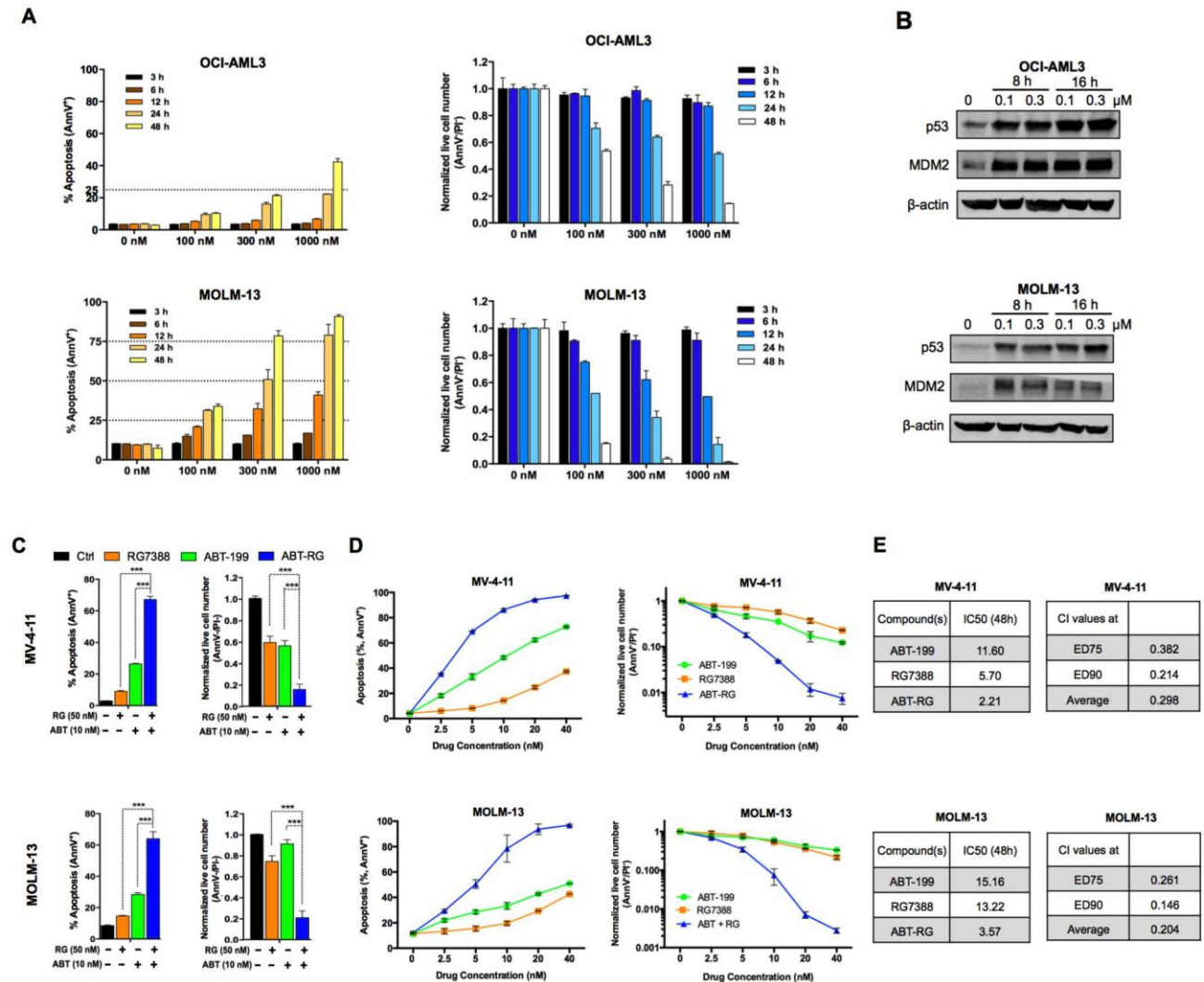


Figure S3.1 related to Figure 3.1.

(A) Time- and dose-dependent induction of apoptosis and reduction of live cell numbers by RG in OCI-AML3 and MOLM-13 cells. (B) Immunoblot of MV-4-11 and OCI-AML3 cells treated with RG for 8 or 16 h. β -actin served as loading control. (C-E) RG synergized with ABT at a 5:1(C) or 1:1 ratio (D) in ABT-sensitive MV-4-11 and MOLM-13 cells. The combination index (CI) and IC₅₀ values were calculated with Calcsyn software based on live cell numbers (E). AML cells were treated with indicated concentration of RG for 48 h (A, C, D). Data in bar/line graphs represent the means of triplicate experiments (A, C, D). Error bars, mean \pm SD. *** $P < 0.001$ as determined by two-tailed unpaired Student's t -test.

3.3.2 p53 Activation Overcomes Acquired Resistance to BCL-2 Inhibition

Although initially sensitive to BCL-2 inhibitor ABT, MOLM-13 and MV-4-11 cells acquired resistance after prolonged exposure to ABT. While BCL-2 inhibition readily induced apoptosis in parental cells, only marginal apoptosis occurred in resistant cells (MOLM-13-R and MV-4-11-R, Figure 3.2A). The ABT IC₅₀ increased by over 30- and 80-fold for MOLM-13-R and MV-4-11-R, respectively. Compared to their parental counterparts, the resistant cells expressed similar levels of BCL-2, but higher levels of MCL-1 (Figure 3.2B). Ectopic MCL-1 expression also conferred resistance to ABT in initially sensitive MOLM-13 and MV-4-11 cells (Figures S3.2A-D), indicating that the acquired resistance could be attributed, at least in part, to the elevated expression of MCL-1.

Next we examined if the acquired resistance to BCL-2 inhibition could be abrogated by p53 activation. BCL-2 inhibition by ABT triggered little apoptosis in the resistant MOLM-13-R/MV-4-11-R cells. However, the combination of p53 activator RG with ABT markedly induced apoptosis and decreased live cell numbers (Figures 3.2C and 3.2E), implying that the acquired resistance could be abrogated by p53 activation (Similarly, RG overcame ABT resistance in MOLM-13/MV-4-11 cells with ectopic MCL-1 expression; Figures S3.2E-F). To test this *in vivo*, we labeled the resistant MOLM-13-R cells with luciferase (Luci) and injected them into NOD SCID gamma (NSG) mice (Figure 3.2D). After confirmation of engraftment by bioluminescence imaging (BLI), the mice were randomly assigned to four groups (n = 10/group) and treated with vehicle, ABT, RG, or the combination. After 2-wk treatment, the leukemic burden in the combination group was ~1/200 of that in the ABT/control groups and ~1/19 of that in the RG group (Figures 3.2F and 3.2H). Meanwhile, the combination dramatically

reduced leukemic infiltration in spleen, liver, and bone marrow (BM, Figure 3.2G). MOLM-13-R cells rapidly killed control and ABT-treated mice at about the same time (Figure 3.2I). p53 activator RG prolonged survival by 6 d, while the combination significantly extended mouse survival by 20 d (a 3.3-fold prolongation relative to RG monotherapy, Figure 3.2I). These results indicate that p53 activation by RG could overcome acquired resistance to BCL-2 inhibition *in vivo*.

Figure 3.2

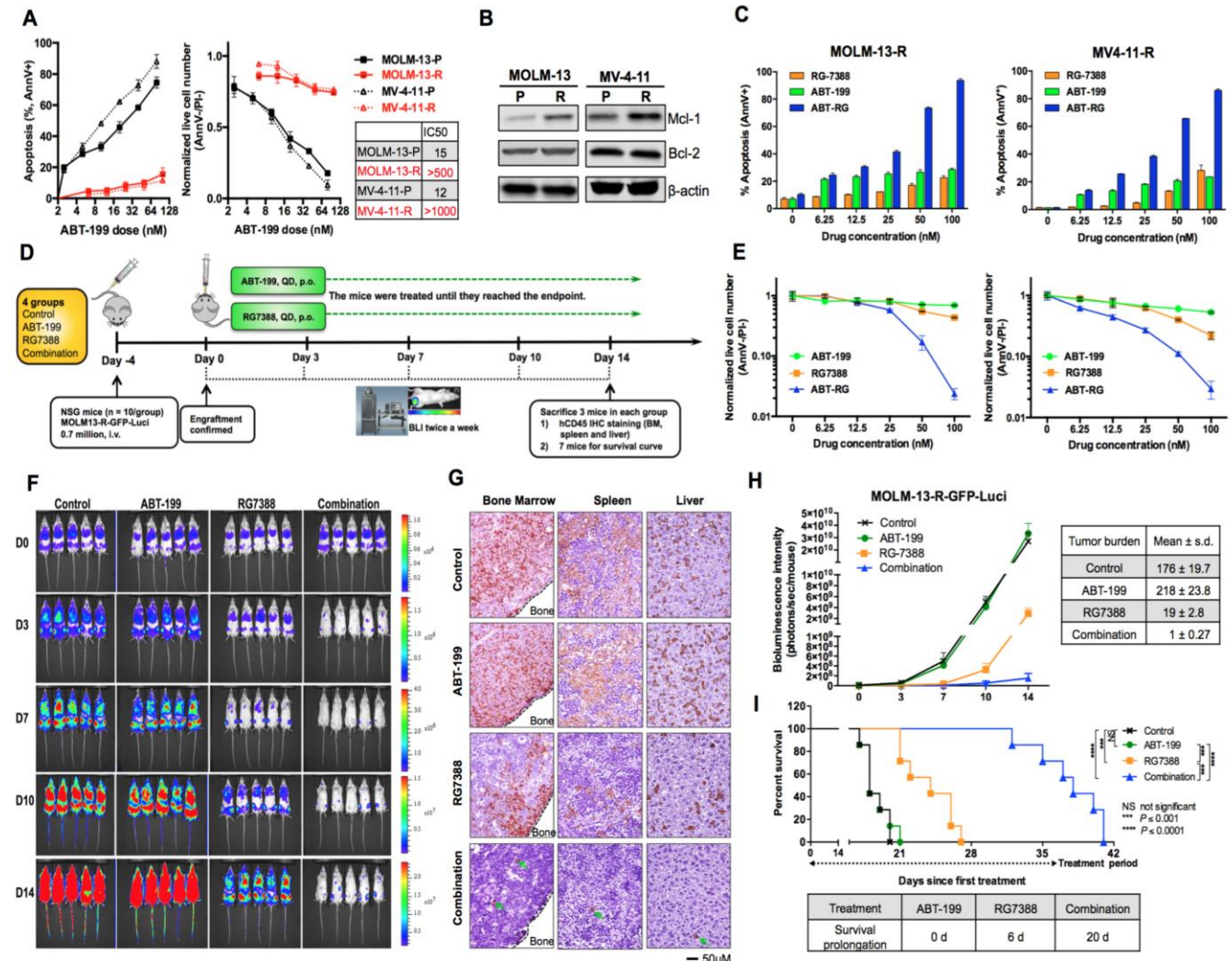


Figure 3.2 Sensitive AML cell lines acquire resistance to BCL-2 inhibitor ABT; p53 activator RG overcomes the acquired resistance *in vitro* and *in vivo*.

(A) Sensitivity comparison of parental (P) and generated resistant (R) cells after treatment with ABT for 48 h. The IC_{50} values were calculated with Calcsyn software based on live cell numbers. (B) Immunoblot showing MCL-1 upregulation in cells with acquired resistance. (C and E) The resistant cells were treated with ABT, RG or ABT-RG combination at a 1:1 ratio for 48 h. (D) Schematic outline of the mouse model of acquired ABT resistance (MOLM-13-R). Treatment was started after confirmation of AML engraftment on day 0 (4 days post-injection). (F) Serial bioluminescence images of mice bearing MOLM-13-R cells treated with vehicle, ABT, RG or the combination. (G) Representative immunohistochemical (IHC) staining of murine bone marrow, spleen and liver for human CD45 antigen on day 14. Three mice from each group were sacrificed. Rare leukemic cells in tissue sections from combination-treated mice were marked by green arrows. (H) Quantification of bioluminescence emitted from the whole body of each mouse. Data represent the mean \pm s.d. of each group. (I) Kaplan-Meier survival curves of mice injected with MOLM-13-R cells ($n = 7$ per group; statistical significance was evaluated by the log-rank test).

Data in bar/line graphs (A, C, E) represent the means of triplicate experiments. Error bars, mean \pm SD.

Figure S3.2

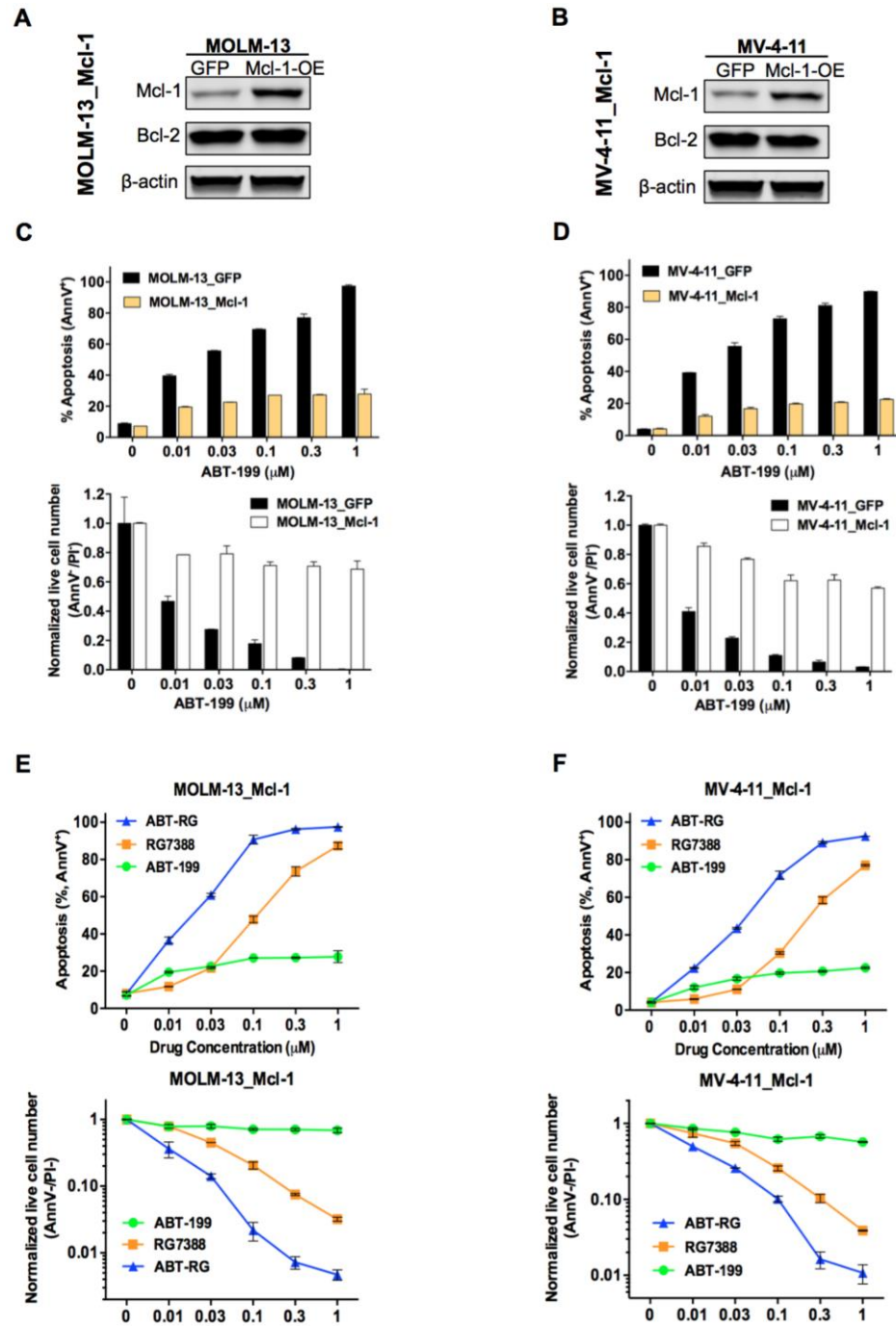


Figure S3.2 related to Figure 3.2. MCL-1 overexpression confers resistance to BCL-2 inhibitor ABT, which can be abrogated by p53 activator RG.

(A, B) Immunoblot showing stable MCL-1 overexpression in MOLM-13 and MV-4-11 cells. GFP, control transfectants. β-actin served as loading control. (C, D) MCL-1 overexpression rendered MOLM-13 and MV-4-11 cells resistant to ABT. Cells were treated with ABT for 48 h. (E, F) RG could overcome MCL-1-mediated resistance to ABT. Control and MCL-1-overexpressing MOLM-13/MV-4-11 cells were treated with RG and ABT at a 1:1 ratio for 48 h. Data in bar/line graphs represent the means of triplicate experiments. Error bars, mean ± SD

3.3.3 p53 Activation Abrogates Inherent Resistance to BCL-2 Inhibition

OCI-AML3 cells express a high level of MCL-1 and are inherently resistant to BCL-2 inhibitor ABT (Figures 3.3A-B). Both MCL-1 knockdown ¹¹ and a selective MCL-1 inhibitor A-1210477 abolished ABT resistance (Figure S3.3), further validating MCL-1 as an inherent resistance factor in OCI-AML3 cells. We then asked whether the inherent resistance could be abrogated by RG-mediated p53 activation. Combining RG with ABT at a 3:1 or 1:1 ratio increased apoptosis and decreased live cell numbers to a significantly greater extent than either agent alone (Figures 3.3C-D). p53 activator RG reduced ABT IC₅₀ from 1590 to 26 nM. These results indicate that p53 activation could overcome the inherent resistance to BCL-2 inhibitor ABT. Importantly, RG failed to overcome the inherent resistance in p53 knockdown cells (Figure 3.3E), implying the pivotal role of p53 activation in this process.

To determine if p53 activation could overcome the inherent resistance *in vivo*, we labeled OCI-AML3 cells with luciferase and injected them into NSG mice (Figures 3.3F-G). Seven days post-injection, engraftment was confirmed by BLI (Figure 3.3H). The mice were then randomly divided into four groups and treated with vehicle, ABT, RG, or the combination. BCL-2 inhibition by ABT slightly reduced leukemic burden as indicated by BLI and immunohistochemical (IHC) analysis (Figures 3.3H-J). p53 activator RG significantly decreased tumor burden, while the combination further slowed leukemia progression and reduced tumor infiltration in BM, spleen, and liver to a greater extent than either agent alone (Figures 3.3H-J). The ABT-RG combination markedly extended mouse survival by 61 d (3.2- and 6.1-fold prolongation relative to RG or ABT monotherapy, respectively; Figure 3.3K). These data suggest that p53 activation can overcome the MCL-1-mediated inherent resistance to BCL-2 inhibition *in vivo*.

Figure 3.3

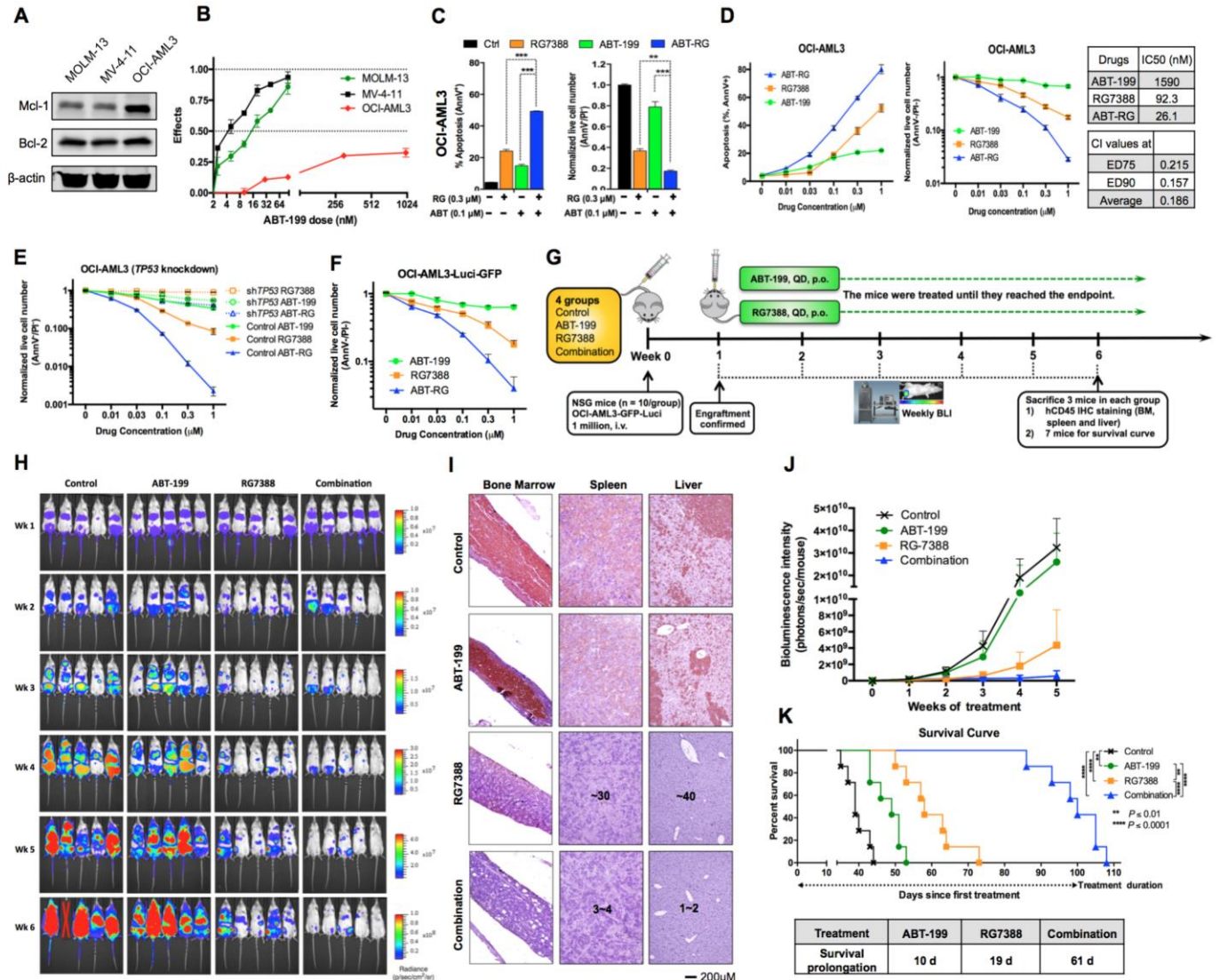


Figure 3.3 p53 activation by RG abrogates inherent resistance to ABT.

(A) Basal expression of MCL-1 and BCL-2 in MOLM-13, MV-4-11 and OCI-AML3 cells. (B) MCL-1^{high} OCI-AML3 cells are inherently resistant to ABT. AML cells were treated with ABT for 48 h. Effects = 1 – live cell number^{treated}/live cell number^{control}. (C and D) RG synergized with ABT at a 3:1 ratio (C) or a 1:1 ratio (D). The combination index (CI) and IC₅₀ values were calculated using Calcsyn software based on live cell numbers. (E) RG overcame ABT resistance in control but not in p53 knockdown OCI-AML3 cells (48 h treatment). (F) RG abrogated ABT resistance in luciferase-labeled OCI-AML3 cells *in vitro* (48 h treatment). (G) Schematic outline of the mouse model of inherent ABT resistance. (H) Serial bioluminescence images of OCI-AML3-engrafted NSG mice. Treatment was initiated on day 7 after confirmation of engraftment. (I) Representative IHC staining of murine BM, spleen and liver for human CD45 antigen at week 6. Three mice from each group were sacrificed. Countable numbers of hCD45⁺ cells were marked on each slide. (J) Quantitation of bioluminescence emitted from the whole body of each mouse. Data represent the mean ± s.d. of each group. (K) Kaplan-Meier survival curves of mice injected with luciferase-labeled OCI-AML3 cells (*n* = 7 per group; statistical significance and median survival were evaluated using the log-rank test). Data in bar/line graphs (B-F) represent the means of triplicate experiments with error bars indicating SD. ***P* < 0.01, ****P* < 0.001 as determined by two-tailed unpaired Student's *t*-test.

Figure S3.3

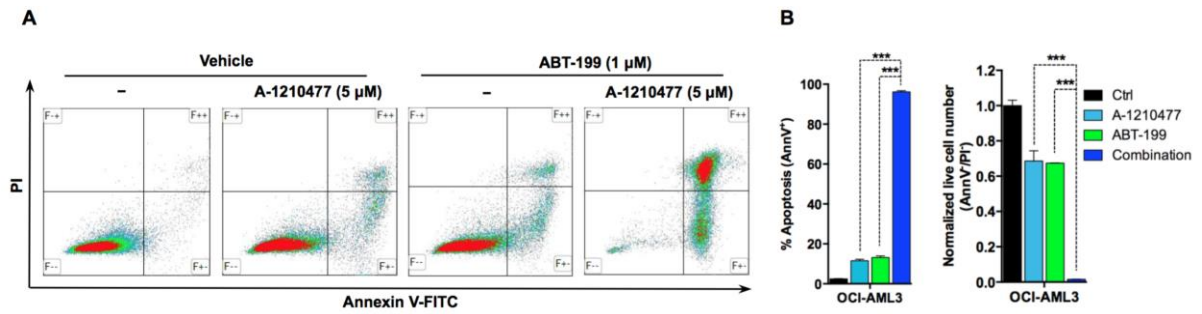


Figure S3.3 related to Figure 3.3. MCL-1 inhibition overcomes inherent ABT resistance in OCI-AML3 cells.

(A) Representative flow cytometry plots of OCI-AML3 cells treated with MCL-1 antagonist A-1210477 (5 μM) in the presence or absence of ABT (1 μM) for 24 h. (B) The cell numbers were enumerated by flow analysis using CountBright counting beads and normalized to untreated control. Data represent the means of triplicate experiments. *P* values were calculated by two-tailed unpaired Student's *t*-test. *** *P* < 0.001. Error bars, mean ± SD.

3.3.4 p53 Activation Induces Pro-Apoptotic Proteins and Reverses ABT-Induced Upregulation of MCL-1

We next sought to address the mechanism by which p53 activation overcame MCL-1-mediated resistance to BCL-2 inhibition. We chose OCI-AML3 for the mechanistic studies because it is not only resistant to BCL-2 inhibitor ABT but also relatively resistant to p53 activator RG (Figure S3.1A). p53 activation by RG significantly increased mRNA levels of p53 target genes *MDM2*, *BBC3*, *BAX* and *BAK* (Figure 3.4A). Similarly, kinetic study using immunoblotting revealed a rapid and strong upregulation of MDM2 and Puma (Figure 3.4B) and a delayed upregulation of Bax and Bak. These observations correspond with previous reports that p53 has lower affinity for *BAX/BAK* promoters than for *MDM2/BBC3* promoters^{42,80}. Since Puma, Bax, and Bak each binds and counteracts MCL-1^{4,9}, their upregulation can contribute to overcoming MCL-1-mediated resistance.

Although OCI-AML3 cells express a high level of MCL-1, MCL-1 was further upregulated (~2-fold) in these cells after acute ABT exposure (Figure 3.4C), which could further enhance resistance to ABT. In contrast, p53 activation by RG induced a time- and dose-dependent downregulation of MCL-1 (Figure 3.4C). The downregulation occurred within 9 h, when no cleavage of PARP-1 was detected and the cell viability was over 97%, excluding the possibility that MCL-1 degradation was a secondary consequence of apoptosis. Moreover, BCL-2 inhibitor ABT quickly upregulated MCL-1 within a few hours, even in the presence of p53 activator RG, but the MCL-1 upregulation could be reversed later by p53 activation (Figure S3.4A). Notably, BCL-2 levels were not affected by ABT or RG treatment (Figure S3.4B). These findings

indicate that p53 activation by RG could reduce MCL-1 levels and reverse ABT-mediated upregulation of MCL-1.

3.3.5 p53 Activation Inhibits pERK and Activates GSK3 to Modulate MCL-1

Phosphorylation

To determine the mechanism underlying the reduction of MCL-1, we first conducted qRT-PCR analysis, which indicated that p53 activation did not significantly affect *MCL1* transcription (Figure 3.4D, lower panel). We postulated that MCL-1 might be regulated by post-translational modifications (PTMs) that affect its stability. The best-characterized MCL-1 PTMs are phosphorylation at threonine 163 (T163) and serine 159 (S159) ^{28,81}. T163 phosphorylation (denoted as pMCL-1T) stabilizes MCL-1 but also primes MCL-1 to be further phosphorylated at S159. The dually phosphorylated MCL-1 (pMCL-1T/S) will be ubiquitinated and targeted for proteasomal degradation ^{28,81}.

Consistent with a PTM mode of regulation, p53 activation by RG decreased pMCL-1T and increased pMCL-1T/S (Figure 3.4E, lane 2), while BCL-2 inhibitor ABT dramatically elevated pMCL-1T (Figure 3.4E, lane 3). Interestingly, p53 activation converted the abundant stabilizing pMCL-1T to destabilizing pMCL-1T/S (Figure 3.4E, lanes 3,4), which could explain how RG reversed ABT-induced upregulation of MCL-1. In contrast, p53 knockdown upregulated pMCL-1T (Figure 3.4F, lane 2) and diminished the ability of RG to convert pMCL-1T to pMCL-1T/S (Figure 3.4F, lanes 3,4), suggesting an indispensable role of p53 in this conversion. The next question was which kinase phosphorylated MCL-1 at T163 or S159 in this context.

pERK and pJNK have been reported to phosphorylate MCL-1 at T163 ^{28,81,82}. It appeared that pJNK did not play a major role here since neither pJNK nor total JNK

levels decreased in response to p53 activation (Figure S3.4C). In contrast, p53 activation decreased pERK and pMCL-1T (Figure 3.4E), whereas p53 knockdown simultaneously increased the two phospho-proteins (Figure 3.4F). Moreover, suppressing pERK with the MEK-specific inhibitor PD0325901 (PD) eliminated both pERK and pMCL-1T (Figure 3.4H). Collectively, these results indicate that pERK, rather than pJNK, regulated MCL-1 phosphorylation at T163 in response to p53 activation or p53 knockdown.

GSK3 has been reported to associate with pMCL-1T and phosphorylate its S159 residue^{81,83}. GSK3 protein is constitutively active, but its activity is diminished by inhibitory phosphorylation at serine 9/21^{83,84}. We found that p53 activation reduced pGSK3 (Figure 3.4E, lane 2) but not total GSK3 (Figure S3.4E), implying a larger fraction of active GSK3, which likely transformed ABT-induced pMCL-1T to a high level of pMCL-1T/S (Figure 3.4E, lane 4). In contrast, p53 knockdown increased GSK3 phosphorylation and restrained GSK3 to transform pMCL-1T to pMCL-1T/S (Figure 3.4F, lane 2). To further verify GSK3's role in this conversion, we pretreated OCI-AML3 cells with GSK3 inhibitor CHIR-99021 (CHIR, Figure 3.4J). Since little pMCL-1T was present in untreated cells, BCL-2 inhibitor ABT was added to increase pMCL-1T (GSK3 substrate). ABT alone induced abundant pMCL-1T but not pMCL-1T/S (Figure 3.4E, lane 3), implying that active GSK3 was probably present at a low level. Therefore p53 activator RG or MEK inhibitor PD was also added to release GSK3 activity (explained in the next paragraph). As expected, ABT-PD or ABT-RG combinations induced abundant pMCL-1T/S, while GSK3 inhibitor CHIR prevented the generation of destabilizing pMCL-1T/S and increased MCL-1 levels (Figure 3.4J). These findings indicate that GSK3 phosphorylated MCL-1 at S159 to promote MCL-1 degradation in

Figure 3.4

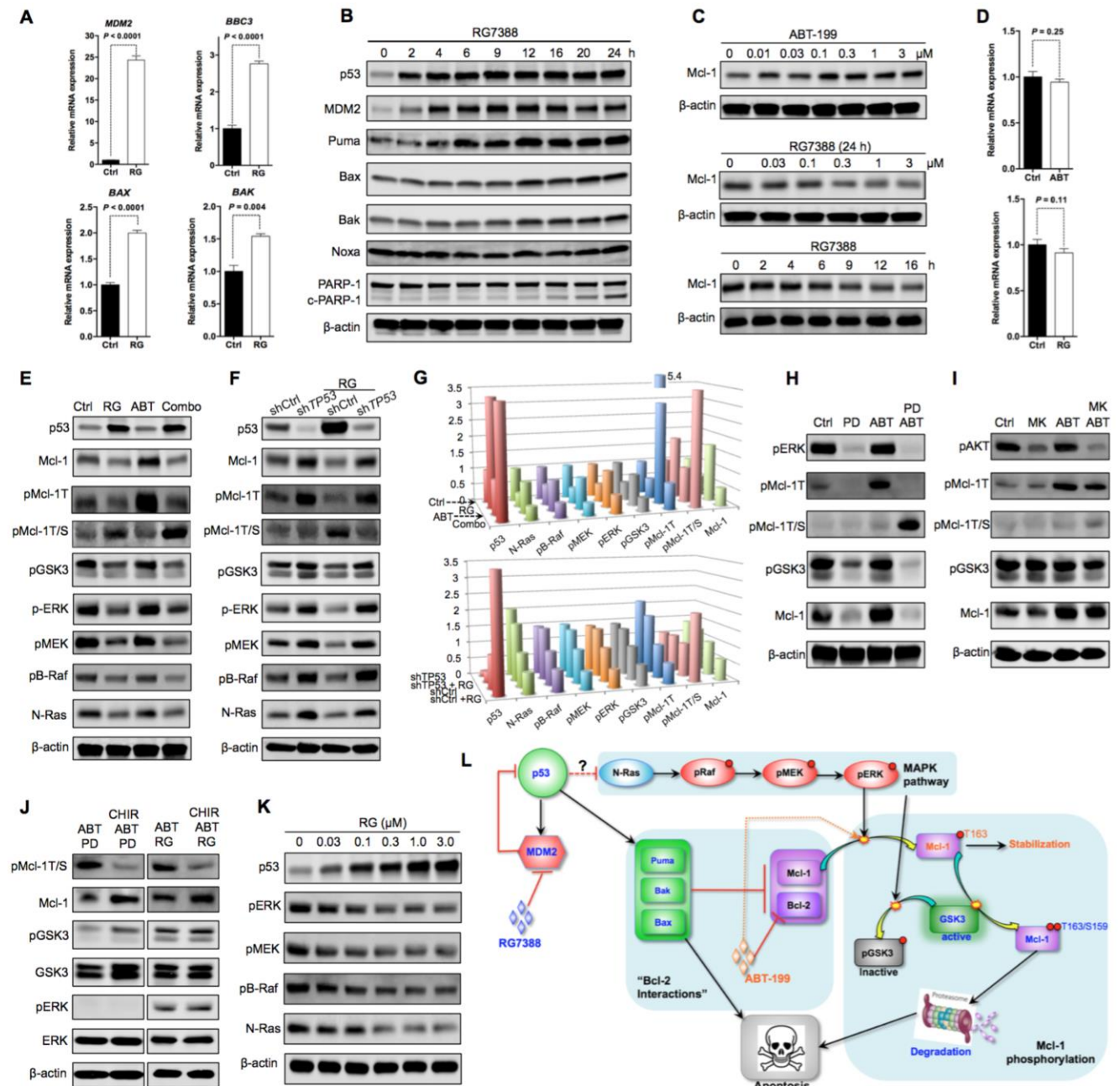


Figure 3.4 p53 negatively regulates N-Ras and downstream MAPK/GSK3 signaling to modulate MCL-1 phosphorylation and degradation.

(A) Relative mRNA expression of *MDM2*, *BAX*, *BAK* and *BBC3* (Puma-encoding gene) in OCI-AML3 cells after 12 h treatment with 1 μ M RG. (B) p53 activation by RG induced time-dependent upregulation of Puma, Bax and Bak but not Noxa in OCI-AML3 cells. (C) ABT treatment (24 h) upregulated MCL-1 whereas RG treatment reduced MCL-1 in OCI-AML3 cells. (D) Relative mRNA expression of *MCL1* in OCI-AML3 cells after incubation with 1 μ M ABT or RG for 12 h. (E) Immunoblot of OCI-AML3 cells treated with vehicle, 1 μ M RG, 1 μ M ABT or the combination for 24 h. The pMCL-1T and pMCL-1T/S antibodies recognize their epitopes in a mutually exclusive manner. (F) Immunoblot of OCI-AML3 cells (control or p53 knockdown)

treated with vehicle or 1 μ M RG for 24 h. **(G)** 3D cylinder charts showing protein levels in panels E & F as measured by quantitative immunoblot using the Odyssey Infrared Imaging System. Value = 1 for untreated control. **(H)** OCI-AML3 cells were treated with vehicle, 100 nM PD0325901 (PD, MEK inhibitor), 1 μ M ABT or the PD-ABT combination for 12 h. **(I)** OCI-AML3 cells were treated with vehicle, 1 μ M MK-2206 (MK, AKT inhibitor), 1 μ M ABT or the MK-ABT combination for 12 h. **(J)** GSK3 inhibition prevented the generation of pMCL-1T/S and increased MCL-1. OCI-AML3 cells were treated for 24 h with different combinations of 1 μ M ABT, 100 nM PD, 1 μ M CHIR-99021 (CHIR, GSK3 inhibitor) and 1 μ M RG. **(K)** p53 activation by RG reduced N-Ras and the Ras/Raf/MEK/ERK signaling cascade. OCI-AML3 cells were treated with escalating doses of RG for 24 h. **(L)** Schematic diagram of the proposed mechanism by which p53 activation overcame MCL-1-mediated resistance to ABT.

Figure S3.4

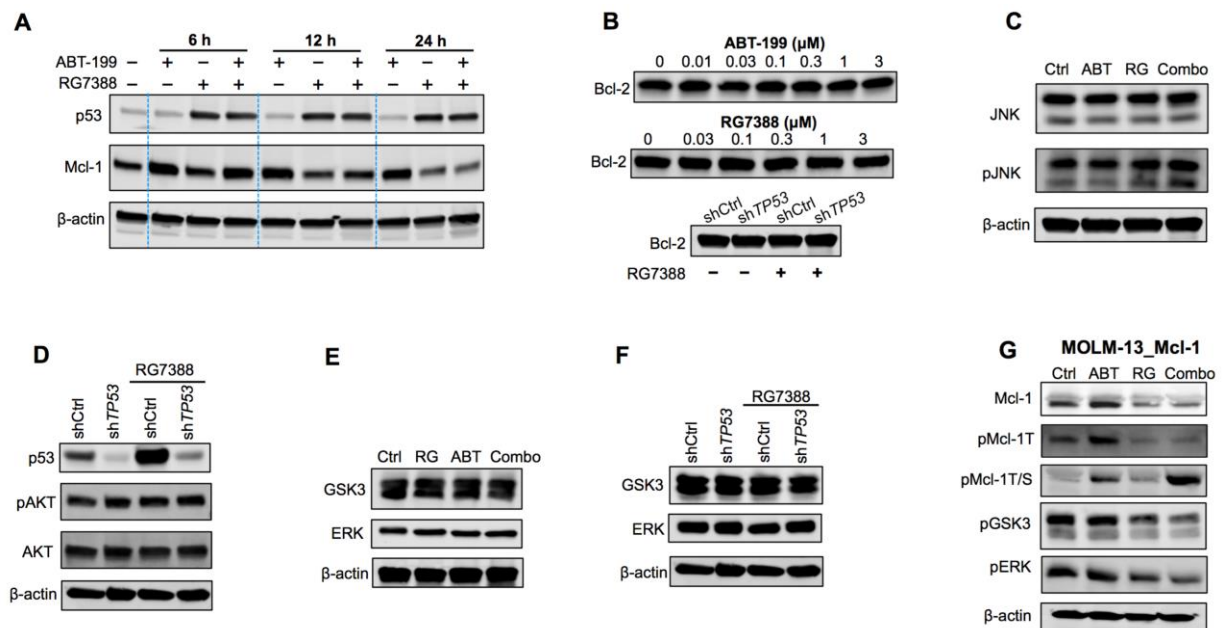


Figure S3.4 related to Figure 3.4.

(A) ABT-199 quickly induced MCL-1 upregulation in the absence or presence of RG, which could be latter reversed by RG-induced p53 activation. OCI-AML3 cells were treated with vehicle, 1 μ M ABT, 1 μ M RG or the combination for indicated time. **(B)** BCL-2 inhibition by ABT, p53 activation by RG or p53 knockdown did not affect BCL-2 protein expression. The loading control immunoblots were the same as in Figure 4C and 4F. **(C)** RG or ABT did not change the levels of active pJNK or total JNK. Cell lysates are the same as in Figure 4E. **(D)** p53 knockdown or p53 activation did not significantly affect pAKT level. p53 and β -actin immunoblots are the same as in Figure 4F. **(E)** p53 activation by RG did not affect the expression of total GSK3 or total ERK, but reduced pERK and pGSK3 as shown in Figure 4E. The immunoblot for loading control is the same as in Figure 4E. **(F)** p53 knockdown did not affect the expression of total GSK3 or total ERK, but increased pERK and pGSK3 as shown in Figure 4F. **(G)** Immunoblot of MCL-1–overexpressing MOLM-13 cells treated with vehicle, 1 μ M ABT, 1 μ M RG or the combination for 24 h. The results are consistent with our findings in OCI-AML3 cells.

this system.

3.3.6 p53 Downregulates N-Ras and Downstream MAPK Signaling and Releases GSK3 Activity

To determine the mechanism by which p53 activation regulates GSK3 activity, we first measured the effects of p53 expression on AKT, which is widely known to phosphorylate and inactivate GSK3^{83,84}. In OCI-AML3 cells, however, p53 knockdown or p53 activation did not significantly affect the pAKT levels (Figure S3.4D). Meanwhile, MK-2206, a selective AKT inhibitor, dramatically decreased pAKT, but only marginally decreased pGSK3 and failed to release GSK3 activity to convert ABT-induced pMCL-1T to pMCL-1T/S (Figure 3.4I), suggesting that AKT did not play a significant role here.

We next examined the MEK/ERK signaling, which has also been implicated in regulating GSK3 inhibitory phosphorylation^{84,85}. p53 activation by RG decreased pGSK3 together with pMEK and pERK, (Figures 3.4E and 3.4K), whereas p53 knockdown resulted in concurrent upregulation of these three phospho-proteins (Figure 3.4F). Furthermore, MEK inhibitor PD markedly reduced pGSK3 (Figure 3.4H) and released GSK3 activity, which robustly converted ABT-induced pMCL-1T to pMCL-1T/S (Figure 3.4H). These findings together implied that the MEK/ERK signaling mediated the inhibitory phosphorylation of GSK3 in this context. Next, we tracked the Ras/Raf/MEK/ERK pathway bottom-up and unexpectedly found that p53 activation downregulated the N-Ras protein levels (Figure 3.4E). Importantly, p53 knockdown upregulated N-Ras levels (Figure 3.4F), while p53 activator RG induced a dose-dependent decrease of N-Ras (Figure 3.4K). These results indicate that p53 could negatively modulate N-Ras expression. It is well established that activation of oncogenic Ras proteins can elevate p53 expression and p53 activity through the ARF-

p53 circuit^{86,87}. Our finding that p53 negatively regulated N-Ras protein levels, identifies a previously unknown connection between p53 and N-Ras. The mechanism through which this is accomplished needs to be defined in future studies. We also quantitated and normalized the levels of proteins involved in this regulatory cascade using Odyssey Infrared Imaging System and the companion software (see Experimental Procedures), and generated two cylinder charts (Figure 3.4G) corresponding to Figures 3.4E and 3.4F. The cylinder charts demonstrate similar trends between the N-Ras/B-Raf/MEK/ERK signaling cascade and MCL-1 protein levels but opposite trends between p53 and MCL-1 levels, or between p53 levels and the MAPK signaling cascade. These correlations are consistent with our proposed mechanism. The findings of these mechanistic studies can be briefly summarized as follows (also summarized in Figure 3.4L). RG mediates activation of p53, which negatively regulates the N-Ras/B-Raf/MEK/ERK pathway and releases GSK3 activity. Active GSK3 then converts ABT-induced stabilizing pMCL-1T to pMCL-1T/S and promotes MCL-1 degradation. Meanwhile, p53 also induces Puma, Bax, and Bak to counteract the remaining MCL-1, thus overcoming MCL-1-mediated resistance to BCL-2 inhibition at multiple levels.

3.3.7 BCL-2 Inhibition Reciprocally Overcomes Resistance to p53 Activation by Switching Cellular Response from Pro-Survival G1 Arrest to Apoptosis

RG induced comparable levels of p53 in MV-4-11, MOLM-13, and OCI-AML3 cells, but substantially less apoptosis occurred in OCI-AML3 cells (Figure 3.5A), suggesting that OCI-AML3 is relatively resistant to apoptosis induction by p53 and has a higher apoptotic threshold. We postulated that if p53 level was not sufficient to push OCI-AML3 cells across the apoptotic threshold, p53 might induce abundant p21 proteins to

trigger pro-survival cell cycle arrest (CCA). Indeed, p53 activation by RG induced little apoptosis in OCI-AML3 cells (Figure 5A) but robustly elevated p21 expression at mRNA and protein levels (Figures 3.5B-C) and triggered CCA at G1 phase (Figure S3.5A). The induced CCA was reversible as OCI-AML3 cells resumed proliferation after removal of RG (Figure 3.5D). Moreover, p21 knockdown (Figure 3.5E) reduced CCA at G1 phase (Figure S3.5A) but significantly increased RG-induced apoptosis (Figure 3.5F). It has been well established that p21 can suppress tumors by inhibiting cell proliferation. Our findings here indicate that p21 can also mediate tumor resistance by protecting cancer cells from p53-induced apoptosis and by promoting reversible G1 arrest.

The apoptotic threshold can be directly modulated up or down by BCL-2 family proteins. OCI-AML3 expresses high levels of BCL-2 and MCL-1, which contribute to its high apoptotic threshold. Unlike MCL-1, BCL-2 protein levels were not affected by p53 activation or knockdown (Figure S3.4B). Although MCL-1 levels decreased upon p53 activation, the high levels of BCL-2 could still be sufficient to keep most cells below apoptotic threshold (We previously demonstrated that knockdown of MCL-1 by 85% did not significantly affect OCI-AML3 viability or proliferation^{11,79}). Under this scenario, cells would preferentially enter G1 arrest in response to p53-induced high levels of p21, rather than undergo apoptosis. Based on these, we proposed that lowering the apoptotic threshold by BCL-2 inhibition might be sufficient to switch the cellular response of p53 activation from pro-survival G1 arrest to apoptotic cell death, thus overcoming apoptosis resistance to p53 activation. To test this hypothesis, we developed a protocol to simultaneously analyze apoptosis (AnnV⁺) and cell cycle distribution of AnnV⁻ live cells (Figure 3.5G). Unlike other commonly used methods, this

Figure 3.5

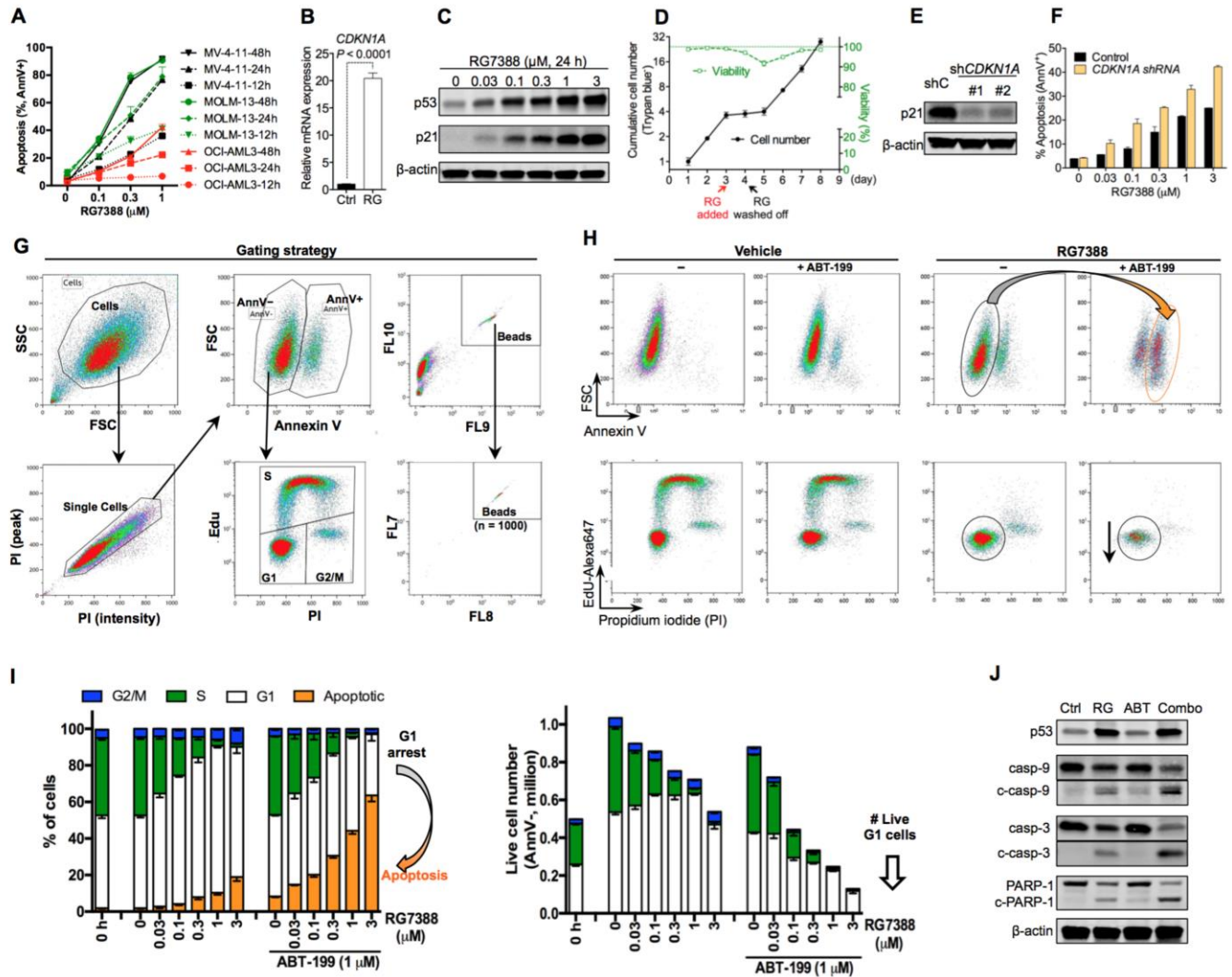


Figure 3.5 BCL-2 inhibition reciprocally overcomes resistance to p53 activation via shifting cellular response from G1 arrest to apoptosis.

(A) OCI-AML3 cells are relatively resistant to RG compared to MV-4-11 and MOLM-13 cells. (B) Relative mRNA expression of *CDKN1A* (p21-encoding gene) in OCI-AML3 cells after 12 h treatment with 1 μ M RG. (C) Immunoblot showing p21 upregulation in OCI-AML3 cells after RG treatment. (D) OCI-AML3 cells resumed exponential proliferation after removal of RG. OCI-AML3 cells were treated with 1 μ M RG7388 which was washed off after 24 h. The cell numbers and viability were determined by Vi-CELL viability analyzer (Trypan blue exclusion assay). (E) Immunoblots showing stable p21 knockdown in OCI-AML3 cells. Because of the low basal expression of p53/p21, the control (shC) or knockdown cells were treated with 1 μ M RG for 24 h prior to immunoblot analysis. (F) p21 knockdown significantly increased RG-induced apoptosis (48 h treatment). (G) Flow cytometry plots showing the gating strategy used to simultaneously analyze apoptosis and cell cycle distribution. The absolute cell numbers were also enumerated with CountBright counting beads. (H) Representative flow cytometry plots of OCI-AML3 cells after indicated treatments for 24 h. The gating was as depicted as in middle panels of Figure 3.5G. (I) Apoptosis and cell cycle analysis of OCI-AML3 cells treated with RG in the absence or presence of ABT for 24 h. The gating was the same as in Figure 3.5G. (J) OCI-AML3 cells were treated with DMSO, 1 μ M RG, 1 μ M ABT or the combination for 24 h. Data in line/bar graphs represent the means of triplicate experiments. Error bars, mean \pm SD.

Figure S3.5

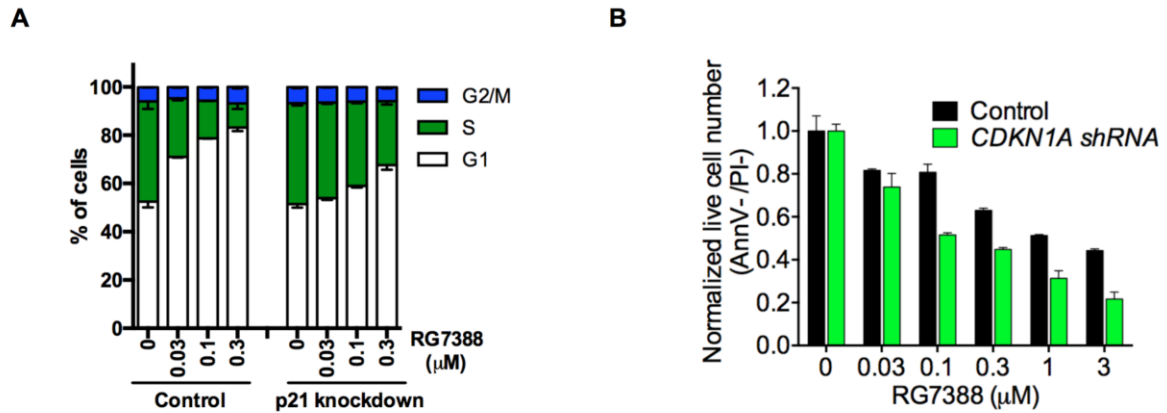


Figure S3.5 related to Figure 3.5.

(A) p21 knockdown attenuated cell cycle arrest at G1 phase. OCI-AML3 cells were treated with RG for 24 h, and then pulsed with 10 μM Edu for 1 h. Next the cells was fixed, permeabilized, stained with Click-iT Plus reaction cocktail (Life Technologies) and analyzed by flow cytometry according to the manufacturer's instruction. (B) p21 knockdown reduced the numbers of live cells (AnnV⁻/PI⁻) after 48 h treatment with indicated concentrations of RG. Data represent the means of triplicate experiments. Error bars, mean ± SD.

protocol avoided the interference of apoptotic cells in mitotic phase analysis. Counting beads were also added to quantify cell numbers in different phases. As shown in Figures 3.5H-I, p53 activator RG triggered little apoptosis but arrested most cells in G1 phase. Although BCL-2 inhibitor ABT did not affect cell cycle distribution, lowering the apoptotic threshold by ABT substantially reduced G1-arrested cells and augmented apoptosis induction by RG (Figures 3.5H-I). Moreover, adding ABT to RG markedly increased cleavage of caspase-9, caspase-3, and PARP-1 (markers of apoptosis, Figure 3.5J), which further supported our hypothesis that BCL-2 inhibition could overcome resistance to p53 activation via switching cellular response from pro-survival G1 arrest to apoptosis.

3.3.8 p53 Activation and BCL-2 Inhibition Reciprocally Overcome Resistance of Primary AML Cells

p53 activator RG effectively induced dose-dependent apoptosis and reduced live cell numbers in p53^{wt} patient samples (7/7 tested, Figure 3.6A). Consistent with the results in cell lines, RG could overcome ABT resistance in p53^{wt} but not in p53 deficient primary AML cells (Figure 3.6B). Notably, one p53^{wt} primary sample was highly resistant to both ABT and RG as 48 h treatment with up to 1 μ M of either compound only induced marginal increase in apoptosis (Figure 3.6B, middle panels). Nonetheless, the combination markedly increased apoptosis and reduced live cell numbers than either treatment alone.

To further test the combination in a patient-derived xenograft (PDX) model, we injected one resistant patient sample (p53^{wt}) into NSG mice, which could rapidly kill injected mice within few weeks (Figure 3.6C for experimental design). To gauge the level of engraftment, we sacrificed one extra group of three mice 10 days post-injection

Figure 3.6

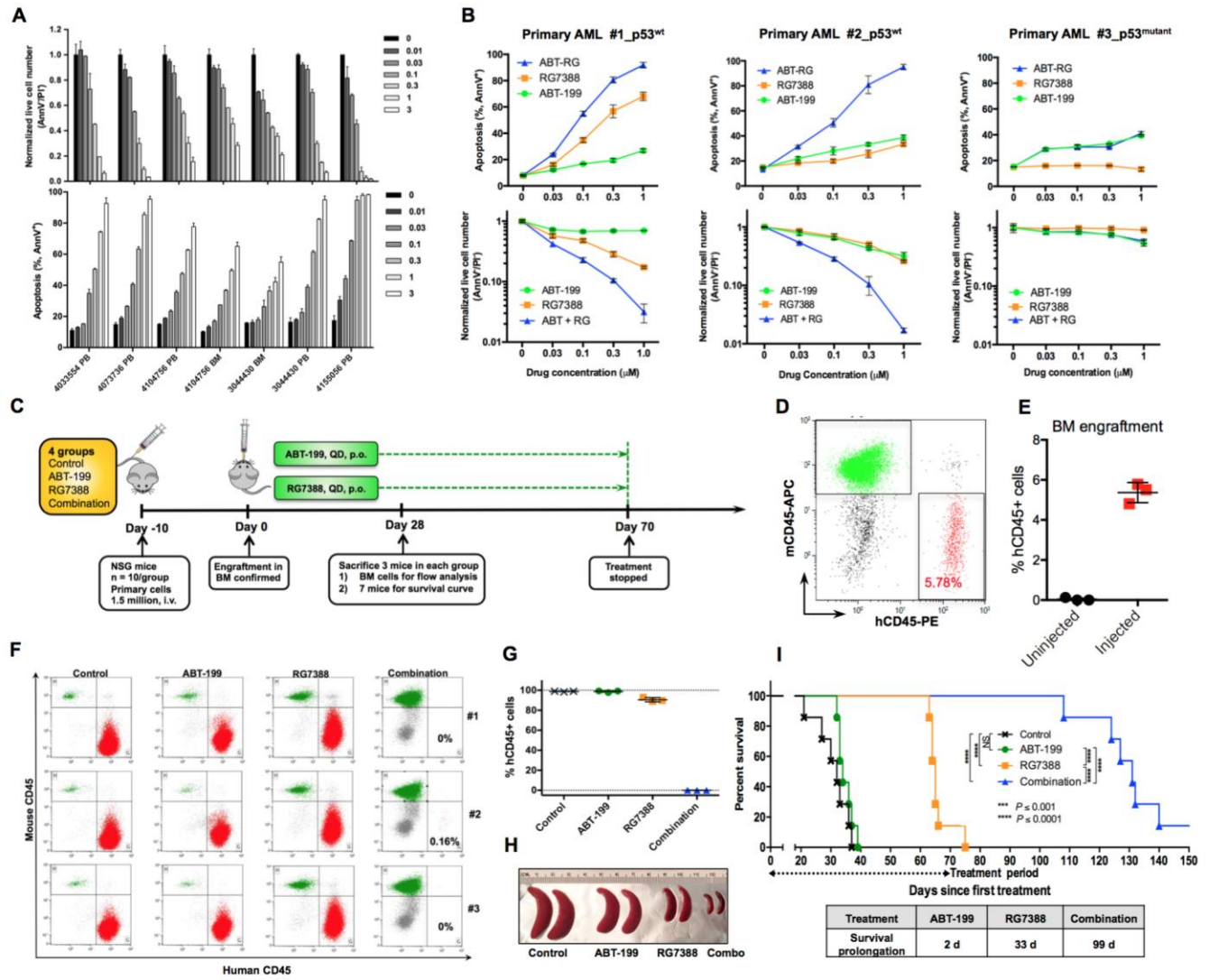


Figure 3.6 BCL-2 inhibition and p53 activation reciprocally overcome drug resistance of AML primary samples *in vitro* and in a PDX mouse model of resistance.

(A) Dose-dependent induction of apoptosis and reduction of live cell numbers by RG in p53^{wt} primary AML samples (48 h treatment). PB, peripheral blood. (B) Representative ABT-resistant primary samples with wild type or mutant p53 treated with ABT, RG or ABT-RG combination for 48 h. (C) Schematic outline of the PDX mouse model of drug resistance. (D) Representative flow cytometry plot showing engraftment of human AML cells (hCD45⁺) in murine femur BM (day 0). (E) Percentage of hCD45⁺ leukemic cells in murine BM, confirming leukemia engraftment. The percentage of hCD45⁺ cells was calculated as: % hCD45⁺ cells = the number of hCD45⁺ cells/the sum of hCD45⁺ and mCD45⁺ cells. (F) Flow cytometry analysis of hCD45⁺ leukemic cells in femur BM on day 28. Three mice from each group were sacrificed on day 28. (G) Percentage of hCD45⁺ cells in femur BM on day 28. (H) Representative murine spleens from sacrificed mice on day 28. (I) Kaplan-Meier survival curves of mice engrafted with resistant primary AML cells ($n = 7$ per group; statistical significance was evaluated using the log-rank test. NS, not significant.)

and found that the BM (3/3) was uniformly engrafted with ~5% human CD45⁺ cells (Figures 3.6D-E). The treatment was then initiated as described above. After 4 weeks, three mice from each group were euthanized and examined. As shown in Figures 3.6F-G, BM from control, ABT or RG groups was heavily infiltrated with leukemic cells (>85% by flow cytometry analysis). Remarkably, the ABT-RG combination reduced leukemic cells to 0.16% in the BM of one mouse and to undetectable levels in the other two (Figure 3.6F). ABT or RG monotherapy slightly or moderately decreased spleen size, whereas the combination dramatically reduced spleen size (Figure 3.6H). BCL-2 inhibitor ABT extended median survival by only 2 days, but combining ABT with p53 activator RG substantially prolonged mouse survival by 99 d (a 3-fold extension relative to RG monotherapy, Figure 3.6I). Collectively, these *in vitro* and *in vivo* data indicate that the combination of BCL-2 inhibition and p53 activation (ABT-RG) could cooperatively overcome apoptosis resistance to either treatment alone in primary AML cells. In the three different types of ABT-resistant mouse models (Figures 3.2D, 3.3G, and 3.6C), p53 activator RG moderately prolonged mouse survival and reduced leukemic burden, suggesting that the three different types of engrafted cells were also relatively resistant to p53 activation. BCL-2 inhibitor ABT by itself prolonged mouse survival only marginally or not at all. Nonetheless, combining ABT with RG extended median survival at least 3-fold compared to RG alone in all three resistant mouse models. These *in vivo* data, together with our *in vitro* results and mechanistic studies, demonstrate that BCL-2 inhibition and p53 activation can reciprocally overcome apoptosis resistance to either strategy alone and induce synthetic lethality of resistant leukemia cells.

Chapter 4 Discussion and Future Directions

4.1 Discussion

Relapsed AML is a difficult cancer to treat effectively; therefore, there is a need for improved treatment options for refractory AML. In Chapter 2, we demonstrate that selective inhibition of BCL-2 by ABT-199 kills AML cell lines and primary patient cells both *ex vivo* and in *in vivo* mouse xenografts as a single agent. The concentrations used in our studies here are in the 0.001-1 µg/ml range, a range readily achievable in clinical trials where serum concentrations of 3-4 µg/ml have been observed. Moreover, the drug acts very quickly *in vitro*, killing cells within 2 hours of drug exposure. We also show that ABT-199 functions on-target at the mitochondria. This is consistent with the observation that AML myeloblasts from chemorefractory patients showed no difference in their BCL-2 dependence, as measured by BH3 profiling, or sensitivity to ABT-199 compared to chemosensitive cells⁶².

Our *in vitro* results suggest there will be heterogeneity in clinical response (IC50s ranged from 0.43 to >1000 nm), so that a predictive biomarker would be of great utility. In Chapter 2, we present four methods that may be predictive of clinical response to ABT-199. The first method is cytogenetics. The cellular death response to ABT-199 appears to be largely independent of cytogenetic and genetic mutation status, except perhaps for complex karyotype and *JAK2* mutant patients, suggesting that treatment with ABT-199 could be useful for patients who have poor prognostic factors. The utility of cytogenetics as a more general predictive biomarker for response to ABT-199 needs to be examined across many more samples.

A second method is *ex vivo* short term culture of the primary patient samples with ABT-199. The disadvantage of this method is that it is difficult to reliably culture primary AML cells for the requisite time frame to observe cell death. We observed that even

after a short 8 h culture there could be upwards of 60% spontaneous apoptotic death in the control un-treated primary AML cells. Therefore, it would not be ideal to rely on an *in vitro* cell death assay where many samples could be potentially lost due to spontaneous cell death during culture.

The third predictive biomarker method is to measure BCL-2 levels by Western blot. We show that increased expression of BCL-2 is associated with increased sensitivity to ABT-199. However, given the complex interactions of the BCL-2 family members, individual measurements of the various anti-apoptotics alone may not provide accurate data on the *in vivo* biology of the anti-apoptotic dependencies in AML. Many of the BCL-2 family members are regulated by post-translational modifications and interactions with other proteins. These types of interactions are difficult to capture in static Western blot measurements.

The fourth method, BH3 profiling, may prove useful as a predictive biomarker. BH3 profiling is a functional assay that accounts for the relative amounts and interactions of all of the BCL-2 family members. We show here that the mitochondrial response to the BAD peptide correlates with mitochondrial response to *ex vivo* ABT-199 treatment. Most significantly, BH3 profiling could discriminate *in vivo* sensitivity of human AML cells to ABT-199 (Figure 2.6). Thus, we may be able to use BH3 profiling of pre-treatment AML samples to direct ABT-199 treatment to AML cases that are most BCL-2 dependent. While the assay is less familiar to many, it is a straightforward protocol using reagents and equipment available in most clinical and research laboratories. Moreover, results are available the same day the sample is acquired. As for the other putative biomarkers, empiric testing in the clinical setting is the only way to truly validate BH3 profiling as a useful predictive biomarker.

BCL-2 was discovered in lymphoid cancer cells, and much of the research on this protein has been conducted in lymphoid cells, where it is highly expressed⁸⁸. It is therefore understandable that clinical testing of ABT-199 has so far focused on lymphomas and CLL. In Chapter 2, we demonstrate that selective, on-target BCL-2 inhibition using a clinically active drug is a promising avenue for clinical investigation in the myeloid malignancy AML. It is particularly important to recognize that even AML myeloblasts that are resistant to conventional therapies appear to be quite sensitive to BCL-2 inhibition. Thus, BCL-2 inhibition by ABT-199 offers hope to those AML cases that most need novel therapeutic intervention. Our results in Chapter 2 strongly support the testing of ABT-199 for treatment of AML patients as the majority of patient samples were sensitive to the drug in *ex vivo* culture. Furthermore, our results support the testing of BH3-profiling as a predictive biomarker for ABT-199 response in the clinic.

Based on this study, a multi-center phase II trial has been conducted to treat relapsed and refractory AML patients or patients unfit for intensive chemotherapy. The overall complete response rate was 19%; an additional 19% of patients demonstrated antileukemic activity not meeting IWG criteria (partial bone marrow response and incomplete hematologic recovery). 38% patients had isocitrate dehydrogenase 1/2 mutations, of which 33% achieved complete response or complete response with incomplete blood count recovery. The BCL-2 inhibitor ABT-199 demonstrated its activity and tolerable safety profile. Our preclinical and clinical findings provide a compelling rationale to evaluate ABT-199 combined with other agents in AML.

In these clinical and preclinical studies, we identified MCL-1 expression confers resistance to ABT-199. p53 is a critical apoptosis regulator which potentially induce pro-apoptotic proteins such as Puma, Noxa, Bax to counteract MCL-1. In Chapter 3, we

studied whether p53 activation could overcome MCL-1-mediated resistance to BCL-2 inhibitor ABT-199. We found that p53 activation combined with BCL-2 inhibition achieved impressive anti-leukemia efficacy *in vitro* and *in vivo*. The combination of p53 activator RG and BCL-2 inhibitor ABT overcame resistance to either treatment alone, and it remarkably prolonged survival in three AML mouse models of resistance. These encouraging results provided the rationale for a multi-center phase II clinical trial in AML (NCT02670044). If this combination therapy is proven successful in the clinic, this concept is not limited to AML. Other hematological malignancies such as MDS, MM, ALL, CML, and CLL also have low p53 mutation rates and express high levels of BCL-2. These p53^{wt} malignancies may respond as well to the proposed combination strategy. Additionally, several compounds have been reported to promote proper folding of mutant p53 and restore its transcriptional function^{8,89}. Combining these compounds with BCL-2 inhibitors might represent a promising direction for p53 mutant cancers. We also found that low doses of ABT-RG combination synergized well with cytarabine and idarubicin (Figure 4.1), revealing its potential to be combined with AML front-line therapeutics.

Anti-apoptotic MCL-1 has been increasingly recognized as an important target in cancer therapy^{4,9,33}. MCL-1 protein has a short half-life and it can be cleaved by activated caspases during apoptotic cell death⁸¹. A number of studies observed MCL-1 reduction after treatment with different anti-tumor therapeutics; but the MCL-1 decrease was often accompanied by a substantial level of apoptosis. Therefore, it is ambiguous whether the observed MCL-1 decrease was the cause of apoptosis or merely a secondary consequence of apoptosis, especially when mechanistic insights were lacking in the majority of these reports. In the current study, (1) we observed that p53

Figure 4.1

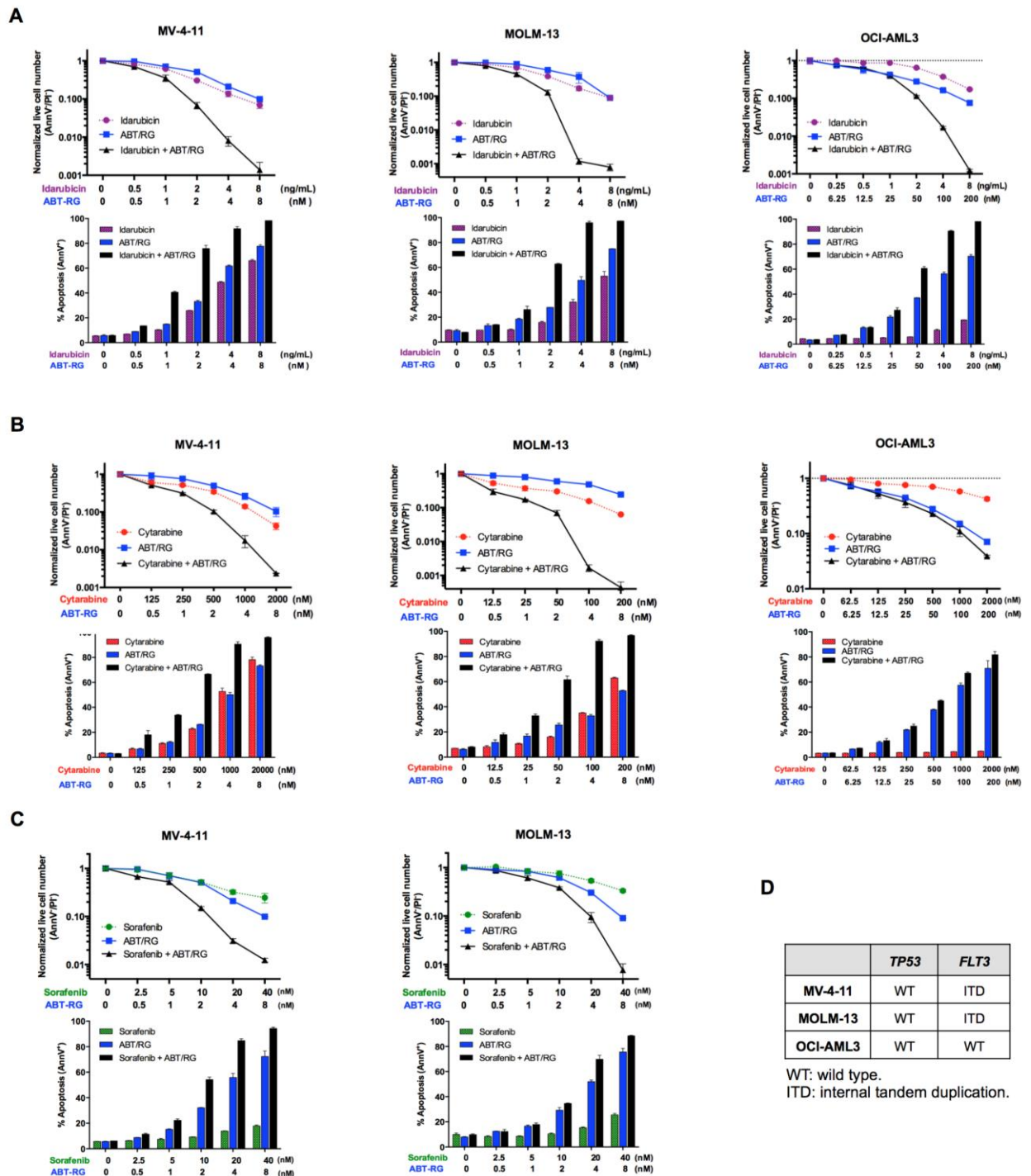


Figure 4.1 Low doses of ABT-RG combination synergizes with idarubicin, cytarabine and sorafenib.

(A-C) MV-4-11, MOLM-13 and OCI-AML3 cells were treated with indicated compounds or combinations for 48 h (ABT-RG, 1:1 ratio). Data in bar/line graphs represent the means of triplicate experiments. Error bars, mean \pm SD. (D) *TP53* and *FLT3* status of the three AML cell lines.

Data in panels A-D represent the means of triplicate experiments. Error bars, mean \pm SD.

activator RG induced MCL-1 reduction prior to apoptotic cell death; (2) p53 knockdown upregulated MCL-1 while both the control and knockdown cells were highly viable, thus excluding potential interference from apoptosis; (3) Moreover, we illustrated the underlying mechanism that p53 activation regulated N-Ras/B-Raf/MEK/ERK/GSK3 signaling to modulate MCL-1 phosphorylation and promote MCL-1 degradation. These points collectively support the negative regulation of MCL-1 by p53 and exclude the possibility that the observed MCL-1 reduction is merely a consequence of apoptosis.

To validate our mechanistic findings in another system, we also ectopically overexpressed MCL-1 in MOLM-13 cells to make them resistant to BCL-2 inhibitor ABT (Figures S3.2A and S3.2C). As in OCI-AML3 cells, p53 activator RG reduced MCL-1 in MOLM-13_MCL-1 cells (Figure S3.4G, lane 3). Moreover, acute ABT exposure similarly induced upregulation of MCL-1 and pMCL-1T (Figure S3.4G, lane 2), which could be reversed by p53 activator RG (Figure S3.4G, lane 4). RG also decreased pERK and pGSK3 (Figure S3.4G), resulting in an increase in active GSK3, which could potentially convert pMCL-1T to pMCL-1T/S. Indeed, combination-treated MOLM13_MCL-1 cells had much lower levels of pMCL-1T but higher levels of pMCL-1T/S than ABT-treated cells (Figure S3.4G, lanes 2,4). These data are in line with and support our mechanistic findings in OCI-AML3 cells.

Biological outcomes of p53 activation can be determined by different cellular thresholds for CCA and apoptosis^{42,80,90}. For tumor cells with high apoptotic threshold, p53 activity might not induce enough pro-apoptotic proteins to push tumor cells through their apoptotic threshold but may induce sufficient cell cycle regulatory proteins to trigger reversible CCA. To minimize CCA-mediated resistance to p53 activation, we proposed to convert the cellular response from CCA to apoptosis by reducing the

apoptotic threshold with BCL-2 inhibitor ABT. Paradoxically, ABT induced an unwelcome increase in MCL-1, which further raised the apoptotic threshold. Given that a low dose of ABT (i.e., 10 nM) was sufficient to upregulate MCL-1 (Figure 3.4C), special attention should be given to possible MCL-1 elevation when using ABT in the laboratory or in the clinic. Nevertheless, in our study, the MCL-1 elevation can be reversed by p53 activator RG. In this scenario, BCL-2 inhibition by ABT could effectively reduce the apoptotic threshold and switch the outcome of p53 activation from G1 arrest to apoptosis. In addition, others and we have shown that AML and other hematologic malignancies widely overexpress BCL-2^{11,91-93}. This may explain why in this study, BCL-2 inhibitor ABT almost always synergized with RG in p53^{wt} AML cell lines, in p53^{wt} primary samples, and in three resistance mouse models of AML.

In Chapter 3, we demonstrated that p53 activation could overcome inherent and acquired resistance to BCL-2 inhibition by regulating the Ras/Raf/MEK/ERK/GSK3 signaling to promote MCL-1 degradation and by promoting the expression of pro-apoptotic proteins. In addition, BCL-2 inhibition reciprocally overcame apoptosis resistance to p53 activation by shifting cellular response from G1 arrest to apoptosis. The mechanistic studies, together with the remarkable *in vitro* and *in vivo* efficacy, strongly support future research and clinical trials testing combinations of BCL-2 inhibitors with p53-reactivating compounds.

4.2 Future Directions and Unanswered Questions

4.2.1 To Systematically Study Mechanisms of Resistance to BCL-2 inhibitor ABT-

199

Directly targeting the apoptosis pathways might potentially minimize the emergence

of acquired resistance mediated by the complex cancer signaling networks. However, the BCL-2 family anti-apoptotic proteins (i.e., BCL-2, MCL-1, BCL-XL, BFL-1, and BCL-W) are functionally redundant, at least in their functions to inhibit apoptotic cell death. Thus, overexpression of other anti-apoptotic protein(s) could potentially render cancer cells resistant to the BCL-2 selective inhibitor ABT-199. Indeed, in Chapter 2, we found that AML cells with high basal levels of MCL-1 are inherently resistant to ABT-199. Moreover, in Chapter 3, we found that initially sensitive AML cells could acquire resistance to ABT-199 by upregulating MCL-1 after long-term exposure to this compound. We also demonstrated that MCL-1 knockdown or Mcl-1 inhibition could re-sensitize these resistant AML cells to ABT-199, whereas MCL-1 overexpression conferred resistance to ABT-199. These results collectively suggest the pivotal roles of MCL-1 in mediating resistance to ABT-199 in this context. Of note, OCI-AML3, MOLM-13 and MV-4-11 cells express relatively low basal levels of BCL-XL, BFL-1, and BCL-W when compared to the levels of BCL-2 or MCL-1, these may explain why BCL-XL, BFL-1, and BCL-W seemingly do not play a significant role in our study. However, BFL-1, BCL-XL, or BCL-W might be potentially important and may mediate resistance to ABT-199 in other systems such as cancer cells with high basal expression of these proteins. It is also reasonable to speculate that sensitive cancer cells might acquire adaptive resistance to ABT-199 by elevating the expression of BFL-1, BCL-XL or BCL-W. Therefore, it will be of great interest to profile the expression changes of all BCL-2 family proteins in a large panel of cancer cell lines before and after exposure to ABT-199, to systematically study mechanisms of resistance to ABT-199.

Another potential mechanism that could promote resistance to ABT-199 is acquisition of mutations in BCL-2 protein. The BH1, BH2, and BH3 domains of BCL-2

protein form a hydrophobic pocket to sequester Bax, Bak, and BH3-only proteins. BH3 mimetic ABT-199 can dock into this pocket to replace and release Bax, Bak, and BH3-only proteins to promote apoptosis. If BCL-2 protein acquired mutations that cause the conformational changes of the hydrophobic pocket to make it less accessible or less avid for ABT-199, cancer cell lines with these Bcl-2 mutations could become resistant to ABT-199. Mutation acquisition mediated resistance to ABT-199 has been reported in mantle cell lymphoma cell lines after chronic exposure to this compound⁹⁴. Of note, the mutations in the BH3-binding pocket might also compromise the ability of BCL-2 to sequester Bax, Bak, or BH3-only proteins and, therefore, may not confer cancer cells survival advantages over cancer cells without these mutations. Based on this scenario, mutation-mediated resistance to BH3 mimetics such as ABT-199 is less likely to happen for BCL-2 anti-apoptotic proteins, when compared to many other cancer targets that do not rely on protein interactions for their oncogenic functions. In the era of omics, high-throughput techniques such as DNA-seq, RNA-seq, Reverse-Phase Protein micro-array (RPPA), can be utilized to systemically investigate the mechanisms of acquired resistance to ABT-199 by comparing the differences between the pre-treated cancer cells and cancer cells with acquired resistance.

4.2.2 To Study Mechanisms of Acquired Resistance to the Combination of BCL-2 Inhibition and p53 Activation

In Chapter 3, we have shown that the concomitant BCL-2 inhibition by ABT-199 and p53 activation by RG7388 could mutually overcome resistance to either treatment alone. As a result, the combination achieved remarkable efficacy *in vitro* and markedly prolonged survival in three resistance models of AML. Although the observed efficacy was impressive enough and actually exceeded our expectations, the combinatorial

treatment did not cure the mice. All mice eventually died of leukemia as manifested by the high leukemic burden of dissected mice, indicating that the engrafted AML cells eventually developed resistance to the combination therapy. It would be very intriguing to study the mechanism of acquired resistance to the combined therapy. The mechanistic findings from this proposed study could be of great significance as they could help devise novel strategies to overcome the acquired resistance so that to release the full potential of such combined therapy. Bearing this in mind, we have had collected and preserved the AML cells from the mice in the control, ABT-199, RG7388, and the combination groups. We are currently using high-throughput techniques such as RNA-seq, Reverse-Phase Protein micro-array (RPPA), and DNA-seq to systemically investigate mechanisms of acquired resistance to either monotherapy or to the combination therapy.

4.2.3 To Illustrate the Underlying Mechanism by Which p53 Negatively Regulates Ras

p53 is arguably the most important tumor suppressor protein, whereas Ras proteins are among the most important oncogenes. Ras proteins are single-subunit small GTPases, which function as binary signaling switches. When bound to GTP, Ras is switched to the “on” state, which initiates downstream signaling cascade to regulate diverse processes such as cell growth, survival, differentiation, and cell migration. When bound to GDP, Ras is switched to the “off” state. H-Ras, K-Ras, and N-Ras are three Ras protein variants in human cells. Mutations of H-, K-, and N-Ras have been implicated in many types of cancers. Ras mutations that lead to constitutive activation of Ras signaling are found in ~30% of all human tumors and up to 90% in certain types of cancers, making Ras mutations the most common abnormality of all human proto-

oncogenes.

It has been well documented that oncogenic Ras activation engages the ARF–p53 circuit to trigger p53 signaling. Our finding that p53 negatively regulates N-Ras at protein levels, identifies a previously unknown connection between p53 and N-Ras. The mechanism through which this is accomplished needs to be defined in future studies and should be of great interest to the p53 and Ras communities. Other intriguing questions are whether p53 also negatively regulates N-Ras in other types of cancers and whether p53 also downregulates the expression of other Ras variants in human, mouse, and other model systems.

4.2.4 To Study the Mechanism by Which ABT-199 Elevates MCL-1 Expression

In Chapter 3, we found that ABT-199, like its predecessor ABT-737, can induce MCL-1 expression within few hours. Yecies, *et al.* reported that ABT-737 exposure increased the expression of MCL-1 mRNA in lymphomas³¹. However, ABT-199 exposure did not elevate MCL-1 mRNA levels in our study (Figure 2.4D). We postulated that MCL-1 might be regulated at post-translational levels. Indeed, we found that ABT-199 treatment dramatically induced MCL-1 phosphorylation at Threonine 163, a post-translational modification that stabilizes MCL-1. The MEK/ERK signaling has been documented to promote MCL-1 phosphorylation at Threonine 163. Konopleva, *et al.* reported that ABT-737 was able to activate MEK/ERK signaling to elevate MCL-1 levels⁹⁵. In our current study with ABT-199, MEK/ERK signaling seemingly did not play a significant role because neither pMEK/pERK nor total MEK/ERK was affected by ABT-199 treatment. The detailed mechanism through which ABT-199 induced MCL-1 expression is beyond the scope of this study. Nevertheless, elucidating the underlying mechanism shall be of great significance, as it would help devise strategies to

circumvent the unwelcome elevation of MCL-1 that can be caused by even a low dose of ABT-199.

4.2.5 To Test the BCL-2 Inhibition/p53 Activation Strategy in immunocompetent Mice or in immunodeficient Mice with Humanized Immune System

For the mouse studies in Chapters 2 and 3, we injected AML cell lines or patient samples intravenously into NOD SCID gamma (NSG) mice. After confirmation of AML engraftment, the injected mice were treated with different therapeutic regimens. NSG mice are a proven host for engraftment of hematopoietic malignancies as well as solid tumors. The immunodeficient NSG mice combine the characteristics of the Non-obese diabetic (NOD) background, the severe combined immune deficiency mutation (*SCID*) background and the IL2 receptor gamma chain deficiency. As a result, NSG mice are severely immune-deficient and don't have mature T cells, B cells, or functional NK cells. NSG mice are also deficient in cytokine signaling because of the deficiency of IL2 receptor gamma chain. These features facilitate the engraftment of human normal or malignant cells, especially for engraftment of human hematopoietic cells and leukemia cells. However, *in vivo* studies using NSG mice may neglect the potential effects of innate and adaptive immunity in fighting cancer cells.

Accumulating pre-clinical and clinical evidence suggests that targeted therapies or conventional chemotherapies not only induce direct cytotoxic/cytostatic effects, but also stimulate immune responses to activate T, NK, and other immune cells to fight cancer cells. Because NSG mice do not have functional immune system, the xenograft mouse models in this study possibly underestimate the efficacy of our proposed combination strategy. The roles of immune system in cancer therapies can be studied using transgenic, syngeneic immunocompetent mouse models or immune-deficient mice with

established human immunity following transplantation with hematopoietic stem cells or peripheral blood mononuclear cells. The humanized mouse hosts recently become commercially available, though expensive, from the Jackson Laboratory. These immunocompetent mouse models could be used to study whether an immunocompetent background could further enhance the efficacy of combined BCL-2 inhibition and p53 activation.

4.2.6 To Study the Efficacy of Concurrent BCL-2 Inhibition and p53 Activation in killing Leukemia Stem Cells (LSCs)

LSCs are at the top of the hierarchy of malignant hematopoiesis and possess the ability to drive leukemogenesis *in vivo*^{96,97}. LSCs are typically quiescent and resistant to conventional chemotherapies and, as a result, potentially drive leukemia relapse after initial responses^{72,98}. Recent evidence suggests that most functionally defined chronic myeloid leukemia LSCs have relatively low levels of reactive oxygen species and aberrantly overexpress BCL-2 protein⁷². Furthermore, BCL-2-mediated oxidative phosphorylation is reportedly essential for LSC energy homeostasis, such that BCL-2 inhibition reduces oxidative phosphorylation and selectively eradicates quiescent CML LSCs⁷². Meanwhile, other published results have demonstrated that putative AML LSCs express high levels of MCL-1⁹⁹ and MCL-1 suppression kills transformed AML blast and stem cells, suggesting a critical role of MCL-1 for LSC survival²⁸, though not ruling out a concomitant requirement for BCL-2. Overall, it is still equivocal that whether BCL-2, MCL-1 or both are critical for LSC survival.

In Chapter 3, we found that p53 activation by RG7388 promoted MCL-1 degradation and induced pro-apoptotic proteins to counteract the remaining MCL-1. Base on this, it is reasonable to speculate that the combination of RG7388 and ABT-

199 may be very effective in killing LSCs by combined inhibition of Mcl-1 and Bcl-2. However, toxicity may be an issue when targeting proteins expressed in both leukemic stem cells and hematopoietic stem cells. In this regard, Opferman and colleagues reported that MCL-1 might play an essential role in the survival of murine hematopoietic stem cells and early myeloid precursors⁶³. In the same study, murine AML cells were demonstrated to be more sensitive to MCL-1 deletion than normal hematopoietic stem and progenitor cells⁶³, suggesting that a therapeutic window might exist. Consistently, we found that a pan-BCL-2 antagonist, which simultaneously inhibits BCL-2, MCL-1, BCL-XL, and BFL-1 but with the highest affinity for MCL-1, killed most LSCs but were well tolerated by hematopoietic stem and progenitor cells⁷⁹. Based on these, we speculate that the combination of BCL-2 inhibition and p53 activation may effectively kill LSCs while sparing the majority of normal hematopoietic stem and progenitor cells. However, the conclusions can only be drawn from systematic pre-clinical or clinical studies to evaluate the toxicity of such combined therapy on normal hematopoiesis.

Bibliography

- 1 Pazarentzos, E. & Bivona, T. G. Adaptive stress signaling in targeted cancer therapy resistance. *Oncogene* **34**, 5599-5606, doi:10.1038/onc.2015.26 (2015).
- 2 Trusolino, L. & Bertotti, A. Compensatory pathways in oncogenic kinase signaling and resistance to targeted therapies: six degrees of separation. *Cancer Discov.* **2**, 876-880, doi:10.1158/2159-8290.CD-12-0400 (2012).
- 3 Chandarlapaty, S. Negative feedback and adaptive resistance to the targeted therapy of cancer. *Cancer Discov.* **2**, 311-319, doi:10.1158/2159-8290.CD-12-0018 (2012).
- 4 Hata, A. N., Engelman, J. A. & Faber, A. C. The BCL2 family: key mediators of the apoptotic response to targeted anticancer therapeutics. *Cancer Discov.* **5**, 475-487, doi:10.1158/2159-8290.CD-15-0011 (2015).
- 5 Delbridge, A. R., Grabow, S., Strasser, A. & Vaux, D. L. Thirty years of BCL-2: translating cell death discoveries into novel cancer therapies. *Nat. Rev. Cancer* **16**, 99-109, doi:10.1038/nrc.2015.17 (2016).
- 6 Letai, A. G. Diagnosing and exploiting cancer's addiction to blocks in apoptosis. *Nature reviews. Cancer* **8**, 121-132, doi:10.1038/nrc2297 (2008).
- 7 Hanahan, D. & Weinberg, R. A. Hallmarks of cancer: the next generation. *Cell* **144**, 646-674, doi:10.1016/j.cell.2011.02.013 (2011).

- 8 Hoe, K. K., Verma, C. S. & Lane, D. P. Drugging the p53 pathway: understanding the route to clinical efficacy. *Nature reviews. Drug discovery* **13**, 217-236, doi:10.1038/nrd4236 (2014).
- 9 Czabotar, P. E., Lessene, G., Strasser, A. & Adams, J. M. Control of apoptosis by the BCL-2 protein family: implications for physiology and therapy. *Nat. Rev. Mol. Cell Biol.* **15**, 49-63, doi:10.1038/nrm3722 (2014).
- 10 Konopleva, M., Pollyea, D. A., Potluri, J., Chyla, B., Hogdal, L., Busman, T., McKeegan, E., Salem, A. H., Zhu, M., Ricker, J. L., Blum, W., DiNardo, C. D., Kadia, T., Dunbar, M., Kirby, R., Falotico, N., Levenson, J., Humerickhouse, R., Mabry, M., Stone, R., Kantarjian, H. & Letai, A. Efficacy and Biological Correlates of Response in a Phase II Study of Venetoclax Monotherapy in Patients with Acute Myelogenous Leukemia. *Cancer Discov.*, doi:10.1158/2159-8290.CD-16-0313 (2016).
- 11 Pan, R., Hogdal, L. J., Benito, J. M., Bucci, D., Han, L., Borthakur, G., Cortes, J., DeAngelo, D. J., Debose, L., Mu, H., Dohner, H., Gaidzik, V. I., Galinsky, I., Golfman, L. S., Haferlach, T., Harutyunyan, K. G., Hu, J., Levenson, J. D., Marcucci, G., Muschen, M., Newman, R., Park, E., Ruvolo, P. P., Ruvolo, V., Ryan, J., Schindela, S., Zweidler-McKay, P., Stone, R. M., Kantarjian, H., Andreeff, M., Konopleva, M. & Letai, A. G. Selective BCL-2 inhibition by ABT-199 causes on-target cell death in acute myeloid leukemia. *Cancer discovery* **4**, 362-375, doi:10.1158/2159-8290.CD-13-0609 (2014).

- 12 Volkmann, N., Marassi, F. M., Newmeyer, D. D. & Hanein, D. The rheostat in the membrane: BCL-2 family proteins and apoptosis. *Cell Death Differ.* **21**, 206-215, doi:10.1038/cdd.2013.153 (2014).
- 13 Taylor, R. C., Cullen, S. P. & Martin, S. J. Apoptosis: controlled demolition at the cellular level. *Nat. Rev. Mol. Cell Biol.* **9**, 231-241, doi:10.1038/nrm2312 (2008).
- 14 Moldoveanu, T., Follis, A. V., Kriwacki, R. W. & Green, D. R. Many players in BCL-2 family affairs. *Trends Biochem. Sci.* **39**, 101-111, doi:10.1016/j.tibs.2013.12.006 (2014).
- 15 Vucic, D., Dixit, V. M. & Wertz, I. E. Ubiquitylation in apoptosis: a post-translational modification at the edge of life and death. *Nat. Rev. Mol. Cell Biol.* **12**, 439-452, doi:10.1038/nrm3143 (2011).
- 16 Youle, R. J. & Strasser, A. The BCL-2 protein family: opposing activities that mediate cell death. *Nat. Rev. Mol. Cell Biol.* **9**, 47-59, doi:10.1038/nrm2308 (2008).
- 17 Juin, P., Geneste, O., Gautier, F., Depil, S. & Campone, M. Decoding and unlocking the BCL-2 dependency of cancer cells. *Nat. Rev. Cancer* **13**, 455-465, doi:10.1038/nrc3538 (2013).
- 18 Delbridge, A. R. & Strasser, A. The BCL-2 protein family, BH3-mimetics and cancer therapy. *Cell Death Differ.* **22**, 1071-1080, doi:10.1038/cdd.2015.50 (2015).
- 19 Shamas-Din, A., Kale, J., Leber, B. & Andrews, D. W. Mechanisms of action of Bcl-2 family proteins. *Cold Spring Harb. Perspect. Biol.* **5**, a008714, doi:10.1101/cshperspect.a008714 (2013).

- 20 Letai, A., Bassik, M. C., Walensky, L. D., Sorcinelli, M. D., Weiler, S. & Korsmeyer, S. J. Distinct BH3 domains either sensitize or activate mitochondrial apoptosis, serving as prototype cancer therapeutics. *Cancer Cell* **2**, 183-192 (2002).
- 21 Jabbour, A. M., Heraud, J. E., Daunt, C. P., Kaufmann, T., Sandow, J., O'Reilly, L. A., Callus, B. A., Lopez, A., Strasser, A., Vaux, D. L. & Ekert, P. G. Puma indirectly activates Bax to cause apoptosis in the absence of Bid or Bim. *Cell Death Differ* **16**, 555-563, doi:10.1038/cdd.2008.179 (2009).
- 22 Ren, D., Tu, H. C., Kim, H., Wang, G. X., Bean, G. R., Takeuchi, O., Jeffers, J. R., Zambetti, G. P., Hsieh, J. J. & Cheng, E. H. BID, BIM, and PUMA are essential for activation of the BAX- and BAK-dependent cell death program. *Science* **330**, 1390-1393, doi:10.1126/science.1190217 (2010).
- 23 Certo, M., Del Gaizo Moore, V., Nishino, M., Wei, G., Korsmeyer, S., Armstrong, S. A. & Letai, A. Mitochondria primed by death signals determine cellular addiction to antiapoptotic BCL-2 family members. *Cancer Cell* **9**, 351-365, doi:10.1016/j.ccr.2006.03.027 (2006).
- 24 Cheng, E. H., Wei, M. C., Weiler, S., Flavell, R. A., Mak, T. W., Lindsten, T. & Korsmeyer, S. J. BCL-2, BCL-X(L) sequester BH3 domain-only molecules preventing BAX- and BAK-mediated mitochondrial apoptosis. *Mol Cell* **8**, 705-711 (2001).
- 25 Oltersdorf, T., Elmore, S. W., Shoemaker, A. R., Armstrong, R. C., Augeri, D. J., Belli, B. A., Bruncko, M., Deckwerth, T. L., Dinges, J., Hajduk, P. J., Joseph, M. K., Kitada, S., Korsmeyer, S. J., Kunzer, A. R., Letai, A., Li, C., Mitten, M. J.,

Nettesheim, D. G., Ng, S., Nimmer, P. M., O'Connor, J. M., Oleksijew, A., Petros, A. M., Reed, J. C., Shen, W., Tahir, S. K., Thompson, C. B., Tomaselli, K. J., Wang, B., Wendt, M. D., Zhang, H., Fesik, S. W. & Rosenberg, S. H. An inhibitor of Bcl-2 family proteins induces regression of solid tumours. *Nature* **435**, 677-681, doi:10.1038/nature03579 (2005).

26 Tse, C., Shoemaker, A. R., Adickes, J., Anderson, M. G., Chen, J., Jin, S., Johnson, E. F., Marsh, K. C., Mitten, M. J., Nimmer, P., Roberts, L., Tahir, S. K., Xiao, Y., Yang, X., Zhang, H., Fesik, S., Rosenberg, S. H. & Elmore, S. W. ABT-263: a potent and orally bioavailable Bcl-2 family inhibitor. *Cancer Res.* **68**, 3421-3428, doi:10.1158/0008-5472.CAN-07-5836 (2008).

27 Souers, A. J., Levenson, J. D., Boghaert, E. R., Ackler, S. L., Catron, N. D., Chen, J., Dayton, B. D., Ding, H., Enschede, S. H., Fairbrother, W. J., Huang, D. C., Hymowitz, S. G., Jin, S., Khaw, S. L., Kovar, P. J., Lam, L. T., Lee, J., Maecker, H. L., Marsh, K. C., Mason, K. D., Mitten, M. J., Nimmer, P. M., Oleksijew, A., Park, C. H., Park, C. M., Phillips, D. C., Roberts, A. W., Sampath, D., Seymour, J. F., Smith, M. L., Sullivan, G. M., Tahir, S. K., Tse, C., Wendt, M. D., Xiao, Y., Xue, J. C., Zhang, H., Humerickhouse, R. A., Rosenberg, S. H. & Elmore, S. W. ABT-199, a potent and selective BCL-2 inhibitor, achieves antitumor activity while sparing platelets. *Nat. Med.* **19**, 202-208, doi:10.1038/nm.3048 (2013).

28 Gores, G. J. & Kaufmann, S. H. Selectively targeting Mcl-1 for the treatment of acute myelogenous leukemia and solid tumors. *Genes Dev.* **26**, 305-311, doi:10.1101/gad.186189.111 (2012).

- 29 Konopleva, M., Contractor, R., Tsao, T., Samudio, I., Ruvolo, P. P., Kitada, S., Deng, X., Zhai, D., Shi, Y. X., Sneed, T., Verhaegen, M., Soengas, M., Ruvolo, V. R., McQueen, T., Schober, W. D., Watt, J. C., Jiffar, T., Ling, X., Marini, F. C., Harris, D., Dietrich, M., Estrov, Z., McCubrey, J., May, W. S., Reed, J. C. & Andreeff, M. Mechanisms of apoptosis sensitivity and resistance to the BH3 mimetic ABT-737 in acute myeloid leukemia. *Cancer Cell* **10**, 375-388, doi:10.1016/j.ccr.2006.10.006 (2006).
- 30 Roberts, A. W., Seymour, J. F., Brown, J. R., Wierda, W. G., Kipps, T. J., Khaw, S. L., Carney, D. A., He, S. Z., Huang, D. C., Xiong, H., Cui, Y., Busman, T. A., McKeegan, E. M., Krivoschik, A. P., Enschede, S. H. & Humerickhouse, R. Substantial susceptibility of chronic lymphocytic leukemia to BCL2 inhibition: results of a phase I study of navitoclax in patients with relapsed or refractory disease. *J. Clin. Oncol.* **30**, 488-496, doi:10.1200/JCO.2011.34.7898 (2012).
- 31 Yecies, D., Carlson, N. E., Deng, J. & Letai, A. Acquired resistance to ABT-737 in lymphoma cells that up-regulate MCL-1 and BFL-1. *Blood* **115**, 3304-3313, doi:10.1182/blood-2009-07-233304 (2010).
- 32 Beroukhim, R., Mermel, C. H., Porter, D., Wei, G., Raychaudhuri, S., Donovan, J., Barretina, J., Boehm, J. S., Dobson, J., Urashima, M., Mc Henry, K. T., Pinchback, R. M., Ligon, A. H., Cho, Y. J., Haery, L., Greulich, H., Reich, M., Winckler, W., Lawrence, M. S., Weir, B. A., Tanaka, K. E., Chiang, D. Y., Bass, A. J., Loo, A., Hoffman, C., Prensner, J., Liefeld, T., Gao, Q., Yecies, D., Signoretti, S., Maher, E., Kaye, F. J., Sasaki, H., Tepper, J. E., Fletcher, J. A., Tabernero, J., Baselga, J., Tsao, M. S., Demichelis, F., Rubin, M. A., Janne, P. A., Daly, M. J., Nucera, C.,

Levine, R. L., Ebert, B. L., Gabriel, S., Rustgi, A. K., Antonescu, C. R., Ladanyi, M., Letai, A., Garraway, L. A., Loda, M., Beer, D. G., True, L. D., Okamoto, A., Pomeroy, S. L., Singer, S., Golub, T. R., Lander, E. S., Getz, G., Sellers, W. R. & Meyerson, M. The landscape of somatic copy-number alteration across human cancers. *Nature* **463**, 899-905, doi:10.1038/nature08822 (2010).

- 33 Belmar, J. & Fesik, S. W. Small molecule Mcl-1 inhibitors for the treatment of cancer. *Pharmacol. Ther.* **145**, 76-84, doi:10.1016/j.pharmthera.2014.08.003 (2015).
- 34 Czabotar, P. E., Lee, E. F., van Delft, M. F., Day, C. L., Smith, B. J., Huang, D. C., Fairlie, W. D., Hinds, M. G. & Colman, P. M. Structural insights into the degradation of Mcl-1 induced by BH3 domains. *Proc. Natl. Acad. Sci. U. S. A.* **104**, 6217-6222, doi:10.1073/pnas.0701297104 (2007).
- 35 Bieging, K. T. & Attardi, L. D. Deconstructing p53 transcriptional networks in tumor suppression. *Trends Cell Biol.* **22**, 97-106, doi:10.1016/j.tcb.2011.10.006 (2012).
- 36 Lehmann, B. D. & Pietenpol, J. A. Targeting mutant p53 in human tumors. *J. Clin. Oncol.* **30**, 3648-3650, doi:10.1200/JCO.2012.44.0412 (2012).
- 37 Wade, M., Li, Y. C. & Wahl, G. M. MDM2, MDMX and p53 in oncogenesis and cancer therapy. *Nat. Rev. Cancer* **13**, 83-96, doi:10.1038/nrc3430 (2013).
- 38 Cheok, C. F., Verma, C. S., Baselga, J. & Lane, D. P. Translating p53 into the clinic. *Nat. Rev. Clin. Oncol.* **8**, 25-37, doi:10.1038/nrclinonc.2010.174 (2011).

- 39 Brady, C. A. & Attardi, L. D. p53 at a glance. *J. Cell Sci.* **123**, 2527-2532, doi:10.1242/jcs.064501 (2010).
- 40 Chene, P. Inhibiting the p53-MDM2 interaction: an important target for cancer therapy. *Nat. Rev. Cancer* **3**, 102-109, doi:10.1038/nrc991 (2003).
- 41 Muller, P. A. & Vousden, K. H. Mutant p53 in cancer: new functions and therapeutic opportunities. *Cancer Cell* **25**, 304-317, doi:10.1016/j.ccr.2014.01.021 (2014).
- 42 Kruiswijk, F., Labuschagne, C. F. & Vousden, K. H. p53 in survival, death and metabolic health: a lifeguard with a licence to kill. *Nat. Rev. Mol. Cell Biol.* **16**, 393-405, doi:10.1038/nrm4007 (2015).
- 43 Muller, P. A. & Vousden, K. H. p53 mutations in cancer. *Nat. Cell Biol.* **15**, 2-8, doi:10.1038/ncb2641 (2013).
- 44 Xu-Monette, Z. Y., Medeiros, L. J., Li, Y., Orlowski, R. Z., Andreeff, M., Bueso-Ramos, C. E., Greiner, T. C., McDonnell, T. J. & Young, K. H. Dysfunction of the TP53 tumor suppressor gene in lymphoid malignancies. *Blood* **119**, 3668-3683, doi:10.1182/blood-2011-11-366062 (2012).
- 45 Kojima, K., Konopleva, M., McQueen, T., O'Brien, S., Plunkett, W. & Andreeff, M. Mdm2 inhibitor Nutlin-3a induces p53-mediated apoptosis by transcription-dependent and transcription-independent mechanisms and may overcome Atm-mediated resistance to fludarabine in chronic lymphocytic leukemia. *Blood* **108**, 993-1000, doi:10.1182/blood-2005-12-5148 (2006).

- 46 Kojima, K., Konopleva, M., Samudio, I. J., Shikami, M., Cabreira-Hansen, M., McQueen, T., Ruvolo, V., Tsao, T., Zeng, Z., Vassilev, L. T. & Andreeff, M. MDM2 antagonists induce p53-dependent apoptosis in AML: implications for leukemia therapy. *Blood* **106**, 3150-3159, doi:10.1182/blood-2005-02-0553 (2005).
- 47 Vassilev, L. T., Vu, B. T., Graves, B., Carvajal, D., Podlaski, F., Filipovic, Z., Kong, N., Kammlott, U., Lukacs, C., Klein, C., Fotouhi, N. & Liu, E. A. In vivo activation of the p53 pathway by small-molecule antagonists of MDM2. *Science* **303**, 844-848, doi:10.1126/science.1092472 (2004).
- 48 Ding, Q., Zhang, Z., Liu, J. J., Jiang, N., Zhang, J., Ross, T. M., Chu, X. J., Bartkovitz, D., Podlaski, F., Janson, C., Tovar, C., Filipovic, Z. M., Higgins, B., Glenn, K., Packman, K., Vassilev, L. T. & Graves, B. Discovery of RG7388, a potent and selective p53-MDM2 inhibitor in clinical development. *J. Med. Chem.*, doi:10.1021/jm400487c (2013).
- 49 Estey, E. & Dohner, H. Acute myeloid leukaemia. *Lancet* **368**, 1894-1907, doi:10.1016/S0140-6736(06)69780-8 (2006).
- 50 Klepin, H. D., Rao, A. V. & Pardee, T. S. Acute Myeloid Leukemia and Myelodysplastic Syndromes in Older Adults. *J. Clin. Oncol.*, doi:10.1200/JCO.2014.55.1564 (2014).
- 51 Dombret, H. & Gardin, C. An update of current treatments for adult acute myeloid leukemia. *Blood* **127**, 53-61, doi:10.1182/blood-2015-08-604520 (2016).
- 52 Dohner, H., Weisdorf, D. J. & Bloomfield, C. D. Acute Myeloid Leukemia. *N. Engl. J. Med.* **373**, 1136-1152, doi:10.1056/NEJMra1406184 (2015).

- 53 Lo-Coco, F., Avvisati, G., Vignetti, M., Thiede, C., Orlando, S. M., Iacobelli, S., Ferrara, F., Fazi, P., Cicconi, L., Di Bona, E., Specchia, G., Sica, S., Divona, M., Levis, A., Fiedler, W., Cerqui, E., Breccia, M., Fioritoni, G., Salih, H. R., Cazzola, M., Melillo, L., Carella, A. M., Brandts, C. H., Morra, E., von Lilienfeld-Toal, M., Hertenstein, B., Wattad, M., Lubbert, M., Hanel, M., Schmitz, N., Link, H., Kropp, M. G., Rambaldi, A., La Nasa, G., Luppi, M., Ciceri, F., Finizio, O., Venditti, A., Fabbiano, F., Dohner, K., Sauer, M., Ganser, A., Amadori, S., Mandelli, F., Dohner, H., Ehninger, G., Schlenk, R. F., Platzbecker, U., Gruppo Italiano Malattie Ematologiche, d. A., German-Austrian Acute Myeloid Leukemia Study, G. & Study Alliance, L. Retinoic acid and arsenic trioxide for acute promyelocytic leukemia. *N. Engl. J. Med.* **369**, 111-121, doi:10.1056/NEJMoa1300874 (2013).
- 54 Chen, Y., Jacamo, R., Konopleva, M., Garzon, R., Croce, C. & Andreeff, M. CXCR4 downregulation of let-7a drives chemoresistance in acute myeloid leukemia. *J. Clin. Invest.* **123**, 2395-2407, doi:10.1172/JCI66553 (2013).
- 55 Karajannis, M. A., Vincent, L., Drenzo, R., Shmelkov, S. V., Zhang, F., Feldman, E. J., Bohlen, P., Zhu, Z., Sun, H., Kussie, P. & Rafii, S. Activation of FGFR1beta signaling pathway promotes survival, migration and resistance to chemotherapy in acute myeloid leukemia cells. *Leukemia* **20**, 979-986, doi:10.1038/sj.leu.2404203 (2006).
- 56 Walter, R. B. & Estey, E. H. Management of older or unfit patients with acute myeloid leukemia. *Leukemia* **29**, 770-775, doi:10.1038/leu.2014.216 (2015).
- 57 Ley, T. J., Mardis, E. R., Ding, L., Fulton, B., McLellan, M. D., Chen, K., Dooling, D., Dunford-Shore, B. H., McGrath, S., Hickenbotham, M., Cook, L., Abbott, R.,

Larson, D. E., Koboldt, D. C., Pohl, C., Smith, S., Hawkins, A., Abbott, S., Locke, D., Hillier, L. W., Miner, T., Fulton, L., Magrini, V., Wylie, T., Glasscock, J., Conyers, J., Sander, N., Shi, X., Osborne, J. R., Minx, P., Gordon, D., Chinwalla, A., Zhao, Y., Ries, R. E., Payton, J. E., Westervelt, P., Tomasson, M. H., Watson, M., Baty, J., Ivanovich, J., Heath, S., Shannon, W. D., Nagarajan, R., Walter, M. J., Link, D. C., Graubert, T. A., DiPersio, J. F. & Wilson, R. K. DNA sequencing of a cytogenetically normal acute myeloid leukaemia genome. *Nature* **456**, 66-72, doi:10.1038/nature07485 (2008).

58 Gandhi, L., Camidge, D. R., Ribeiro de Oliveira, M., Bonomi, P., Gandara, D., Khaira, D., Hann, C. L., McKeegan, E. M., Litvinovich, E., Hemken, P. M., Dive, C., Enschede, S. H., Nolan, C., Chiu, Y. L., Busman, T., Xiong, H., Krivoshik, A. P., Humerickhouse, R., Shapiro, G. I. & Rudin, C. M. Phase I study of Navitoclax (ABT-263), a novel Bcl-2 family inhibitor, in patients with small-cell lung cancer and other solid tumors. *J Clin Oncol* **29**, 909-916, doi:10.1200/JCO.2010.31.6208 (2011).

59 Schoenwaelder, S. M., Jarman, K. E., Gardiner, E. E., Hua, M., Qiao, J., White, M. J., Josefsson, E. C., Alwis, I., Ono, A., Willcox, A., Andrews, R. K., Mason, K. D., Salem, H. H., Huang, D. C., Kile, B. T., Roberts, A. W. & Jackson, S. P. Bcl-xL-inhibitory BH3 mimetics can induce a transient thrombocytopathy that undermines the hemostatic function of platelets. *Blood* **118**, 1663-1674, doi:10.1182/blood-2011-04-347849 (2011).

60 Vandenberg, C. J. & Cory, S. ABT-199, a new Bcl-2-specific BH3 mimetic, has in vivo efficacy against aggressive Myc-driven mouse lymphomas without provoking

thrombocytopenia. *Blood* **121**, 2285-2288, doi:10.1182/blood-2013-01-475855 (2013).

- 61 Vaillant, F., Merino, D., Lee, L., Breslin, K., Pal, B., Ritchie, M. E., Smyth, G. K., Christie, M., Phillipson, L. J., Burns, C. J., Mann, G. B., Visvader, J. E. & Lindeman, G. J. Targeting BCL-2 with the BH3 Mimetic ABT-199 in Estrogen Receptor-Positive Breast Cancer. *Cancer Cell* **24**, 120-129, doi:10.1016/j.ccr.2013.06.002 (2013).
- 62 Vo, T. T., Ryan, J., Carrasco, R., Neuberg, D., Rossi, D. J., Stone, R. M., Deangelo, D. J., Frattini, M. G. & Letai, A. Relative mitochondrial priming of myeloblasts and normal HSCs determines chemotherapeutic success in AML. *Cell* **151**, 344-355, doi:10.1016/j.cell.2012.08.038 (2012).
- 63 Opferman, J. T., Iwasaki, H., Ong, C. C., Suh, H., Mizuno, S., Akashi, K. & Korsmeyer, S. J. Obligate role of anti-apoptotic MCL-1 in the survival of hematopoietic stem cells. *Science* **307**, 1101-1104, doi:10.1126/science.1106114 (2005).
- 64 Deng, J., Carlson, N., Takeyama, K., Dal Cin, P., Shipp, M. & Letai, A. BH3 profiling identifies three distinct classes of apoptotic blocks to predict response to ABT-737 and conventional chemotherapeutic agents. *Cancer Cell* **12**, 171-185, doi:10.1016/j.ccr.2007.07.001 (2007).
- 65 Ni Chonghaile, T., Sarosiek, K. A., Vo, T. T., Ryan, J. A., Tammareddi, A., Moore, V. e. G., Deng, J., Anderson, K. C., Richardson, P., Tai, Y. T., Mitsiades, C. S., Matulonis, U. A., Drapkin, R., Stone, R., Deangelo, D. J., McConkey, D. J., Sallan,

S. E., Silverman, L., Hirsch, M. S., Carrasco, D. R. & Letai, A. Pretreatment mitochondrial priming correlates with clinical response to cytotoxic chemotherapy. *Science* **334**, 1129-1133, doi:10.1126/science.1206727 (2011).

66 Brunelle, J. K., Ryan, J., Yecies, D., Opferman, J. T. & Letai, A. MCL-1-dependent leukemia cells are more sensitive to chemotherapy than BCL-2-dependent counterparts. *J Cell Biol* **187**, 429-442, doi:10.1083/jcb.200904049 (2009).

67 Ruvolo, V. R., Karanjeet, K. B., Schuster, T. F., Brown, R., Deng, Y., Hinchcliffe, E. & Ruvolo, P. P. Role for PKC δ in Fenretinide-Mediated Apoptosis in Lymphoid Leukemia Cells. *J Signal Transduct* **2010**, 584657, doi:10.1155/2010/584657 (2010).

68 Chen, Y., Jacamo, R., Shi, Y. X., Wang, R. Y., Battula, V. L., Konoplev, S., Strunk, D., Hofmann, N. A., Reinisch, A., Konopleva, M. & Andreeff, M. Human extramedullary bone marrow in mice: a novel in vivo model of genetically controlled hematopoietic microenvironment. *Blood* **119**, 4971-4980, doi:10.1182/blood-2011-11-389957 (2012).

69 Haferlach, T., Kohlmann, A., Wiczorek, L., Basso, G., Kronnie, G. T., Béné, M. C., De Vos, J., Hernández, J. M., Hofmann, W. K., Mills, K. I., Gilkes, A., Chiaretti, S., Shurtleff, S. A., Kipps, T. J., Rassenti, L. Z., Yeoh, A. E., Papenhausen, P. R., Liu, W. M., Williams, P. M. & Foà, R. Clinical utility of microarray-based gene expression profiling in the diagnosis and subclassification of leukemia: report from the International Microarray Innovations in Leukemia Study Group. *J Clin Oncol* **28**, 2529-2537, doi:10.1200/JCO.2009.23.4732 (2010).

- 70 John Francis Seymour, M. S. D., John M. Pagel, Brad S. Kahl, William G. Wierda, Thomas P. Miller, John F. Gerecitano, Thomas J. Kipps, Mary Ann Anderson, David C.S. Huang, David E. Darden, Lori A. Gressick, Cathy E. Nolan, Jianning Yang, Todd A. Busman, Alison M. Graham, Elisa Cerri, Sari H. Enschede, Rod A. Humerickhouse, Andrew Warwick Roberts. (J Clin Oncol 31, 2013 (suppl; abstr 7018), 2013).
- 71 Jordan, C. T., Upchurch, D., Szilvassy, S. J., Guzman, M. L., Howard, D. S., Pettigrew, A. L., Meyerrose, T., Rossi, R., Grimes, B., Rizzieri, D. A., Luger, S. M. & Phillips, G. L. The interleukin-3 receptor alpha chain is a unique marker for human acute myelogenous leukemia stem cells. *Leukemia* **14**, 1777-1784 (2000).
- 72 Lagadinou, E. D., Sach, A., Callahan, K., Rossi, R. M., Neering, S. J., Minhajuddin, M., Ashton, J. M., Pei, S., Grose, V., O'Dwyer, K. M., Liesveld, J. L., Brookes, P. S., Becker, M. W. & Jordan, C. T. BCL-2 inhibition targets oxidative phosphorylation and selectively eradicates quiescent human leukemia stem cells. *Cell stem cell* **12**, 329-341, doi:10.1016/j.stem.2012.12.013 (2013).
- 73 Del Gaizo Moore, V., Brown, J. R., Certo, M., Love, T. M., Novina, C. D. & Letai, A. Chronic lymphocytic leukemia requires BCL2 to sequester prodeath BIM, explaining sensitivity to BCL2 antagonist ABT-737. *J Clin Invest* **117**, 112-121, doi:10.1172/JCI28281 (2007).
- 74 Del Gaizo Moore, V., Schlis, K. D., Sallan, S. E., Armstrong, S. A. & Letai, A. BCL-2 dependence and ABT-737 sensitivity in acute lymphoblastic leukemia. *Blood* **111**, 2300-2309, doi:10.1182/blood-2007-06-098012 (2008).

- 75 Weinberg, R. A. (Garland Science, Taylor & Francis Group LLC, New York, NY, 2014).
- 76 Cerami, E., Gao, J., Dogrusoz, U., Gross, B. E., Sumer, S. O., Aksoy, B. A., Jacobsen, A., Byrne, C. J., Heuer, M. L., Larsson, E., Antipin, Y., Reva, B., Goldberg, A. P., Sander, C. & Schultz, N. The cBio cancer genomics portal: an open platform for exploring multidimensional cancer genomics data. *Cancer Discov.* **2**, 401-404, doi:10.1158/2159-8290.CD-12-0095 (2012).
- 77 Kubbutat, M. H., Jones, S. N. & Vousden, K. H. Regulation of p53 stability by Mdm2. *Nature* **387**, 299-303, doi:10.1038/387299a0 (1997).
- 78 Haupt, Y., Maya, R., Kazaz, A. & Oren, M. Mdm2 promotes the rapid degradation of p53. *Nature* **387**, 296-299, doi:10.1038/387296a0 (1997).
- 79 Pan, R., Ruvolo, V. R., Wei, J., Konopleva, M., Reed, J. C., Pellecchia, M., Andreeff, M. & Ruvolo, P. P. Inhibition of Mcl-1 with the pan-Bcl-2 family inhibitor (-)BI97D6 overcomes ABT-737 resistance in acute myeloid leukemia. *Blood* **126**, 363-372, doi:10.1182/blood-2014-10-604975 (2015).
- 80 Kracikova, M., Akiri, G., George, A., Sachidanandam, R. & Aaronson, S. A. A threshold mechanism mediates p53 cell fate decision between growth arrest and apoptosis. *Cell Death Differ.* **20**, 576-588, doi:10.1038/cdd.2012.155 (2013).
- 81 Opferman, J. T. Unraveling MCL-1 degradation. *Cell Death Differ.* **13**, 1260-1262, doi:10.1038/sj.cdd.4401978 (2006).

- 82 Morel, C., Carlson, S. M., White, F. M. & Davis, R. J. Mcl-1 integrates the opposing actions of signaling pathways that mediate survival and apoptosis. *Mol. Cell. Biol.* **29**, 3845-3852, doi:10.1128/MCB.00279-09 (2009).
- 83 Maurer, U., Charvet, C., Wagman, A. S., Dejardin, E. & Green, D. R. Glycogen synthase kinase-3 regulates mitochondrial outer membrane permeabilization and apoptosis by destabilization of MCL-1. *Mol. Cell* **21**, 749-760, doi:10.1016/j.molcel.2006.02.009 (2006).
- 84 Cohen, P. & Frame, S. The renaissance of GSK3. *Nat. Rev. Mol. Cell Biol.* **2**, 769-776, doi:10.1038/35096075 (2001).
- 85 Ding, Q., Xia, W., Liu, J. C., Yang, J. Y., Lee, D. F., Xia, J., Bartholomeusz, G., Li, Y., Pan, Y., Li, Z., Bargou, R. C., Qin, J., Lai, C. C., Tsai, F. J., Tsai, C. H. & Hung, M. C. Erk associates with and primes GSK-3 β for its inactivation resulting in upregulation of β -catenin. *Mol. Cell* **19**, 159-170, doi:10.1016/j.molcel.2005.06.009 (2005).
- 86 Karnoub, A. E. & Weinberg, R. A. Ras oncogenes: split personalities. *Nat. Rev. Mol. Cell Biol.* **9**, 517-531, doi:10.1038/nrm2438 (2008).
- 87 Lowe, S. W., Cepero, E. & Evan, G. Intrinsic tumour suppression. *Nature* **432**, 307-315, doi:10.1038/nature03098 (2004).
- 88 Tsujimoto, Y., Finger, L. R., Yunis, J., Nowell, P. C. & Croce, C. M. Cloning of the chromosome breakpoint of neoplastic B cells with the t(14;18) chromosome translocation. *Science* **226**, 1097-1099 (1984).

- 89 Gulpinar, E. & Vousden, K. H. Hitting cancers' weak spots: vulnerabilities imposed by p53 mutation. *Trends Cell Biol.* **25**, 486-495, doi:10.1016/j.tcb.2015.04.001 (2015).
- 90 Chen, X., Ko, L. J., Jayaraman, L. & Prives, C. p53 levels, functional domains, and DNA damage determine the extent of the apoptotic response of tumor cells. *Genes Dev.* **10**, 2438-2451 (1996).
- 91 Coustan-Smith, E., Kitanaka, A., Pui, C. H., McNinch, L., Evans, W. E., Raimondi, S. C., Behm, F. G., Arico, M. & Campana, D. Clinical relevance of BCL-2 overexpression in childhood acute lymphoblastic leukemia. *Blood* **87**, 1140-1146 (1996).
- 92 Iqbal, J., Neppalli, V. T., Wright, G., Dave, B. J., Horsman, D. E., Rosenwald, A., Lynch, J., Hans, C. P., Weisenburger, D. D., Greiner, T. C., Gascoyne, R. D., Campo, E., Ott, G., Muller-Hermelink, H. K., Delabie, J., Jaffe, E. S., Grogan, T. M., Connors, J. M., Vose, J. M., Armitage, J. O., Staudt, L. M. & Chan, W. C. BCL2 expression is a prognostic marker for the activated B-cell-like type of diffuse large B-cell lymphoma. *J. Clin. Oncol.* **24**, 961-968, doi:10.1200/JCO.2005.03.4264 (2006).
- 93 Reed, J. C. Bcl-2-family proteins and hematologic malignancies: history and future prospects. *Blood* **111**, 3322-3330, doi:10.1182/blood-2007-09-078162 (2008).
- 94 Fresquet, V., Rieger, M., Carolis, C., Garcia-Barchino, M. J. & Martinez-Climent, J. A. Acquired mutations in BCL2 family proteins conferring resistance to the BH3 mimetic ABT-199 in lymphoma. *Blood*, doi:10.1182/blood-2014-03-560284 (2014).

- 95 Konopleva, M., Milella, M., Ruvolo, P., Watts, J. C., Ricciardi, M. R., Korchin, B., McQueen, T., Bornmann, W., Tsao, T., Bergamo, P., Mak, D. H., Chen, W., McCubrey, J., Tafuri, A. & Andreeff, M. MEK inhibition enhances ABT-737-induced leukemia cell apoptosis via prevention of ERK-activated MCL-1 induction and modulation of MCL-1/BIM complex. *Leukemia* **26**, 778-787, doi:10.1038/leu.2011.287 (2012).
- 96 Walter, R. B., Appelbaum, F. R., Estey, E. H. & Bernstein, I. D. Acute myeloid leukemia stem cells and CD33-targeted immunotherapy. *Blood* **119**, 6198-6208, doi:10.1182/blood-2011-11-325050 (2012).
- 97 Jordan, C. T. Targeting myeloid leukemia stem cells. *Sci. Transl. Med.* **2**, 31ps21, doi:10.1126/scitranslmed.3000914 (2010).
- 98 Saito, Y., Kitamura, H., Hijikata, A., Tomizawa-Murasawa, M., Tanaka, S., Takagi, S., Uchida, N., Suzuki, N., Sone, A., Najima, Y., Ozawa, H., Wake, A., Taniguchi, S., Shultz, L. D., Ohara, O. & Ishikawa, F. Identification of therapeutic targets for quiescent, chemotherapy-resistant human leukemia stem cells. *Sci. Transl. Med.* **2**, 17ra19, doi:10.1126/scitranslmed.3000349 (2010).
- 99 Kornblau, S. M., Qutub, A., Yao, H., York, H., Qiu, Y. H., Graber, D., Ravandi, F., Cortes, J., Andreeff, M., Zhang, N. & Coombes, K. R. Proteomic profiling identifies distinct protein patterns in acute myelogenous leukemia CD34+CD38- stem-like cells. *PLoS One* **8**, e78453, doi:10.1371/journal.pone.0078453 (2013).

Vita

Rongqing Pan was born in Cangzhou, China, the son of Shuqin Li and Shouxiang Pan. After graduating from Cangzhou No.1 High School, he entered Nanjing Agricultural University in Nanjing, China. He received the degree of Bachelor of Sciences with a major in Biological Sciences in June 2007. For the next three years, he studied in the Department of Microbiology at Nanjing Agricultural University for his Master degree. During the course of his Master study, he designed novel methods to improve protein production in yeast and devised a marker-free technique for repetitive genome editing of yeast. In August of 2010, he entered The University of Texas Graduate School of Biomedical Sciences at Houston to pursue his doctoral degree in Cancer Biology Program at MD Anderson Cancer Center.

Permanent contact information:

Rongqing.Pan@gmail.com